

The one loop $\overline{\text{MS}}$ static potential in the Gribov-Zwanziger Lagrangian

J.A. Gracey,
Theoretical Physics Division,
Department of Mathematical Sciences,
University of Liverpool,
P.O. Box 147,
Liverpool,
L69 3BX,
United Kingdom.

Abstract. We compute the static potential in the Gribov-Zwanziger Lagrangian as a function of the Gribov mass, γ , in the $\overline{\text{MS}}$ scheme in the Landau gauge at one loop. The usual gauge independent one loop perturbative static potential is recovered in the limit as $\gamma \rightarrow 0$. By contrast the Gribov-Zwanziger static potential contains the term $\gamma^2/(p^2)^2$. However, the linearly rising potential in coordinate space as a function of the radial variable r does not emerge due to a compensating behaviour as $r \rightarrow \infty$. Though in the short distance limit a dipole behaviour is present. We also demonstrate enhancement in the propagator of the bosonic localizing Zwanziger ghost field when the one loop Gribov gap equation is satisfied. The explicit form of the one loop gap equation for the Gribov mass parameter is also computed in the MOM scheme and the zero momentum value of the renormalization group invariant effective coupling constant is shown to be the same value as that in the $\overline{\text{MS}}$ scheme.

1 Introduction.

One of the main outstanding problems in quantum field theory is to understand the confinement of the quarks and gluons associated with the strong nuclear force. The underlying field theory is Yang-Mills or Quantum Chromodynamics (QCD) which is a non-abelian gauge theory based on the $SU(3)$ colour group. Whilst its ultraviolet properties such as asymptotic freedom, [1, 2], are relatively straightforward to extract from perturbative calculations, it is the infrared properties which are difficult to truly access. These lie at the heart of the confinement problem. In early analyses of trying to understand how quarks and gluons are confined, it was recognised that the force separating these fundamental quanta of QCD behaved as a constant at large distances. In other words the potential energy at a colour charge separation distance of r was proportional to r . Known as the linearly rising potential it has been studied using lattice regularization which goes beyond perturbation theory. Indeed there is widespread acceptance that such numerical analyses do produce a linearly rising potential. See, for example, [3, 4, 5]. Another aspect of early attempts to understand such a potential has been clearly given in Mandelstam's review, [6], which emphasises the infrared behaviour of the gluon field, as well as in the work of others, [7, 8, 9]. Briefly, in the ultraviolet the gluon behaves as a standard fundamental massless particle with a simple propagator proportional to $1/p^2$ where p is the gluon momentum. However, such a behaviour can really only be valid asymptotically at high energy. Unlike the photon and overlooking for the moment the fact that the gluon is not a gauge invariant concept, if the gluon propagator's behaviour was of this form *for all* momenta then it could naively but erroneously be identified as a real physical object contrary to its accepted confined property. Instead due to the non-linear nature of the non-abelian gauge theory the gluon's propagator must be modified non-perturbatively or dynamically to a non-fundamental form without a simple pole. Given this, one natural form which it might take in order to fit with the linear potential is a dipole, $1/(p^2)^2$. The justification for this is that considering the force between coloured sources, the exchange of such a gluon at low energies will *naturally* produce a linear potential in coordinate space after taking a simple Fourier transform. However, whilst such a behaviour is an ultimate goal, the evidence for a dipole behaviour in the gluon propagator never actually manifested itself in subsequent studies. Indeed with the use of more powerful computers, lattice gauge theories have been able to probe the infrared behaviour of the gluon propagator more deeply at low energy. Without getting drawn too deeply for the moment into the current debate over which of the scaling, [10, 11, 12, 13, 14, 15, 16, 17, 18, 19, 20, 21], or decoupling solutions, [22, 23, 24, 25, 26, 27, 28, 29], is correct, it is fair to say that the gluon does not appear to have a dipole form at low momenta. Instead the propagator freezes either to zero or a finite non-zero value for each of these respective current scenarios. Therefore, the extraction of the dipole behaviour is currently in abeyance.

The next key breakthrough in the pursuit of gluon confinement effectively dawned with Gribov's seminal work noting the ambiguity in gauge fixing in the Landau gauge, [10]. In essence gauge fixing locally in a non-abelian gauge theory can be achieved uniquely but globally one will always end up with gauge or Gribov copies hindering the process. This was resolved by Gribov, [10], by restricting the path integral measure to the first Gribov region, Ω , defined as that region encompassing the trivial gauge solution, $A_\mu^a = 0$, where A_μ^a is the gluon field or gauge potential, such that the Faddeev-Popov operator has strictly positive eigenvalues. This restriction of the path integral produces a radically different gluon propagator which is clearly non-fundamental and vanishes in the infrared limit. Moreover, a mass parameter is introduced, known as the Gribov mass and denoted by γ , which is not an independent parameter of the theory. Indeed γ satisfies a gap equation which can be evaluated at one loop, [10]. One major consequence is that the propagator of the Faddeev-Popov ghost, which is required for the Landau

gauge fixing, also has a modification. Instead of a simple $1/p^2$ form, it behaves as $1/(p^2)^2$ as $p^2 \rightarrow 0$. Whilst this is a dipole, a Faddeev-Popov ghost clearly cannot be exchanged between colour sources as it is Grassmann in nature as it is required to restore unitarity. Subsequent progress in this area was via a series of articles in the main by Zwanziger and collaborators, [11, 12, 13, 14, 15, 16, 17, 18, 19, 20, 21]. Briefly, the drawback of the Gribov semi-classical analysis is that the resultant effective Lagrangian is non-local and therefore essentially inadequate for practical quantum computations. However, in a series of articles Zwanziger managed to localize the non-locality at the expense of introducing extra localizing fields, [12, 13, 17, 18]. The resulting Lagrangian was renormalizable, [18, 30, 31], meaning that it was possible to perform calculations with it. Indeed its renormalization is such that the known ultraviolet structure of Yang-Mills or QCD is totally unaltered by the extra localizing fields. Instead they only effectively play a role in the infrared. Subsequently, the two loop $\overline{\text{MS}}$ extension to Gribov's gap equation was determined in [32] verifying the Faddeev-Popov ghost enhancement at two loops and gluon suppression at one loop, [33]. The former property is not inconsistent with the Kugo-Ojima confinement criterion, [34, 35], derived for a BRST invariant Yang-Mills theory. Indeed it was shown that the Grassmann localizing ghost also was enhanced at two loops, [33], giving a propagator of dipole form but it is equally not directly relevant for confinement of coloured sources for the same reason as the Faddeev-Popov ghost.

Given the potential for the Gribov-Zwanziger Lagrangian to be a candidate for understanding confined gluons we now indicate the primary aim of this article. The explicit calculations of [32, 33] at one and two loops have opened the possibility of calculating the potential between two coloured sources using the Gribov-Zwanziger localized Lagrangian, [12, 13, 17, 18]. One aim is to see whether the behaviour of the potential is significantly different from that computed in the usual version of QCD. Indeed this was first discussed by Susskind in [36] and other authors at around the same time, [37, 38]. They considered the Wilson loop definition and examined the energy between two coloured sources fixed in time but at a spatial separation. This is known as the static limit. An advantage of the Wilson loop is that it is gauge invariant and in principle one can extract the resulting potential in any gauge. Originally this was achieved in the Feynman gauge at one loop in the $\overline{\text{MS}}$ scheme, [36, 37, 38]. Subsequently, the two loop static potential was determined in the same gauge in [39, 40]. This calculation was subsumed into a more general computation by Schröder in [41, 42]. There the full two loop potential was constructed in an arbitrary linear covariant gauge in ordinary (massless) perturbation theory. It clearly demonstrated the explicit cancellation of the linear gauge fixing parameter (and en route corrected a minor error in the original expression given in [39, 40]). The two loop static potential for a general colour state emerged later in [43]. More recently the three loop static potential has been the subject of interest with both the quark, [44, 45, 46], and purely gluonic contributions now available, [47, 48]. Since such an extensive formalism already exists (and is comprehensively reviewed in [49]) it is a rather straightforward exercise to apply it to the Gribov-Zwanziger Lagrangian at one loop. At the very least any perturbative potential, which will depend on γ , is needed since it would have to match onto the behaviour of the potential beyond the perturbative approximation. At this point it is worth noting that Zwanziger considered the Wilson loop in the Gribov-Zwanziger context using a lattice approach in [19]. There it was argued that a linear rising potential could emerge if there was ghost enhancement and gluon suppression, including gluon propagator freezing to a non-zero value. Moreover, the string tension was proportional to a combination of the zero momentum values of the gluon and Faddeev-Popov ghost form factors.

Although the static potential forms a main part of our article, we will also consider the structure of all the contributing fields to see whether a dipole exchange between coloured sources could somehow emerge in the Gribov-Zwanziger Lagrangian. In making this previous statement we have been careful in our wording and not mentioned the gluon. The reason for this is simple.

The premise that it is solely the gluon field itself which is responsible for confinement in the Gribov-Zwanziger context may need to be refined. This is primarily due to the appearance of the Zwanziger localizing ghosts in the work of [12, 13, 17, 18]. These play no role in the ultraviolet dynamics of QCD but do become important in the infrared. There is a *bosonic* Zwanziger ghost which is spin-1 and carries non-abelian colour charge. In some ways it could be regarded as a gluon component since its equation of motion implies it is a non-local projection of A_μ^a . However, in the full Gribov-Zwanziger Lagrangian we regard it as a separate entity. Therefore, in principle the appearance of a dipole behaviour in the infrared between coloured sources could also derive from other spin-1 fields aside from the gluon itself. Indeed this is indicated very strongly in Zwanziger's recent article, [50], where Dyson Schwinger techniques are applied to the bosonic localizing ghost to produce an enhancement akin to that of both Grassmann ghost fields. Though the enhancement is actually beyond dipole being $1/(p^2)^3$ as $p^2 \rightarrow 0$. However, since it is non-Grassmann, [50], it is evidently a much better candidate for an exchange field between coloured sources. Therefore, in the current context of the full one loop $\overline{\text{MS}}$ static potential in the Gribov-Zwanziger Lagrangian we will speculate how it might be possible to go beyond the one loop potential and qualitatively produce a linearly rising potential. En route we will record some new properties of the underlying Gribov gap equation. As emphasised by Zwanziger, in the Gribov-Zwanziger context the theory can only be regarded as a gauge theory when the Gribov mass, γ , explicitly satisfies this equation. In the original calculations of Gribov, [10], to produce the Faddeev-Popov ghost enhancement the main lesson was that the gap equation was central to seeing towards the infrared. To a lesser extent it also played a role in qualitatively producing the freezing to a non-zero value, [33], of a renormalization group invariant definition of the coupling constant based on the Landau gauge properties of the gluon ghost vertex, [51]. Therefore, we believe that the gap equation, which is derived from the condition defining the first Gribov region, should be a central requirement to producing the infrared property of a linearly rising potential. In our calculations we will follow the more recent formulation of the Gribov-Zwanziger Lagrangian of [50] where the localizing bosonic ghosts were resolved into their real and imaginary parts. Whilst this will be different from the earlier loop computations of [32, 33], it transpires that those results are not correct since the propagator of the real part of the bosonic localizing ghost was treated erroneously. Therefore, throughout the discussion we will re-address some of the results of [32, 33] and provide the correct details. It turns out that the main features such as one loop gluon suppression, two loop Faddeev-Popov ghost enhancement and the freezing of a renormalization group invariant effective coupling constant to a finite non-zero value remain unaltered. It is only the actual numerical details which are revised since the omission affects the finite parts of Feynman graphs upon which there are no non-trivial independent checks. Finally, given the current interest in the alternative infrared structure known as the decoupling solution, [22, 23, 24, 25, 26, 27, 28, 29], we will briefly discuss its status within the static potential approach. Indeed in [52] a novel way of producing the decoupling solution within the Gribov-Zwanziger Lagrangian was considered and later tested in explicit calculations, [53].

The paper is organised as follows. In section 2 we review the static potential formalism of [36, 37, 38, 39, 40, 41, 42] as well as the necessary ingredients from the Gribov-Zwanziger Lagrangian, [12, 13, 17, 18]. Section 3 is devoted to the formal construction of the one loop corrections to the propagators in the reformulation of the Gribov-Zwanziger Lagrangian in terms of the real and imaginary parts of the localizing bosonic ghost discussed in [50]. The explicit one loop $\overline{\text{MS}}$ static potential is constructed in section 4 prior to considering several new calculational aspects of the Gribov gap equation for γ in section 5 including the correct two loop $\overline{\text{MS}}$ expression. The role the original gap equation plays in the one loop enhancement of the bosonic localizing ghosts is discussed in section 6 and its implications for trying to extract the linearly rising potential

qualitatively in the Gribov-Zwanziger static potential are also considered. Section 7 focuses on considering power corrections to the potential and other quantities which can be computed in the Gribov-Zwanziger Lagrangian as well as elementary ideas on the underlying properties of higher order Feynman graphs. We give our conclusions in section 8. Several appendices are provided. The first details the decomposition of products of colour group structure functions into a standard basis which is required in the discussion of the bosonic ghost enhancement. The next two appendices provide the explicit *exact* one loop corrections respectively to the transverse and longitudinal parts of all the 2-point functions of the spin-1 fields in the Gribov-Zwanziger Lagrangian. The longitudinal parts are presented as they are relevant to the current debate on the BRST structure of the Gribov-Zwanziger Lagrangian. The final appendix records the explicit values of scalar amplitudes in the decomposition of the correlation function of a Lorentz tensor operator involving the field strength. It extends the power correction computation of the analogous scalar operator considered in section 7.

2 Formalism.

We begin by briefly summarizing the static potential formalism in both the original QCD and Gribov-Zwanziger contexts. The key is the definition of the Wilson loop where the loop is taken to be a rectangle. The spatial extent is length r and the time interval is denoted by T . When the temporal side of the rectangle is very much in excess of the spatial extent, $T \gg r$, then the potential, $V(r)$, between two heavy static colour sources is given by

$$V(r) = - \lim_{T \rightarrow \infty} \frac{1}{iT} \ln \left\langle 0 \left| \text{Tr} \mathcal{P} \exp \left(ig \oint dx^\mu A_\mu^a T^a \right) \right| 0 \right\rangle . \quad (2.1)$$

Here \mathcal{P} denotes the path ordering prescription, A_μ^a is the gluon field and T^a are the colour group generators satisfying

$$[T^a, T^b] = if^{abc} T^c \quad (2.2)$$

where f^{abc} are the structure constants. Throughout our discussion on the definition and properties of the static potential we make the same general assumptions as have been discussed extensively in [36, 37, 38, 39, 40, 41, 42] such as gauge invariance of $V(r)$. Also, for instance, it is accepted that the potential of (2.1) can be reformulated in terms of a functional integral with an external colour source, $J_\mu^a(x)$. In other words

$$V(r) = - \lim_{T \rightarrow \infty} \frac{1}{iT} \frac{\text{tr} Z[J]}{\text{tr} Z[0]} \quad (2.3)$$

where formally

$$Z[J] = \int \mathcal{D}A_\mu \mathcal{D}\psi \mathcal{D}\bar{\psi} \mathcal{D}c \mathcal{D}\bar{c} \exp \left[- \int d^4x \left(L + J^{a\mu} A_\mu^a \right) \right] \quad (2.4)$$

and the Lagrangian L will be discussed later in detail but will either be the original QCD Lagrangian or that of the Gribov-Zwanziger theory. The denominator, $Z[0]$, is included as a normalization. The other main assumption, which also occurs in the usual QCD case and has been discussed in [36, 37, 38, 39, 40, 41], is that of the exponentiation of the values of the actual Feynman diagrams in order to properly extract the static potential implicit in the definition, (2.1). This has been proved to all orders in the abelian case. For the non-abelian case the exponentiation for the Wilson loop for ordinary QCD has been demonstrated in [54, 55]. Although we assume that that analysis extends to the Gribov-Zwanziger case we note that

for our one loop computation, the exponentiation does indeed occur which is sufficient for our present purpose.

For the moment we follow the early approach of [36, 37, 38] for the canonical formalism of QCD and the Lagrangian is given by

$$L^{\text{QCD}} = -\frac{1}{4}G_{\mu\nu}^a G^{a\mu\nu} - \frac{1}{2\alpha}(\partial^\mu A_\mu^a)^2 - \bar{c}^a \partial^\mu D_\mu c^a + i\bar{\psi}^{iI} \not{D}\psi^{iI} \quad (2.5)$$

where $G_{\mu\nu}^a$ is the field strength, the covariant derivative, D_μ , is defined by

$$\begin{aligned} D_\mu c^a &= \partial_\mu c^a - gf^{abc} A_\mu^b c^c \\ D_\mu \psi^{iI} &= \partial_\mu \psi^{iI} + igT_{IJ}^a A_\mu^a \psi^{iJ} \end{aligned} \quad (2.6)$$

g is the coupling constant and we have included the usual linear covariant gauge fixing term with parameter α . It is formally present to allow for the non-singular inversion of the quadratic part of the Lagrangian in momentum space to determine the propagators but we will set $\alpha = 0$ throughout thereafter. Associated with this are the Faddeev-Popov ghosts, c^a and \bar{c}^a , and massless quarks, ψ^{iI} , are included where the indices have the ranges $1 \leq a \leq N_A$, $1 \leq i \leq N_f$ and $1 \leq I \leq N_F$ where N_F and N_A are the respective dimensions of the fundamental and adjoint representations and N_f is the number of quark flavours. To recover the static set-up of the colour sources we take, [36, 37, 38],

$$J_\mu^a(x) = gv_\mu T^a \left[\delta^{(3)}(\mathbf{x} - \frac{1}{2}\mathbf{r}) - \delta^{(3)}(\mathbf{x} - \frac{1}{2}\mathbf{r}') \right] \quad (2.7)$$

where $v_\mu = \eta_{\mu 0}$ is a unit vector and we will set $r = |\mathbf{r} - \mathbf{r}'|$. This vector v_μ will be present throughout our calculations and in effect projects out the time component of the gluon it couples to. Whilst we will be concentrating on the Gribov-Zwanziger case throughout, which relates to a theory of a confined gluon, we note that the group generator present in the source will be taken as being the fundamental representation initially. Though one can regard the heavy sources as being gluons in which case one would use the adjoint representation of the source interaction. The calculation of the one loop static potential is the same irrespective of whether the generator is in the fundamental or adjoint representations. Computationally differences will only arise in the two loop static potential, [43]. At this point it is worth briefly mentioning that in the Coulomb gauge, which Gribov also considered in [10], it is the time component of the gluon propagator which receives attention in regard to confinement. So the vector v_μ is in effect the bridge between the Landau gauge we use here and the Coulomb gauge results in relation to a confining potential through the gauge invariant Wilson loop.

Given this formulation of the static potential, it is possible to evaluate $V(r)$ either directly in coordinate space, [36, 37, 38], or in momentum space, [39, 40, 41, 42]. For the latter $V(r)$ emerges after a Fourier transform and in our conventions we take

$$V(r) = \int \frac{d^3\mathbf{k}}{(2\pi)^3} e^{i\mathbf{k}\cdot\mathbf{r}} \tilde{V}(\mathbf{k}) \quad (2.8)$$

where $\tilde{V}(\mathbf{k})$ is the momentum space static potential. Performing the angular integrations since $\tilde{V}(\mathbf{k})$ will only depend on the momentum length k then

$$V(r) = \frac{1}{2\pi^2} \int_0^\infty dk k^2 \tilde{V}(k) \frac{\sin(kr)}{kr}. \quad (2.9)$$

At this point it is perhaps apt to recall differing forms of $\tilde{V}(k)$ and examine their implications for coordinate space. Although we will consider forms relevant for this article, a more general

library of mappings between spaces can be found, for instance, in [56]. Taking

$$\tilde{V}_C(k) = \frac{A_C}{k^2} \quad , \quad \tilde{V}_l(k) = \frac{A_l}{(k^2)^2} \quad \text{and} \quad \tilde{V}_b(k) = \frac{A_b}{(k^2)^3} \quad (2.10)$$

then

$$V_C(r) = \frac{A_C}{4\pi r} \quad , \quad V_l(r) = -\frac{A_l}{8\pi} r \quad \text{and} \quad V_b(r) = \frac{A_b}{96\pi} r^3 \quad (2.11)$$

respectively which result from the elementary integrals

$$\int_0^\infty dx \frac{\sin x}{x} = \frac{\pi}{2} \quad , \quad \int_0^\infty dx \frac{\sin x}{x^3} = -\frac{\pi}{4} \quad \text{and} \quad \int_0^\infty dx \frac{\sin x}{x^5} = \frac{\pi}{96} \quad (2.12)$$

respectively. So a linearly rising potential will emerge from a simple dipole term. However, it is amusing to note that an asymptotic linear behaviour as $r \rightarrow \infty$ can also emerge from other forms of $\tilde{V}(k)$ such as that given by including in $\tilde{V}_l(k)$ any reasonable function of k , which is non-singular and does not upset the integral convergence, purely on dimensional grounds.

In the early work of [36, 37, 38] the static potential was calculated at one loop directly in coordinate space. The presence of the static sources modifies the Feynman rules and introduces Heaviside step functions of the source interaction positions. Whilst it is relatively straightforward to compute the one loop potential, since we will ultimately be dealing with a formulation of QCD which is effectively massive, it is more natural to work in momentum space. The momentum space formalism was developed in [39, 40, 41, 42] and we defer to those articles for the justification of the more technical aspects rather than unnecessarily repeat them here. Suffice to say that the momentum space Feynman rules for the source gluon couplings do not alter from those recorded in an appendix of [41] and we note that [41] gives comprehensive detail on many of the technical aspects of computing the static potentials. Moreover, the advantage of a momentum space approach is that it is in principle more straightforward to extend to two loops. For completeness in reviewing the earlier static potential result for pure QCD, we note that the one loop $\overline{\text{MS}}$ result of [36, 37, 38] is

$$\tilde{V}(\mathbf{p}) \Big|_{\text{QCD}} = -\frac{16\pi^2 C_F a}{\mathbf{p}^2} \left[1 + \left[\left[\frac{31}{9} - \frac{11}{3} \ln \left[\frac{\mathbf{p}^2}{\mu^2} \right] \right] C_A + \left[\frac{4}{3} \ln \left[\frac{\mathbf{p}^2}{\mu^2} \right] - \frac{20}{9} \right] T_F N_f \right] a + O(a^2) \right] \quad (2.13)$$

where μ is the mass scale introduced to ensure the coupling constant is dimensionless when dimensional regularization is used, $a = g^2/(16\pi^2)$ and the colour group Casimirs are defined by

$$\text{Tr} \left(T^a T^b \right) = T_F \delta^{ab} \quad , \quad T^a T^a = C_F I \quad , \quad f^{acd} f^{bcd} = C_A \delta^{ab} \quad (2.14)$$

and I is the N_F dimensional unit matrix.

To extend the static potential to the Gribov-Zwanziger case we return to the definition (2.1) and (2.3). In Gribov's original work, [10], the key observation in the Landau gauge was that of the partition of configuration space into regions defined by zeroes of the Faddeev-Popov operator $\mathcal{M}(A) = -\partial^\mu D_\mu$ which is hermitian. This is because one has copies of the gauge configuration satisfying the *same* gauge fixing condition. The region containing the origin, $A_\mu^a = 0$, is referred to as the Gribov region and denoted by Ω . Gribov showed that to exclude copies from the gauge fixing procedure, the path integral measure must be restricted to the region Ω which effectively introduced a cutoff into the theory. Consequently, the structure of the theory was altered in that the gluon propagator ceased to be of a fundamental form in the infrared region. This was primarily due to the appearance in the Lagrangian of an additional non-local term. Its origin is

in defining the boundary of Ω by the no-pole or horizon condition and leads to the presence of a mass parameter, γ , known as the Gribov mass. This is not an independent object but must satisfy a gap equation derived from the horizon condition, [10]. One outcome of this is that the propagator of the Faddeev-Popov ghost takes a dipole form in the infrared. Whilst this is of the form for a linear confining potential in coordinate space, the Faddeev-Popov ghost is never directly exchanged between gluons or quarks. Given this position it is straightforward to see what one must do to determine the static potential in the Gribov picture. One simply returns to (2.3) and restricts the integration measure to Ω

$$Z[J] = \int_{\Omega} \mathcal{D}A_{\mu} \mathcal{D}\psi \mathcal{D}\bar{\psi} \mathcal{D}c \mathcal{D}\bar{c} \exp \left[- \int d^4x \left(L + J^{a\mu} A_{\mu}^a \right) \right] . \quad (2.15)$$

Implementing the horizon condition this equates to, [12],

$$Z[J] = \int \mathcal{D}A_{\mu} \mathcal{D}\psi \mathcal{D}\bar{\psi} \mathcal{D}c \mathcal{D}\bar{c} \exp \left[- \int d^4x \left(L^{\text{Grib}} + J^{a\mu} A_{\mu}^a \right) \right] \quad (2.16)$$

where

$$L^{\text{Grib}} = L^{\text{QCD}} + \frac{C_A \gamma^4}{2} A^{a\mu} \frac{1}{\partial^{\nu} D_{\nu}} A_{\mu}^a - \frac{d N_A \gamma^4}{2g^2} \quad (2.17)$$

where d is the dimension of spacetime.

To proceed we now use the localization of the horizon non-locality introduced in [12, 13, 17, 18] by Zwanziger. This involves introducing an additional set of fields called localizing or Zwanziger ghosts, $\{\phi_{\mu}^{ab}, \bar{\phi}_{\mu}^{ab}\}$ and $\{\omega_{\mu}^{ab}, \bar{\omega}_{\mu}^{ab}\}$, where the former are commuting and the latter are anti-commuting. They are regarded as *internal* fields, similar to the Faddeev-Popov ghosts, in that they do not couple directly to quarks. The resulting path integral becomes

$$Z[J] = \int \mathcal{D}A_{\mu} \mathcal{D}\psi \mathcal{D}\bar{\psi} \mathcal{D}c \mathcal{D}\bar{c} \mathcal{D}\xi \mathcal{D}\rho \mathcal{D}\omega \mathcal{D}\bar{\omega} \exp \left[- \int d^4x \left(L^{\text{GZ}} + J^{a\mu} A_{\mu}^a \right) \right] \quad (2.18)$$

where

$$\begin{aligned} L^{\text{GZ}} = & L^{\text{QCD}} + \frac{1}{2} \rho^{ab\mu} \partial^{\nu} (D_{\nu} \rho_{\mu})^{ab} + \frac{i}{2} \rho^{ab\mu} \partial^{\nu} (D_{\nu} \xi_{\mu})^{ab} - \frac{i}{2} \xi^{ab\mu} \partial^{\nu} (D_{\nu} \rho_{\mu})^{ab} \\ & + \frac{1}{2} \xi^{ab\mu} \partial^{\nu} (D_{\nu} \xi_{\mu})^{ab} - \bar{\omega}^{ab\mu} \partial^{\nu} (D_{\nu} \omega_{\mu})^{ab} - \frac{1}{\sqrt{2}} g f^{abc} \partial^{\nu} \bar{\omega}_{\mu}^{ae} (D_{\nu} c)^b \rho^{ec\mu} \\ & - \frac{i}{\sqrt{2}} g f^{abc} \partial^{\nu} \bar{\omega}_{\mu}^{ae} (D_{\nu} c)^b \xi^{ec\mu} - i\gamma^2 f^{abc} A^{a\mu} \xi_{\mu}^{bc} - \frac{d N_A \gamma^4}{2g^2} \end{aligned} \quad (2.19)$$

and we have introduced the real and imaginary fields ρ_{μ}^{ab} and ξ_{μ}^{ab} similar to [50] given by

$$\phi_{\mu}^{ab} = \frac{1}{\sqrt{2}} \left(\rho_{\mu}^{ab} + i \xi_{\mu}^{ab} \right) , \quad \bar{\phi}_{\mu}^{ab} = \frac{1}{\sqrt{2}} \left(\rho_{\mu}^{ab} - i \xi_{\mu}^{ab} \right) . \quad (2.20)$$

In choosing to work with the real fields ρ_{μ}^{ab} and ξ_{μ}^{ab} we will en route be correcting the error in earlier loop calculations, [32, 33], where the ρ_{μ}^{ab} propagator was erroneously treated in the initial computer algebra derivation. One main benefit is that (2.19) is renormalizable, [18, 30, 31], which allows us to do explicit calculations. We briefly note that in using (2.19) to perform computations the gauge symmetry is broken in much the same fashion as in the $\gamma^2 = 0$ situation via the (local) gauge fixing criterion in (2.5). However, the usefulness of (2.19) in determining quantities of physical interest, in addition to renormalizability, resides essentially on two criteria. These are the gauge invariance of the object which is apparent, for instance, in the local or ultraviolet limit and the fact that γ is constrained in the Gribov gap equation to be a (non-perturbative)

function of the coupling constant and is not an independent parameter of the theory. In other words (2.19) has no meaning as a gauge theory unless γ satisfies the gap equation defined by the horizon condition, [11, 12, 13, 14, 15, 16, 17, 18, 19]. For completeness we note the Landau gauge propagators of the gauge sector required for that computation and the current one are,

$$\begin{aligned}
\langle A_\mu^a(p) A_\nu^b(-p) \rangle &= - \frac{\delta^{ab} p^2}{[(p^2)^2 + C_A \gamma^4]} P_{\mu\nu}(p) \\
\langle A_\mu^a(p) \xi_\nu^{bc}(-p) \rangle &= \frac{i f^{abc} \gamma^2}{[(p^2)^2 + C_A \gamma^4]} P_{\mu\nu}(p) \\
\langle A_\mu^a(p) \rho_\nu^{bc}(-p) \rangle &= 0 \\
\langle \xi_\mu^{ab}(p) \xi_\nu^{cd}(-p) \rangle &= - \frac{\delta^{ac} \delta^{bd}}{p^2} \eta_{\mu\nu} + \frac{f^{abe} f^{cde} \gamma^4}{p^2 [(p^2)^2 + C_A \gamma^4]} P_{\mu\nu}(p) \\
\langle \xi_\mu^{ab}(p) \rho_\nu^{cd}(-p) \rangle &= 0 \\
\langle \rho_\mu^{ab}(p) \rho_\nu^{cd}(-p) \rangle &= \langle \omega_\mu^{ab}(p) \bar{\omega}_\nu^{cd}(-p) \rangle = - \frac{\delta^{ac} \delta^{bd}}{p^2} \eta_{\mu\nu}
\end{aligned} \tag{2.21}$$

where

$$P_{\mu\nu}(p) = \eta_{\mu\nu} - \frac{p_\mu p_\nu}{p^2} \tag{2.22}$$

is the transverse projector and we have a procedure similar to that discussed in [33] for handling the mixed propagator. The explicit renormalization properties of the Gribov mass and fields ρ_μ^{ab} , ξ_μ^{ab} and ω_μ^{ab} are predetermined by Slavnov-Taylor identities, [18, 30, 31], which have been verified by explicit computations in the $\overline{\text{MS}}$ scheme, [32, 33], in the ultraviolet situation where one can work with the $\gamma = 0$ limit. Those calculations were carried out with the symbolic manipulation machinery of FORM, [57], which we will also use here. The absence of a mixed ρ_μ^{ab} - ξ_μ^{ab} propagator is due to the fact that the cross-term of the quadratic part of the Lagrangian is a total derivative which can be dropped, [50]. However, we have retained the gluon ρ_μ^{ab} - ξ_μ^{ab} vertex even though it can be written with a factor proportional to the Landau gauge condition, $\partial^\mu A_\mu^a$, [50]. Whilst this will vanish for transverse gluons in the Landau gauge we retain it as part of our Feynman rules since we will consider longitudinal corrections to the 2-point functions at one loop.

Indeed given this, it is worth recalling how the propagators of (2.21) are constructed in practice since it is partly related to the situation with regard to other linear covariant gauges and justifies why we focus solely on the Landau gauge in the Gribov case. Also these comments are based around the more detailed analysis of [58], to which we refer the interested reader, where Gribov copies were considered for linear covariant gauges when the gauge parameter is small. First, we recall, [33], that in deriving (2.21) in order to avoid a singular determinant in Lorentz space in inverting the quadratic part of the momentum space Lagrangian, the gauge parameter is kept non-zero. The Landau gauge expressions, (2.21), emerge when α is set to zero, [33]. Specifically, if we work in the basis of fields $\{A_\mu^a, \xi_\mu^{ab}, \rho_\mu^{ab}\}$ then with a non-zero α the matrix of quadratic terms in the Lagrangian in momentum space is

$$\begin{aligned}
\Lambda_{\mu\nu}^{\{ab|cd\}}(p) &= \begin{pmatrix} -p^2 \delta^{ac} & -i\gamma^2 f^{acd} & 0 \\ -i\gamma^2 f^{cab} & -p^2 \delta^{ac} \delta^{bd} & 0 \\ 0 & 0 & -p^2 \delta^{ac} \delta^{bd} \end{pmatrix} P_{\mu\nu}(p) \\
&+ \begin{pmatrix} -\frac{p^2}{\alpha} \delta^{ac} & -i\gamma^2 f^{acd} & 0 \\ -i\gamma^2 f^{cab} & -p^2 \delta^{ac} \delta^{bd} & 0 \\ 0 & 0 & -p^2 \delta^{ac} \delta^{bd} \end{pmatrix} L_{\mu\nu}(p)
\end{aligned} \tag{2.23}$$

where

$$L_{\mu\nu}(p) = \frac{p_\mu p_\nu}{p^2} \quad (2.24)$$

is the longitudinal projector which satisfies the trivial relation $P_{\mu\nu}(p) + L_{\mu\nu}(p) = \eta_{\mu\nu}$. If we denote the matrix of propagators by $\Pi_{\mu\nu}^{\{ab|cd\}}(p)$ then the propagators must satisfy

$$\Lambda_{\mu\sigma}^{\{ab|cd\}}(p) \Pi_{\nu}^{\{cd|pq\}\sigma}(p) = \begin{pmatrix} \delta^{cp} & 0 & 0 \\ 0 & \delta^{cp} \delta^{dq} & 0 \\ 0 & 0 & \delta^{cp} \delta^{dq} \end{pmatrix} \eta_{\mu\nu} \quad (2.25)$$

and the matrix on the right hand side is the unit matrix on the colour space for this sector of fields. Equipped with this the non-zero α propagators are

$$\begin{aligned} \langle A_\mu^a(p) A_\nu^b(-p) \rangle &= - \frac{\delta^{ab} p^2}{[(p^2)^2 + C_A \gamma^4]} P_{\mu\nu}(p) - \frac{\alpha \delta^{ab} p^2}{[(p^2)^2 + \alpha C_A \gamma^4]} L_{\mu\nu}(p) \\ \langle A_\mu^a(p) \xi_\nu^{bc}(-p) \rangle &= \frac{i f^{abc} \gamma^2}{[(p^2)^2 + C_A \gamma^4]} P_{\mu\nu}(p) + \frac{i \alpha f^{abc} \gamma^2}{[(p^2)^2 + \alpha C_A \gamma^4]} L_{\mu\nu}(p) \\ \langle A_\mu^a(p) \rho_\nu^{bc}(-p) \rangle &= 0 \\ \langle \xi_\mu^{ab}(p) \xi_\nu^{cd}(-p) \rangle &= - \frac{\delta^{ac} \delta^{bd}}{p^2} \eta_{\mu\nu} + \frac{f^{abe} f^{cde} \gamma^4}{p^2 [(p^2)^2 + C_A \gamma^4]} P_{\mu\nu}(p) + \frac{\alpha f^{abe} f^{cde} \gamma^4}{p^2 [(p^2)^2 + \alpha C_A \gamma^4]} L_{\mu\nu}(p) \\ \langle \xi_\mu^{ab}(p) \rho_\nu^{cd}(-p) \rangle &= 0 \\ \langle \rho_\mu^{ab}(p) \rho_\nu^{cd}(-p) \rangle &= \langle \omega_\mu^{ab}(p) \bar{\omega}_\nu^{cd}(-p) \rangle = - \frac{\delta^{ac} \delta^{bd}}{p^2} \eta_{\mu\nu} . \end{aligned} \quad (2.26)$$

These reduce to those of (2.21) in the $\alpha \rightarrow 0$ limit. Though we have included the non-zero α forms since the longitudinal pieces play an important role in determining the one loop corrections to the gluon propagator. However, the propagators of (2.26) have no meaning as such and must not be regarded as the propagators for the extension of the Gribov-Zwanziger Lagrangian to other linear covariant gauges. The Gribov-Zwanziger Lagrangian is purely a Landau gauge construction. To clarify this we recall certain properties in the construction of (2.19) based on [58]. First, in the set of linear covariant gauges the Faddeev-Popov operator is only hermitian in the Landau gauge which allows for the classification of its eigenvalues into positive and negative values in that case only, [10, 11, 12, 13, 14, 15, 15, 16, 17, 18, 19]. This gives a natural way of dividing configuration space into definite regions. For other linear covariant gauges the loss of hermiticity means the eigenvalues can be complex and therefore there is not a natural or straightforward way of partitioning configuration space to even examine how Gribov copies are mapped between regions as one can do in the Landau gauge. Therefore, for non-Landau linear covariant gauges it does not seem clear how the path integral could be cut-off and the analogous first Gribov region defined by a no-pole condition as in the Landau case. Moreover, as the latter condition manifests itself as the non-locality to be localized in the Landau gauge one might simply assume that the natural extension to other linear covariant gauges is to merely use (2.17) and proceed with a non-zero gauge parameter. However, this overlooks the fact that in the Landau gauge the gluon is transverse but in other linear covariant gauges it is not. Therefore, in the non-local term of (2.17) the gauge field in the denominator covariant derivative itself actually involves an additional non-local projection, [58]. Thus, for non-zero α the analogous Gribov-Zwanziger Lagrangian, (2.19), would have additional non-localities which would also need to be localized before any computations could proceed assuming any final local Lagrangian would actually be renormalizable, [58]. So, for instance, the intermediate propagators of (2.26) that exist for non-zero α in deriving (2.21) have no true meaning.

3 2-point function corrections.

Given that we are now using a version of the Gribov-Zwanziger Lagrangian which correctly involves the real and imaginary parts of the bosonic localizing ghosts, it is appropriate to discuss the one loop corrections to all the 2-point functions and propagators of the fields. Though we will concentrate primarily on the mixed sector for reasons which will become apparent later. Whilst the main details of this analysis parallels that given in [33], which was incorrect, we include it here for completeness. We define the 3×3 matrix of one loop 2-point functions formally by

$$\begin{aligned}
\Lambda_{\mu\nu}^{\{ab|cd\}}(p) &= \begin{pmatrix} -p^2\delta^{ac} & -i\gamma^2 f^{acd} & 0 \\ -i\gamma^2 f^{cab} & -p^2\delta^{ac}\delta^{bd} & 0 \\ 0 & 0 & -p^2\delta^{ac}\delta^{bd} \end{pmatrix} P_{\mu\nu}(p) \\
&+ \begin{pmatrix} -p^2\delta^{ac} & -i\gamma^2 f^{acd} & 0 \\ -i\gamma^2 f^{cab} & -p^2\delta^{ac}\delta^{bd} & 0 \\ 0 & 0 & -p^2\delta^{ac}\delta^{bd} \end{pmatrix} L_{\mu\nu}(p) \\
&+ \begin{pmatrix} X\delta^{ac} & U f^{acd} & V f^{acd} \\ U f^{cab} & Q_\xi^{abcd} & 0 \\ V f^{cab} & 0 & Q_\rho^{abcd} \end{pmatrix} P_{\mu\nu}(p)a \\
&+ \begin{pmatrix} X^L\delta^{ac} & U^L f^{acd} & V^L f^{acd} \\ U^L f^{cab} & Q_\xi^L{}^{abcd} & 0 \\ V^L f^{cab} & 0 & Q_\rho^L{}^{abcd} \end{pmatrix} L_{\mu\nu}(p)a + O(a^2) \tag{3.1}
\end{aligned}$$

with respect to the same basis $\{A_\mu^a, \xi_\mu^{ab}, \rho_\mu^{ab}\}$ where

$$\begin{aligned}
Q_\xi^{abcd} &= Q_\xi\delta^{ac}\delta^{bd} + W_\xi f^{ace} f^{bde} + R_\xi f^{abe} f^{cde} + S_\xi d_A^{abcd} \\
Q_\rho^{abcd} &= Q_\rho\delta^{ac}\delta^{bd} + W_\rho f^{ace} f^{bde} + R_\rho f^{abe} f^{cde} + S_\rho d_A^{abcd} \\
Q_\xi^L{}^{abcd} &= Q_\xi^L\delta^{ac}\delta^{bd} + W_\xi^L f^{ace} f^{bde} + R_\xi^L f^{abe} f^{cde} + S_\xi^L d_A^{abcd} \\
Q_\rho^L{}^{abcd} &= Q_\rho^L\delta^{ac}\delta^{bd} + W_\rho^L f^{ace} f^{bde} + R_\rho^L f^{abe} f^{cde} + S_\rho^L d_A^{abcd} \tag{3.2}
\end{aligned}$$

represents the colour decomposition and

$$d_A^{abcd} = \frac{1}{6} \text{Tr} \left(T_A^a T_A^b T_A^c T_A^d \right) \tag{3.3}$$

is totally symmetric and T_A^a is the adjoint representation of the colour group generators. The quantities in the final two matrices of (3.1) represent the one loop corrections and we have incorporated the fact that there is no one loop correction to the $\rho_\mu^{ab} - \xi_\nu^{cd}$ 2-point functions. The longitudinal 2-point functions are indicated by the superscript L . Given (3.1) we define a similar formal form for the inverse to one loop by

$$\begin{aligned}
\Pi_{\mu\nu}^{\{cd|pq\}}(p) &= \begin{pmatrix} -\frac{p^2}{[(p^2)^2 + C_A\gamma^4]} \delta^{cp} & \frac{i\gamma^2}{[(p^2)^2 + C_A\gamma^4]} f^{cpq} & 0 \\ \frac{i\gamma^2}{[(p^2)^2 + C_A\gamma^4]} f^{pcd} & -\frac{1}{p^2} \delta^{cp} \delta^{dq} + \frac{\gamma^4}{p^2 [(p^2)^2 + C_A\gamma^4]} f^{cdr} f^{pqr} & 0 \\ 0 & 0 & -\frac{\delta^{cp} \delta^{dq}}{p^2} \end{pmatrix} P_{\mu\nu}(p) \\
&+ \begin{pmatrix} -\frac{\alpha p^2}{[(p^2)^2 + \alpha C_A\gamma^4]} \delta^{cp} & \frac{i\alpha\gamma^2}{[(p^2)^2 + \alpha C_A\gamma^4]} f^{cpq} & 0 \\ \frac{i\alpha\gamma^2}{[(p^2)^2 + \alpha C_A\gamma^4]} f^{pcd} & -\frac{1}{p^2} \delta^{cp} \delta^{dq} + \frac{\alpha\gamma^4}{p^2 [(p^2)^2 + \alpha C_A\gamma^4]} f^{cdr} f^{pqr} & 0 \\ 0 & 0 & -\frac{\delta^{cp} \delta^{dq}}{p^2} \end{pmatrix} L_{\mu\nu}(p) \\
&+ \begin{pmatrix} A\delta^{cp} & B f^{cpq} & C f^{cpq} \\ B f^{pcd} & D_\xi^{cdpq} & E^{cdpq} \\ C f^{pcd} & E^{cdpq} & D_\rho^{cdpq} \end{pmatrix} P_{\mu\nu}(p)a
\end{aligned}$$

$$+ \begin{pmatrix} A^L \delta^{cp} & B^L f^{cpq} & C^L f^{cpq} \\ B^L f^{pcd} & D_\xi^{cdpq} & E^L cdpq \\ C^L f^{pcd} & E^L cdpq & D_\rho^{cdpq} \end{pmatrix} L_{\mu\nu}(p)a + O(a^2) \quad (3.4)$$

for non-zero α , where

$$\begin{aligned} E^{cdpq} &= E \delta^{cp} \delta^{dq} + F f^{cpe} f^{dqe} + G f^{cde} f^{pqe} + H d_A^{cdpq} \\ D_\xi^{cdpq} &= D_\xi \delta^{cp} \delta^{dq} + J_\xi f^{cpe} f^{dqe} + K_\xi f^{cde} f^{pqe} + L_\xi d_A^{cdpq} \\ D_\rho^{cdpq} &= D_\rho \delta^{cp} \delta^{dq} + J_\rho f^{cpe} f^{dqe} + K_\rho f^{cde} f^{pqe} + L_\rho d_A^{cdpq} \\ E^L cdpq &= E^L \delta^{cp} \delta^{dq} + F^L f^{cpe} f^{dqe} + G^L f^{cde} f^{pqe} + H^L d_A^{cdpq} \\ D_\xi^L cdpq &= D_\xi^L \delta^{cp} \delta^{dq} + J_\xi^L f^{cpe} f^{dqe} + K_\xi^L f^{cde} f^{pqe} + L_\xi^L d_A^{cdpq} \\ D_\rho^L cdpq &= D_\rho^L \delta^{cp} \delta^{dq} + J_\rho^L f^{cpe} f^{dqe} + K_\rho^L f^{cde} f^{pqe} + L_\rho^L d_A^{cdpq} \end{aligned} \quad (3.5)$$

and the inverse satisfies (2.25) again. The quantities in the final two matrices of (3.4) represent the one loop corrections to the propagators. By multiplying out the elements of the left hand side of (2.25) to one loop we can determine the relation of the one loop propagator corrections to those of the 2-point functions. For the transverse sector we find

$$\begin{aligned} A &= -\frac{1}{[(p^2)^2 + C_A \gamma^4]^2} \left[(p^2)^2 X - 2i C_A \gamma^2 p^2 U - C_A \gamma^4 [Q_\xi + C_A R_\xi + \frac{1}{2} C_A W_\xi] \right] \\ B &= \frac{1}{[(p^2)^2 + C_A \gamma^4]^2} \left[i \gamma^2 p^2 X - ((p^2)^2 - C_A \gamma^4) U + i \gamma^2 p^2 [Q_\xi + C_A R_\xi + \frac{1}{2} C_A W_\xi] \right] \\ C &= -\frac{V}{[(p^2)^2 + C_A \gamma^4]}, \quad D_\xi = -\frac{Q_\xi}{(p^2)^2}, \quad J_\xi = -\frac{W_\xi}{(p^2)^2}, \quad L_\xi = -\frac{S_\xi}{(p^2)^2} \\ K_\xi &= \frac{1}{[(p^2)^2 + C_A \gamma^4]^2} \left[\gamma^4 X + 2i \gamma^2 p^2 U - (p^2)^2 R_\xi + \gamma^4 [Q_\xi + \frac{1}{2} C_A W_\xi] \right] \\ &\quad + \frac{\gamma^4 [Q_\xi + \frac{1}{2} C_A W_\xi]}{(p^2)^2 [(p^2)^2 + C_A \gamma^4]} \\ E &= 0, \quad F = 0, \quad G = \frac{i \gamma^2 V}{p^2 [(p^2)^2 + C_A \gamma^4]}, \quad H = 0 \\ D_\rho &= -\frac{Q_\rho}{(p^2)^2}, \quad J_\rho = -\frac{W_\rho}{(p^2)^2}, \quad K_\rho = -\frac{R_\rho}{(p^2)^2}, \quad L_\rho = -\frac{S_\rho}{(p^2)^2} \end{aligned} \quad (3.6)$$

to one loop. For the longitudinal sector, we retain for the moment the non-zero α and find formally,

$$\begin{aligned} A^L &= -\frac{\alpha^2}{[(p^2)^2 + \alpha C_A \gamma^4]^2} \left[(p^2)^2 X^L - 2i C_A \gamma^2 p^2 U^L - C_A \gamma^4 [Q_\xi^L + C_A R_\xi^L + \frac{1}{2} C_A W_\xi^L] \right] \\ B^L &= \frac{\alpha}{[(p^2)^2 + \alpha C_A \gamma^4]^2} \left[i \alpha \gamma^2 p^2 X^L - [(p^2)^2 - \alpha C_A \gamma^4] U^L + i \gamma^2 p^2 [Q_\xi^L + C_A R_\xi^L + \frac{1}{2} C_A W_\xi^L] \right] \\ C^L &= -\frac{\alpha V^L}{[(p^2)^2 + \alpha C_A \gamma^4]}, \quad D_\xi^L = -\frac{Q_\xi^L}{(p^2)^2}, \quad J_\xi^L = -\frac{W_\xi^L}{(p^2)^2}, \quad L_\xi^L = -\frac{S_\xi^L}{(p^2)^2} \\ K_\xi^L &= \frac{\alpha}{[(p^2)^2 + \alpha C_A \gamma^4]^2} \left[\alpha \gamma^4 X^L + 2i \gamma^2 p^2 U^L - \frac{(p^2)^2}{\alpha} R_\xi^L + \gamma^4 [Q_\xi^L + \frac{1}{2} C_A W_\xi^L] \right] \\ &\quad + \frac{\alpha \gamma^4 [Q_\xi^L + \frac{1}{2} C_A W_\xi^L]}{(p^2)^2 [(p^2)^2 + \alpha C_A \gamma^4]} \\ E^L &= 0, \quad F^L = 0, \quad G^L = \frac{i \alpha \gamma^2 V^L}{p^2 [(p^2)^2 + \alpha C_A \gamma^4]}, \quad H^L = 0 \end{aligned}$$

$$D_\rho^L = -\frac{Q_\rho^L}{(p^2)^2}, \quad J_\rho^L = -\frac{W_\rho^L}{(p^2)^2}, \quad K_\rho^L = -\frac{R_\rho^L}{(p^2)^2}, \quad L_\rho^L = -\frac{S_\rho^L}{(p^2)^2} \quad (3.7)$$

to one loop too. We note that the exact one loop expressions for each of these 2-point functions are recorded in appendices B and C. Whilst these represent our arbitrary α manipulations, we must restrict α to the Landau gauge for the propagators corrections to have any meaning in the Gribov-Zwanziger context. Since the one loop corrections are non-singular in α then taking $\alpha \rightarrow 0$ for the longitudinal sector we find

$$\begin{aligned} A^L &= B^L = C^L = E^L = F^L = G^L = H^L = 0 \\ D_\xi^L &= -\frac{Q_\xi^L}{(p^2)^2}, \quad J_\xi^L = -\frac{W_\xi^L}{(p^2)^2}, \quad K_\xi^L = -\frac{R_\xi^L}{(p^2)^2}, \quad L_\xi^L = -\frac{S_\xi^L}{(p^2)^2} \\ D_\rho^L &= -\frac{Q_\rho^L}{(p^2)^2}, \quad J_\rho^L = -\frac{W_\rho^L}{(p^2)^2}, \quad K_\rho^L = -\frac{R_\rho^L}{(p^2)^2}, \quad L_\rho^L = -\frac{S_\rho^L}{(p^2)^2}. \end{aligned} \quad (3.8)$$

Using the explicit values from appendices B and C one can in principle deduce the formal expressions for the one loop corrections to the propagators. For instance, given that $A^L = 0$ when $\alpha = 0$ then the one loop correction to the gluon propagator is actually transverse as is the mixed gluon ξ_μ^{ab} propagator. Given the structures of D_ξ^{Labcd} and D_ρ^{Labcd} then both the ξ_μ^{ab} and ρ_μ^{ab} propagator corrections are not transverse like (2.21).

For the remaining fields c^a and ω_μ^a , if we write the ghost form factors as

$$\langle c^a(p)\bar{c}^b(-p) \rangle = \frac{D_c(p^2)}{p^2}\delta^{ab}, \quad \langle \omega_\mu^{ab}(p)\bar{\omega}_\nu^{cd}(-p) \rangle = \delta^{ac}\delta^{bd}\frac{D_\omega(p^2)}{p^2}\eta_{\mu\nu} \quad (3.9)$$

then

$$\begin{aligned} D_c(p^2) = D_\omega(p^2) &= \left[-1 + \left[\frac{5}{4} - \frac{3}{8} \ln\left(\frac{C_A\gamma^4}{\mu^4}\right) + \frac{3\sqrt{C_A}\gamma^2}{4p^2} \tan^{-1}\left[\frac{\sqrt{C_A}\gamma^2}{p^2}\right] \right. \right. \\ &\quad - \frac{3\pi\sqrt{C_A}\gamma^2}{8p^2} + \frac{C_A\gamma^4}{8(p^2)^2} \ln\left[1 + \frac{(p^2)^2}{C_A\gamma^4}\right] - \frac{3}{8} \ln\left[1 + \frac{(p^2)^2}{C_A\gamma^4}\right] \\ &\quad \left. \left. - \frac{p^2}{4\sqrt{C_A}\gamma^2} \tan^{-1}\left[\frac{\sqrt{C_A}\gamma^2}{p^2}\right] \right] C_A a \right]^{-1} + O(a^2). \end{aligned} \quad (3.10)$$

Using the one loop Gribov gap equation, [10], then $D_c^{-1}(p^2)$ is $O((p^2)^2)$ as $p^2 \rightarrow 0$ and hence both propagators enhance. Likewise the ρ_μ^{ab} propagator enhances whilst one colour component of the ξ_μ^{ab} propagator also suggests there will be some sort of enhancement for that field too, [33]. We will return to this latter point in more detail in section 6.

Equipped with these 2-point functions and the formal expressions for the one loop corrections to the $\{A_\mu^a, \xi_\mu^{ab}, \rho_\mu^{ab}\}$ matrix of propagators we can study the effective renormalization group invariant coupling constant. The behaviour of this effective coupling constant in the zero momentum limit has been the subject of debate over the years and whether it freezes to a finite non-zero or zero value is still unresolved. Defining the gluon propagator form factor as

$$\langle A_\mu^a(p)A_\nu^b(-p) \rangle = -\delta^{ab}\frac{D_A(p^2)}{p^2}P_{\mu\nu}(p) \quad (3.11)$$

then the effective coupling constant is defined by

$$\alpha^{\text{eff}}(p^2) = \alpha_s(\mu)D_A(p^2)\left(D_c(p^2)\right)^2 \quad (3.12)$$

where we have introduced the more common strong coupling constant $\alpha_s = g^2/(4\pi)$. Using the zero momentum values for the 2-point functions recorded in appendix B we have

$$\alpha_s^{\text{eff}}(0) = \lim_{p^2 \rightarrow 0} \left[\frac{\alpha(\mu) \left[1 + C_A \left(\frac{3}{8} \ln \left(\frac{C_A \gamma^4(\mu)}{\mu^4} \right) - \frac{9}{16} \right) a(\mu) \right] (p^2)^2}{C_A \gamma^4(\mu) \left[1 + C_A \left(\frac{3}{8} \ln \left(\frac{C_A \gamma^4(\mu)}{\mu^4} \right) - \frac{5}{8} + \frac{\pi p^2}{8\sqrt{C_A} \gamma^2(\mu)} \right) a(\mu) \right]^2} \right]. \quad (3.13)$$

Hence, evaluating this we find

$$\alpha_s^{\text{eff}}(0) = \frac{16}{\pi C_A} \quad (3.14)$$

which is different to that of [33] since the effect of the omitted propagator has been correctly included. Numerically for $SU(3)$ we have $\alpha_s^{\text{eff}}(0) = 1.698$ which is 4% lower than the value quoted in [33].

4 Static potential.

We now return to the problem of computing the static potential. Given the reformulation of the basic QCD Lagrangian, (2.5), to incorporate the Gribov problem in terms of additional fields ρ_μ^{ab} , ξ_μ^{ab} , ω_μ^{ab} and $\bar{\omega}_\mu^{ab}$, it is important to stress that these localizing fields are regarded as *internal* and do not couple to the static potential source (2.7) of (2.4). Ultimately one begins with a Lagrangian, (2.19), involving a gluon and it is this quantum which is confined. Thus the Feynman rules for the source coupling are the same as those for the usual perturbative case. The main difference is that one uses the Feynman rules for the Gribov-Zwanziger Lagrangian, (2.19). The latter is not a trivial point if one considers the Feynman diagrams contributing to the static potential. Concentrating, for the moment, on the single particle exchange graphs, the leading graph is illustrated in Figure 1 where the sources are represented by the thick vertical lines and the gluon by the spring. However, at the next order there are corrections to the exchanged particle and due to the mixing in the $\{A_\mu^a, \xi_\mu^{ab}\}$ sector, there are extra graphs aside from the gluon self-energy corrections. These are illustrated in Figure 2 where the central blob denotes all possible one particle irreducible one loop corrections. The split propagators involving gluons and ξ_μ^{ab} , denoted by the double line, are the $A_\mu^a \xi_\nu^{bc}$ propagators. One key point is that as there is no direct coupling of either bosonic localizing ghost to a source then there is no single exchange of this field akin to the diagram of Figure 1. Whilst the exact one loop corrections to all the 2-point functions, which lead to the propagator corrections, are known explicitly, we still have to assemble all the pieces for the full static potential. For instance, in addition to the graphs of Figures 1 and 2, there are source gluon vertex corrections as well as double gluon exchange boxes at one loop.

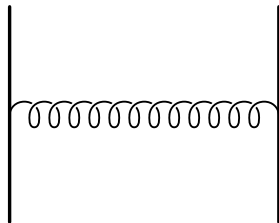


Figure 1: Tree contribution to static potential.

Our calculation proceeds in general terms along the same lines as the earlier work of [39, 40, 41, 42]. The main difference is that Feynman integrals with source propagators as well as

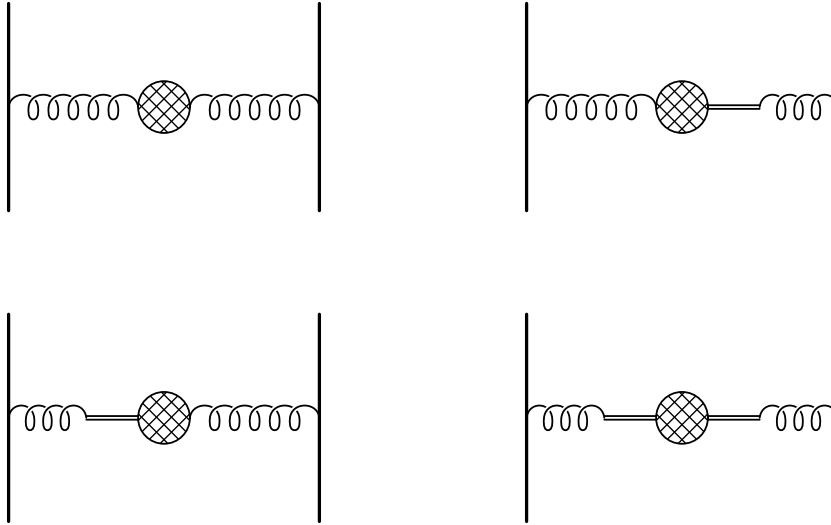


Figure 2: Self-energy corrections to single gluon exchange graph.

Gribov type propagators, as opposed to massless ones, have to be handled for non-single exchange Feynman graphs. For those where either the source propagator or vertex is corrected one has the potential problem of infrared divergences occurring. In the perturbative case the momentum space resolution of this was given in, for example, [39, 40, 41]. Briefly with massless propagators and a source propagator, $1/(kv)$, an infrared divergence arises at the vertex correction but this cancels the double gluon exchange infrared divergence. However, this statement needs to be qualified since in dimensional regularization, which we use here, the regularizing parameter ϵ , where $d = 4 - 2\epsilon$, cannot distinguish between infrared or ultraviolet infinities. Indeed in the original one loop Feynman gauge calculation of [37] they actually cancel in the one loop correction to each of the vertices of Figure 1. For other linear covariant gauges the infrared infinities cancel in the combination of double gluon exchange and source vertex corrections. In [41] this infrared problem was discussed in detail where a fictitious infrared regularizing mass was introduced to explicitly isolate the infrared divergences. They were then shown to cancel for an arbitrary linear covariant gauge. Indeed it was argued that at one loop these infrared divergences are expected to cancel since the full Wilson loop graph that the infrared divergent graphs each actually originate from, is the same diagram before it is cut open for the static limit. As that original Wilson loop topology is infrared safe the infrared cancellation could be regarded as a consistency check and the intermediate regularizing fictitious mass safely removed. In the Gribov case the presence of a natural mass arising from the Gribov parameter in the gluon propagators serves to act as a non-fictitious infrared regularization. Therefore, one can trace the infrared infinity naturally and verify its explicit cancellation.

Having discussed this technical issue then all that remains is to describe the calculational set-up. The Feynman diagrams contributing to the one loop static potential are generated using the QGRAF package, [59]. In total there are 1 tree graph and 31 one loop graphs which is more than the non-Gribov case due to the extra fields and mixed propagators. This latter total is broken down into one snail graph correcting the Gribov parameter of Figure 1, 18 single exchange graphs, 10 source vertex corrections and 2 double (gluon) exchange graphs. The topologies which are additional to those of Figures 1 and 2 are provided in Figure 3. All the graphs in QGRAF notation are then converted into FORM notation in order to harness the power necessary to handle all the resulting intermediate algebra. This conversion adds all the colour

and Lorentz indices to the fields. The Feynman rules are automatically inserted to produce the set of Feynman integrals which need to be evaluated explicitly. For the single particle exchange diagrams this amounts to applying the basic integrals which were already treated in [33] where the exact one loop corrections to all the 2-point functions in the theory were given.

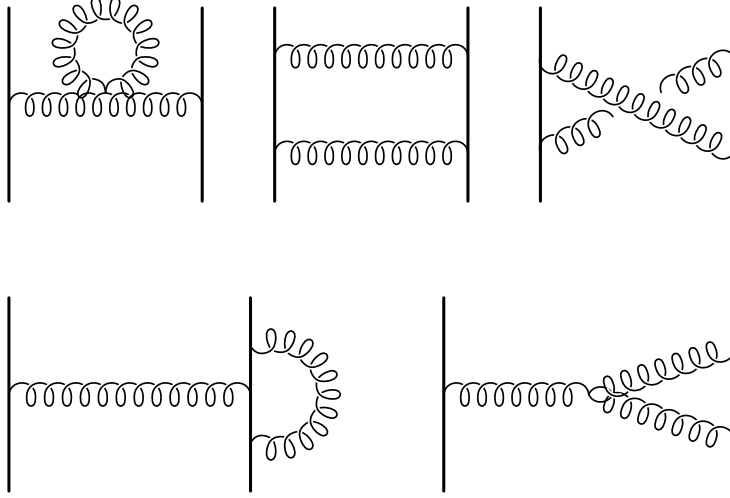


Figure 3: Additional one loop topologies for static potential.

The final part is to handle the remaining box and source vertex corrections which will involve source propagators. Therefore, we define the general scalar master integral

$$I_1(\alpha, \beta, \lambda, m_1^2, m_2^2, p, v) = \int \frac{d^d k}{(2\pi)^d} \frac{1}{[k^2 + m_1^2]^\alpha [(k-p)^2 + m_2^2]^\beta (kv)^\lambda} \quad (4.1)$$

for arbitrary masses m_1 and m_2 where p_μ is the external or exchange momentum and will satisfy $pv = 0$, with $v^2 = 1$, in the static limit throughout. Such integrals emerge after repeated substitution of the elementary relations

$$kp = \frac{1}{2} [k^2 + p^2 - (k-p)^2] \quad (4.2)$$

and

$$\frac{1}{[(k^2)^2 + C_A \gamma^4]} = \frac{1}{2i\sqrt{C_A} \gamma^2} \left[\frac{1}{[k^2 - i\sqrt{C_A} \gamma^2]} - \frac{1}{[k^2 + i\sqrt{C_A} \gamma^2]} \right]. \quad (4.3)$$

Although (4.1) has been given in [41], for completeness we give several intermediate results we used, in our notation. Using integration by parts it is possible to write a recurrence relation for (4.1) as

$$\begin{aligned} \lambda I_1(\alpha, \beta, \lambda + 1, m_1^2, m_2^2, p, v) &= -2\alpha I_1(\alpha + 1, \beta, \lambda - 1, m_1^2, m_2^2, p, v) \\ &\quad - 2\beta I_1(\alpha, \beta + 1, \lambda - 1, m_1^2, m_2^2, p, v) \end{aligned} \quad (4.4)$$

for $\lambda \geq 2$, which allows one to reduce integrals with two source propagators to a standard source free integral which has already been considered in the Gribov case in [33]. For an odd number of source propagators, this reduction will eventually lead to one source propagator but it can be treated using elementary contour integration in the time integral. So, for instance, we have, [41],

$$I_1(1, 1, 1, m_1^2, m_2^2, p, v) = -\frac{i}{2} \int \frac{d^{d-1} \mathbf{k}}{(2\pi)^{d-1}} \frac{1}{[k^2 + m_1^2][(\mathbf{k} - \mathbf{p})^2 + m_2^2]}. \quad (4.5)$$

In other words in this case the treatment of the source propagator reduces the dimensionality of the original integral by one. Finally, any remaining source propagator free integral with propagator powers greater than unity can be reduced by standard integration by parts identities. One final aspect of the automatic calculation concerns the internal renormalization of the parameters and sources. We follow the standard procedure of [60] for this and compute the static potential initially as a function of bare parameters. The renormalized variables, and hence the underlying counterterms, are introduced by replacing the bare parameters by the renormalized ones with the explicit Landau gauge renormalization constants included. This also includes the renormalization associated with the source itself and that renormalization constant is derived in the same way as discussed in [37] but for the Landau gauge. For completeness, we note that the relevant $\overline{\text{MS}}$ Landau gauge renormalization constants, in our conventions, are

$$\begin{aligned}
Z_A &= 1 + \left[\frac{13}{6}C_A - \frac{4}{3}T_F N_f \right] \frac{a}{\epsilon} + O(a^2) \\
Z_g &= 1 + \left[\frac{2}{3}T_F N_f - \frac{11}{6}C_A \right] \frac{a}{\epsilon} + O(a^2) \\
Z_\gamma &= 1 + \left[\frac{1}{3}T_F N_f - \frac{35}{48}C_A \right] \frac{a}{\epsilon} + O(a^2) \\
Z_J &= 1 + O(a^2)
\end{aligned} \tag{4.6}$$

where $J_O^{a\mu} = \sqrt{Z_J} J^{a\mu}$ relates the bare and renormalized sources. Obviously a non-trivial check on the renormalization procedure and the implementation of the explicit values for the master Feynman integrals is that the ultimate static potential is finite and no poles in ϵ remain when all the contributing diagrams are assembled. We note now that this is indeed the case.

Having described the underlying tools for our calculation we now record that the one loop static potential for the Gribov-Zwanziger Lagrangian in the Landau gauge is

$$\begin{aligned}
\tilde{V}(\mathbf{p}) &= - \frac{C_F \mathbf{p}^2 g^2}{[(\mathbf{p}^2)^2 + C_A \gamma^4]} \\
&+ \left[\frac{\pi \sqrt{C_A}}{768 \gamma^2} - \frac{1}{768 \gamma^4} \tan^{-1} \left[- \frac{\sqrt{4C_A \gamma^4 - (\mathbf{p}^2)^2}}{\mathbf{p}^2} \right] \right] \sqrt{4C_A \gamma^4 - (\mathbf{p}^2)^2} \\
&+ \frac{\sqrt{2}}{\gamma^2} \left[\frac{\sqrt{C_A}}{768} \eta_1(\mathbf{p}^2) - \frac{\sqrt{C_A}}{192 \sqrt{2}} \tan^{-1} \left[\frac{\sqrt{C_A} \gamma^2}{\mathbf{p}^2} \right] \right] + \frac{231 \pi C_A^{3/2} \gamma^2}{128 [(\mathbf{p}^2)^2 + C_A \gamma^4]} \\
&+ \frac{\sqrt{2} C_A \gamma^2}{[(\mathbf{p}^2)^2 + C_A \gamma^4]} \left[\frac{13 \sqrt{C_A}}{24 \sqrt{2}} \tan^{-1} \left[\frac{\sqrt{C_A} \gamma^2}{\mathbf{p}^2} \right] + \frac{79 \sqrt{C_A}}{128} \eta_1(\mathbf{p}^2) \right] \\
&+ \frac{2 \pi C_A^{3/2} \gamma^2}{[(\mathbf{p}^2)^2 - 4 C_A \gamma^4]} - \frac{1201 \pi C_A^{5/2} \gamma^6}{768 [(\mathbf{p}^2)^2 + C_A \gamma^4]^2} + \frac{\sqrt{2} C_A^{3/2} \gamma^2}{[(\mathbf{p}^2)^2 + 16 C_A \gamma^4]} \eta_1(\mathbf{p}^2) \\
&- \frac{685 C_A^2 \gamma^4}{768 [(\mathbf{p}^2)^2 + C_A \gamma^4]^2} \tan^{-1} \left[- \frac{\sqrt{4C_A \gamma^4 - (\mathbf{p}^2)^2}}{\mathbf{p}^2} \right] \sqrt{4C_A \gamma^4 - (\mathbf{p}^2)^2} \\
&- \frac{395 \sqrt{2} C_A^{5/2} \gamma^6 \eta_1(\mathbf{p}^2)}{768 [(\mathbf{p}^2)^2 + C_A \gamma^4]^2} + \frac{C_A}{\mathbf{p}^2} \left[\frac{13}{96} \ln \left[1 + \frac{(\mathbf{p}^2)^2}{C_A \gamma^4} \right] - \frac{1}{192} \right] \\
&+ \frac{455 C_A}{384 [(\mathbf{p}^2)^2 + C_A \gamma^4]} \tan^{-1} \left[- \frac{\sqrt{4C_A \gamma^4 - (\mathbf{p}^2)^2}}{\mathbf{p}^2} \right] \sqrt{4C_A \gamma^4 - (\mathbf{p}^2)^2} \\
&+ \frac{\pi C_A^{3/2} \gamma^2}{384 (\mathbf{p}^2)^2} - \frac{C_A^{3/2} \gamma^2}{192 (\mathbf{p}^2)^2} \tan^{-1} \left[\frac{\sqrt{C_A} \gamma^2}{\mathbf{p}^2} \right]
\end{aligned}$$

$$\begin{aligned}
& - \frac{C_A}{[(\mathbf{p}^2)^2 - 4C_A\gamma^4]} \tan^{-1} \left[\frac{\sqrt{4C_A\gamma^4 - (\mathbf{p}^2)^2}}{\mathbf{p}^2} \right] \sqrt{4C_A\gamma^4 - (\mathbf{p}^2)^2} \\
& + \frac{C_A T_F N_f \gamma^4 \mathbf{p}^2}{[(\mathbf{p}^2)^2 + C_A\gamma^4]^2} \left[\frac{4}{3} \ln \left[\frac{\mathbf{p}^2}{\mu^2} \right] - \frac{20}{9} \right] - \frac{T_F N_f \mathbf{p}^2}{[(\mathbf{p}^2)^2 + C_A\gamma^4]} \left[\frac{4}{3} \ln \left[\frac{\mathbf{p}^2}{\mu^2} \right] - \frac{20}{9} \right] \\
& + \frac{C_A^2 \gamma^4 \mathbf{p}^2}{[(\mathbf{p}^2)^2 + C_A\gamma^4]^2} \left[\frac{365}{72} - \frac{251}{192} \ln \left[\frac{C_A\gamma^4}{\mu^4} \right] - \frac{895\sqrt{2}}{3072} \eta_2(\mathbf{p}^2) - \frac{29}{96} \ln \left[\frac{\mathbf{p}^2}{\mu^2} \right] \right] \\
& + \frac{C_A \mathbf{p}^2}{[(\mathbf{p}^2)^2 + C_A\gamma^4]} \left[\frac{125}{64} \ln \left[\frac{C_A\gamma^4}{\mu^4} \right] - \frac{13}{48} \ln \left[\frac{[C_A\gamma^4 + (\mathbf{p}^2)^2]}{\mu^4} \right] - \frac{31}{9} \right. \\
& \quad \left. + \frac{167\sqrt{2}}{1536} \eta_2(\mathbf{p}^2) + \frac{29}{96} \ln \left[\frac{\mathbf{p}^2}{\mu^2} \right] \right] \\
& + \frac{\sqrt{2} C_A \mathbf{p}^2}{4[(\mathbf{p}^2)^2 + 16C_A\gamma^4]} \eta_2(\mathbf{p}^2) + \frac{\sqrt{2} \mathbf{p}^2}{3072\gamma^4} \eta_2(\mathbf{p}^2) \left] \frac{C_F g^4}{16\pi^2} + O(g^6) \tag{4.7}
\end{aligned}$$

where we use the notation that in four dimensions $p_\mu = (p_0, \mathbf{p})$ and we have introduced the intermediate functions $\eta_1(\mathbf{p}^2)$ and $\eta_2(\mathbf{p}^2)$ for compactness where

$$\begin{aligned}
\eta_1(\mathbf{p}^2) &= - \ln \left[1 + \sqrt{1 + \frac{16C_A\gamma^4}{(\mathbf{p}^2)^2}} \right] \sqrt{-1 + \sqrt{1 + \frac{16C_A\gamma^4}{(\mathbf{p}^2)^2}}} \\
& + \ln \left[\frac{16C_A\gamma^4}{(\mathbf{p}^2)^2} \right] \sqrt{-1 + \sqrt{1 + \frac{16C_A\gamma^4}{(\mathbf{p}^2)^2}}} \\
& - 2 \ln \left[\sqrt{1 + \sqrt{1 + \frac{16C_A\gamma^4}{(\mathbf{p}^2)^2}}} - \sqrt{2} \right] \sqrt{-1 + \sqrt{1 + \frac{16C_A\gamma^4}{(\mathbf{p}^2)^2}}} \\
& - 2 \tan^{-1} \left[\frac{\sqrt{2}}{\sqrt{-1 + \sqrt{1 + \frac{16C_A\gamma^4}{(\mathbf{p}^2)^2}}}} \right] \sqrt{1 + \sqrt{1 + \frac{16C_A\gamma^4}{(\mathbf{p}^2)^2}}} \tag{4.8}
\end{aligned}$$

and

$$\begin{aligned}
\eta_2(\mathbf{p}^2) &= \ln \left[\frac{16C_A\gamma^4}{(\mathbf{p}^2)^2} \right] \sqrt{1 + \sqrt{1 + \frac{16C_A\gamma^4}{(\mathbf{p}^2)^2}}} - \ln \left[1 + \sqrt{1 + \frac{16C_A\gamma^4}{(\mathbf{p}^2)^2}} \right] \sqrt{1 + \sqrt{1 + \frac{16C_A\gamma^4}{(\mathbf{p}^2)^2}}} \\
& - 2 \ln \left[\sqrt{1 + \sqrt{1 + \frac{16C_A\gamma^4}{(\mathbf{p}^2)^2}}} - \sqrt{2} \right] \sqrt{1 + \sqrt{1 + \frac{16C_A\gamma^4}{(\mathbf{p}^2)^2}}} \\
& + 2 \tan^{-1} \left[\frac{\sqrt{2}}{\sqrt{-1 + \sqrt{1 + \frac{16C_A\gamma^4}{(\mathbf{p}^2)^2}}}} \right] \sqrt{-1 + \sqrt{1 + \frac{16C_A\gamma^4}{(\mathbf{p}^2)^2}}}. \tag{4.9}
\end{aligned}$$

There is one main check on this result aside from the finiteness one above. This is that we recover the usual perturbative result in the $\gamma^2 \rightarrow 0$ limit. In other words we find

$$\begin{aligned}
\lim_{\gamma \rightarrow 0} \tilde{V}(\mathbf{p}) &= - \frac{4\pi C_F \alpha_s(\mu)}{\mathbf{p}^2} \left[1 + \left[\left[\frac{31}{9} - \frac{11}{3} \ln \left[\frac{\mathbf{p}^2}{\mu^2} \right] \right] C_A + \left[\frac{4}{3} \ln \left[\frac{\mathbf{p}^2}{\mu^2} \right] - \frac{20}{9} \right] T_F N_f \right] a \right. \\
& \quad \left. + O(a^2) \right] \tag{4.10}
\end{aligned}$$

where we note that (4.10) agrees exactly with the earlier result of [36, 37, 38]. Whilst that was originally computed for the Feynman gauge taking the limit where the Gribov mass is removed recovers the perturbative result in the Landau gauge and its agreement with a gauge independent result is another non-trivial check on our computational set-up.

We can now examine (4.7) in the zero momentum limit by expanding the exact result in powers of \mathbf{p}^2 and find

$$\tilde{V}(\mathbf{p}) = -\frac{C_F \mathbf{p}^2 g^2}{C_A \gamma^4} - C_F \left[\frac{\pi \sqrt{C_A}}{32 \gamma^2} + \left(\frac{13}{72} - \frac{3}{8} \ln \left(\frac{C_A \gamma^4}{\mu^4} \right) \right) \frac{\mathbf{p}^2}{\gamma^4} \right] \frac{g^4}{16 \pi^2} + O((\mathbf{p}^2)^2; g^6) \quad (4.11)$$

where the order symbols denote the higher order terms in the momentum expansion and two loop corrections separately. Thus (4.11) would imply that

$$\tilde{V}(0) = -\frac{C_F \sqrt{C_A} g^4}{512 \pi \gamma^2} + O(g^6) \quad (4.12)$$

as a first approximation with no emergence of a dipole. To try and understand the implications of this freezing for the one loop coordinate space potential we first consider the leading term of (4.11). For $\gamma = 0$ the exchange of Figure 1 leads to the usual Coulomb potential but for non-zero γ it is not clear what the $p^2 \rightarrow 0$ limit of the leading term of (4.11) implies for the corresponding $r \rightarrow \infty$ limit. If we write

$$\tilde{V}(\mathbf{p}) = \sum_{n=0}^{\infty} \tilde{V}_n(\mathbf{p}) \quad (4.13)$$

where the subscript n labels the *loop* order, then the first term of (4.7) gives

$$\tilde{V}_0(\mathbf{p}) = -\frac{C_F \mathbf{p}^2 g^2}{[(\mathbf{p}^2)^2 + C_A \gamma^4]} \quad (4.14)$$

whence the Fourier transform, (2.8), leads to

$$V_0(r) = -\frac{C_F g^2}{4 \pi r} \exp \left[-\frac{C_A^{\frac{1}{4}} \gamma r}{\sqrt{2}} \right] \cos \left(\frac{C_A^{\frac{1}{4}} \gamma r}{\sqrt{2}} \right). \quad (4.15)$$

The presence of the exponential factor is not unexpected since it is reminiscent of the Yukawa potential for a massive field. However, the Gribov situation effectively corresponds to a width which is reflected in the trigonometric factor. Now examining the limit corresponding to $p^2 \rightarrow 0$, which is $r \rightarrow \infty$ for *real* r , we see that $V_0(r) \rightarrow 0$. This is consistent on dimensional grounds with naively taking the Fourier transform of the leading term of (4.11). As an aside we remark that similar potentials of this Friedel form have recently emerged in leading order in models of plasmas and stellar nuclear reactions, [61, 62, 63, 64, 65]. Briefly the underlying theory is based on a Higgs-like effective Lagrangian. By considering perturbations about a background then the gauge field fluctuations develop a Gribov type propagator. One claim is that a linearly rising potential will emerge in a particular limit if the effective Higgs mass term has the wrong sign.

Turning to the one loop correction we do not have the luxury of being able to take the full Fourier transform of (4.7) analytically. However, by the same heuristic argument as leading order, the freezing to a finite value, (4.12), leads to a similar large distance limit for our potential. In other words $V(r) \rightarrow 0$ at one loop and there is no linear growth. However, on dimensional grounds such a term will clearly not be Coulombic in this limit. A $1/\mathbf{p}^2$ term would be required for that in the zero momentum limit. Indeed given this the next step would be to try and

understand how the Lüscher term, [66], emerges in the Gribov-Zwanziger formalism as $r \rightarrow \infty$. Within the present context it is not clear how such a term could appear. For instance, aside from the fact that the analysis of [66] producing this term was based on chromoelectric flux tubes, the coefficient of the Lüscher term is universal and independent of the coupling constant. One prospective way this could happen is that the coefficient of a $1/\mathbf{p}^2$ term, when it arises, is fixed by the gap equation satisfied by γ with or without some renormalization group running of parameters to some non-perturbative fixed point. Moreover, the Lüscher term appears together with a linearly rising potential term, [66], which would originate in momentum space from a dipole. However, a dipole behaviour in the zero momentum limit is clearly not evident in (4.7). Although we have not taken the complete Fourier transform of (4.7), we have examined it in detail for a confining behaviour to understand why a dipole is absent and there are some promising features.

Clearly in (4.7) there is an explicit $1/(\mathbf{p}^2)^2$ term which gives a stronger singularity than that of the usual Coulomb case. Indeed concentrating on this term for the moment and setting

$$A_l = \frac{C_F C_A^{3/2} \gamma^2 g^4}{6144\pi} \quad (4.16)$$

in (2.10) we would have

$$V_l(r) = - \frac{C_F C_A^{3/2} \gamma^2 g^4}{49152\pi^2} r \quad (4.17)$$

which would actually be a linearly *decreasing* potential. Ignoring this point for the moment, there is, however, another dipole singularity in (4.7) and this occurs in such a way that there is no overall singularity as $p^2 \rightarrow 0$. The specific term is

$$- \frac{C_F C_A^{3/2} \gamma^2 g^4}{3072\pi^2 (\mathbf{p}^2)^2} \tan^{-1} \left[\frac{\sqrt{C_A} \gamma^2}{\mathbf{p}^2} \right] \quad (4.18)$$

and in the zero momentum limit the inverse tan function tends to $\pi/2$ to cancel the previous pure dipole we considered. Thus, a linearly rising potential will not emerge. Actually for (4.18) it is in fact possible to take the Fourier transform (2.8) and verify that the overall absolute asymptotic behaviour as $r \rightarrow 0$ is linear and precisely cancels that from the pure dipole term Fourier transform. However, we recall what was noted in [33] concerning the overall sign of γ^2 . In studying the zero momentum limits of (4.16) and (4.18) we have tacitly assumed that γ^2 is positive. The sign of γ^2 , though, is not predetermined in (2.19). It can only strictly be determined in relation to other evidence. Indeed it was suggested in [33] that for consistency with other results, such as the power correction structure of the strong coupling constant in the next to high energy limit, that γ^2 was negative and our sign convention needed to be modified by mapping $\gamma^2 \rightarrow -\gamma^2$ in situations where results depended explicitly on γ^2 . It is worth noting that this is not cause for alarm since a similar situation always occurs with the choice of the sign of the coupling constant, g , in the covariant derivative. Its sign cannot be determined since in any computations it appears in the combination g^2 . In other words the choice of sign of g is a convention as is that of γ^2 with the difference being here that one can actually make contact with other methods, such as the strong coupling constant power corrections, to determine it, [33]. In our current set-up we had not made any a priori choice of sign and so there is a degree of freedom to make a specific choice. Therefore, if we return to (4.16) and (4.18), then since the former is an odd function and the latter is an even function of γ^2 , flipping the sign of γ^2 would mean that in fact the terms add and there is a net dipole. This would lead to a linearly *rising* potential. Although this is encouraging and would very much be consistent with the expectation that the Gribov-Zwanziger Lagrangian describes a confined gluon since, for instance, it satisfies

the Kugo-Ojima criterion, [34, 35], it would on the other hand destroy gluon suppression, [16]. This can be seen if one examines the explicit one loop corrections to the gluon propagator given in appendix B. More specifically examining the relevant pieces there, the net dipole arises purely from the ξ_μ^{ab} 2-point function corrections in the one loop gluon propagator. Indeed this would be consistent with the Zwanziger localizing fields dominating the infrared as one moves towards the Gribov horizon. If such a scenario is to be credible, however, one needs to check that at next loop order a triple pole in \mathbf{p}^2 does not arise in the static potential. Such a term is possible on dimensional grounds, for instance. We stress, though, at this point that these are merely interim speculative remarks on the consequences of the sign choice of γ^2 , which would require deeper consideration, and we will omit reference to this point hereafter.

Therefore, returning to our original γ^2 convention this dipole cancellation is not unexpected. Indeed if one examines the explicit exact one loop corrections to each of the transverse parts of the 2-point functions in the $\{A_\mu^a, \xi_\mu^{ab}, \rho_\mu^{ab}\}$ sector, this dipole structure is present in each case in individual terms but with no net dipole. Thus the apparent dipole behaviour is not truly present overall. However, on more general terms this lack of a linearly rising potential should not emerge in the present set-up. Although we have followed an inherently perturbative approach the main lesson from Gribov's original article, which also underlies Zwanziger's construction, is that infrared properties emerge when the gap equation is realised. Then one is dealing with a gauge theory. For example, the gap equation leads to Faddeev-Popov ghost enhancement and more recently produced a qualitative non-zero value of a renormalization group invariant coupling constant in the zero momentum limit, (3.14). However, at no point have we implemented the gap equation within our static potential. (The simple replacement of γ by a non-perturbative function of a is not what we mean by this here.) Somehow, one would expect that a linearly rising potential can only emerge when the gap equation is used *explicitly*. In a later section we will present some considerations towards this point in the context of the static potential considered here. Though, recalling an earlier remark, at higher loop orders there would appear to be nothing in principle preventing pure terms such as $1/(\mathbf{p}^2)^3$ and higher emerging on dimensional grounds. These would have to have a compensating piece to exclude power terms in r remaining in the coordinate space potential. Of course such terms would be irrelevant if the sign associated with it indicated a decreasing contribution to the potential in contrast to an increasing part. Alternatively such terms might resum in such a way that there is matching to a linear type potential. One final point concerning the linear term relates to the soft BRST breaking of (2.19) arising from the γ^2 term, [12, 13, 18, 30]. There is an understanding that for gauge independent quantities results should depend on γ^4 and not on γ^2 . However, on dimensional grounds a linear term in a potential must be accompanied by a factor of γ^2 and therefore it seems impossible to avoid having a γ^2 dependence in the ultimate static potential which is derived from the underlying gauge independent Wilson loop. Though, of course, any such scale can eventually in principle be related back to $\Lambda_{\overline{\text{MS}}}$.

Next we make some specific remarks concerning (4.7). Given that the gluon is now not a massless entity in (2.19), we note that (4.7) has a pole and physical cut at $p^2 = 2\sqrt{C_A}\gamma^2$. This is a threshold type feature due to massless fields with a non-zero width. The associated denominator factor in the term with this cut arises from the Gram determinant of the integration by parts reduction formula for the one loop Feynman integrals without source propagators. In [13], the glueball correlation function was analysed as a spectral density function and it was argued that there was a bound state of the same mass squared value, $2\sqrt{C_A}\gamma^2$, and it was identified as a potential glueball state. It is amusing that there is a threshold effect at the *same* mass value in the static potential which is in some sense a scattering amplitude. It is not clear, though, if this corresponds to a *stable* bound state. However, it is worth recalling the computation of [67] where the glueball spectrum was determined by including a massive gluon in

the evaluation of the leading order gluon scattering amplitude. This was then used to construct a potential within which bound states could be formed. However, the scattering amplitude with the massive gluons did not contain an explicit confining potential but this was added by hand prior to solving for the spectrum. Though strictly speaking the additional confining piece not only incorporated a linear rising part but also modelled string breaking. This final form of the potential energy appears to have endowed a stability on the glueball states. Therefore, it does not seem unreasonable to expect that bound state stability requires an explicit dipole term in (4.7), with string breaking, for similar reasons. For completeness we note that in [41] massive W and Z gauge bosons were included in the static potential formalism for a standard model study but there the *real* mass did not lead to the same threshold singularity as (4.7). Next we note that one can isolate the contribution to (4.7) from purely single particle exchange diagrams corresponding to all the graphs of Figures 1 and 2, since it too has similar dipole behaviour. Indeed it could be the case that the single exchange graphs have a net dipole term which is cancelled by a matching piece from the box and vertex graphs. However, analysing the single exchange contribution in the same way as (4.7) the zero momentum limit is also non-singular. Though in comparison with (4.7) there is an additional dipole-like term. As $p^2 \rightarrow 0$ these three terms conspire in a similar way as before to exclude an overall $1/(p^2)^2$ singularity.

Although the dipole term does not emerge, we close this section by discussing other aspects of (4.7) in the context of [36, 37, 38, 39, 40, 41]. In the perturbative approach one can define a strong coupling constant which matches the usual ultraviolet behaviour of a strong coupling constant in the large momentum limit. It is based on the momentum space behaviour of the potential and is defined by

$$\tilde{V}(\mathbf{p}) = - \frac{4\pi C_F}{\mathbf{p}^2} \alpha_V(\mathbf{p}) \quad (4.19)$$

where the subscript V denotes the V -scheme, [68, 69]. One advantage of this definition is that it is derived from a gauge independent quantity which is effectively the force between two coloured objects. The low momentum behaviour can be studied. Clearly in the Gribov-Zwanziger case at both leading order and one loop $\alpha_V(0) = 0$. Though for the former the behaviour in the zero momentum limit is $O((p^2)^2)$ but $O(p^2)$ in the latter. If, however, an overall dipole piece dominated the infrared then $\alpha_V(\mathbf{p})$ would be singular at low momentum when one factor of \mathbf{p}^2 is cancelled from the coupling constant definition. This would be consistent with confinement in this scheme when the strength of a suitably defined coupling constant increases to produce infrared slavery. Though in the absence of quarks there would appear to be no string breaking related to saturation discussed, for example, in [67]. Given these comments it might be an interesting exercise for lattice or Dyson Schwinger methods to be applied to the static potential specifically in the Gribov-Zwanziger Landau gauge case. This may be particularly apt given the current debate over whether the scaling or decoupling solution is the correct picture. Briefly, in essence we have concentrated on using the formalism associated with the scaling solution. In the decoupling scenario, [22, 23, 24, 25, 26, 27, 28, 29], it transpires that the gluon is not suppressed in the infrared, since the propagator freezes to a finite non-zero value but the form factor vanishes, and the Faddeev-Popov ghost is not enhanced. It has a behaviour which is close to a $1/p^2$ dependence as $p^2 \rightarrow 0$ rather than the dipole of the Gribov scenario, [22, 23, 24, 25, 26, 27, 28, 29].

5 Gap equation.

In this section we focus on several aspects of the Gribov gap equation which defines the Gribov parameter γ using (2.19) to correct the error in the earlier two loop gap equation of [32]. In our

current notation the gap equation is defined by the expectation value

$$f^{abc}\langle A^{a\mu}(x)\xi_{\mu}^{bc}(x)\rangle = \frac{idN_A\gamma^2}{g^2}. \quad (5.1)$$

Whilst the new features we present here are not immediately related to the static potential, we believe they are important and the computations do contribute to understanding further underlying properties of the Gribov-Zwanziger Lagrangian. Throughout our calculations γ appears explicitly but is not an independent parameter of the theory. As emphasised in [11, 12, 13, 14, 15, 16, 17, 18], the Lagrangian can only be interpreted as a gauge theory when the gap equation is satisfied explicitly. The original one loop expression was derived in [10] in the $\overline{\text{MS}}$ scheme and it is straightforward to invert it to determine γ as an explicit function of the coupling constant. For instance, we have, [10],

$$1 = C_A \left[\frac{5}{8} - \frac{3}{8} \ln \left(\frac{C_A \gamma^4}{\mu^4} \right) \right] a + O(a^2) \quad (5.2)$$

which gives

$$\frac{C_A \gamma^4}{\mu^4} = \exp \left[\frac{5}{3} - \frac{32\pi}{3C_A \alpha_s(\mu)} \right] \quad (5.3)$$

or expressing it in numerical form we have

$$\frac{C_A \gamma^4}{\mu^4} = 5.294 \exp \left[- \frac{33.510}{C_A \alpha_s(\mu)} \right]. \quad (5.4)$$

(In this section we revert to the $\overline{\text{MS}}$ scheme rather than continue with the V -scheme.) This clearly demonstrates the non-perturbative behaviour of the Gribov mass parameter. However, as the two loop $\overline{\text{MS}}$ correction to the mass gap is now available, [32], one interesting question is whether it is possible to rearrange the explicit expression to preserve the non-perturbative property emerging from the one loop result. Therefore, to do this we take

$$\frac{C_A \gamma^4}{\mu^4} = c_0 [1 + c_1 C_A \alpha_s(\mu)] \exp \left[- \frac{b_0}{C_A \alpha_s(\mu)} \right]. \quad (5.5)$$

as an ansatz for a corrected form of (5.3). Substituting this into the explicit gap equation, whose correct form now is,

$$\begin{aligned} 1 = & C_A \left[\frac{5}{8} - \frac{3}{8} \ln \left(\frac{C_A \gamma^4}{\mu^4} \right) \right] a \\ & + \left[C_A^2 \left(\frac{3893}{1536} - \frac{22275}{4096} s_2 + \frac{29}{128} \zeta(2) - \frac{65}{48} \ln \left(\frac{C_A \gamma^4}{\mu^4} \right) + \frac{35}{128} \left(\ln \left(\frac{C_A \gamma^4}{\mu^4} \right) \right)^2 \right. \right. \\ & \quad \left. \left. + \frac{411}{1024} \sqrt{5} \zeta(2) - \frac{1317\pi^2}{4096} \right) \right. \\ & \quad \left. + C_A T_F N_f \left(\frac{\pi^2}{8} - \frac{25}{24} - \zeta(2) + \frac{7}{12} \ln \left(\frac{C_A \gamma^4}{\mu^4} \right) - \frac{1}{8} \left(\ln \left(\frac{C_A \gamma^4}{\mu^4} \right) \right)^2 \right) \right] a^2 \\ & + O(a^3) \end{aligned} \quad (5.6)$$

where $s_2 = (2\sqrt{3}/9)\text{Cl}_2(2\pi/3)$ and $\text{Cl}_2(x)$ is the Clausen function, it ought to be possible to determine explicit expressions for the unknown coefficients b_0 and c_i . If one cannot find a

solution then an alternative approach would be needed. Remarkably, it transpires that to two loop order one can achieve the inversion for arbitrary numbers of massless quarks and we find

$$\begin{aligned}
b_0 &= \frac{32\pi \left[3C_A - \sqrt{79C_A^2 - 32C_A T_F N_f} \right]}{[35C_A - 16T_F N_f]} \\
c_0 &= \exp \left[\frac{1}{[105C_A - 48T_F N_f]} \left[260C_A - 112T_F N_f - \frac{[255C_A - 96T_F N_f]C_A}{\sqrt{79C_A^2 - 32C_A T_F N_f}} \right] \right] \\
c_1 &= \left[25855714080\sqrt{5}\zeta(2)C_A^4 - 32766156288\sqrt{5}\zeta(2)C_A^3 N_f T_F + 13817806848\sqrt{5}\zeta(2)C_A^2 N_f^2 T_F^2 \right. \\
&\quad - 1939341312\sqrt{5}\zeta(2)C_A N_f^3 T_F^3 - 20712880440\pi^2 C_A^4 - 350326053000s_2 C_A^4 \\
&\quad + 14594952960\zeta(2)C_A^4 + 56581367360C_A^4 + 34301188224\pi^2 C_A^3 N_f T_F \\
&\quad + 443957500800s_2 C_A^3 N_f T_F - 82914840576\zeta(2)C_A^3 N_f T_F - 94986935296C_A^3 N_f T_F \\
&\quad - 21273919488\pi^2 C_A^2 N_f^2 T_F^2 - 187221196800s_2 C_A^2 N_f^2 T_F^2 + 89436192768\zeta(2)C_A^2 N_f^2 T_F^2 \\
&\quad + 59735801856C_A^2 N_f^2 T_F^2 + 5856952320\pi^2 C_A N_f^3 T_F^3 + 26276659200s_2 C_A N_f^3 T_F^3 \\
&\quad - 35521560576\zeta(2)C_A N_f^3 T_F^3 - 16679698432C_A N_f^3 T_F^3 - 603979776\pi^2 N_f^4 T_F^4 \\
&\quad \left. + 4831838208\zeta(2)N_f^4 T_F^4 + 1744830464N_f^4 T_F^4 \right] \\
&\quad \times \frac{1}{36864\pi[79C_A - 32T_F N_f]^{5/2}[35C_A - 16T_F N_f]\sqrt{C_A}}. \tag{5.7}
\end{aligned}$$

To assist with comparisons we have evaluated the coefficients numerically for both $SU(2)$ and $SU(3)$ colour groups and for several values of N_f and these are given respectively in Tables 1 and 2. Finally, we note that to this order in the gap equation (5.5) can be rewritten as

$$\frac{C_A \gamma^4}{\mu^4} = c_0 \exp \left[-\frac{b_0}{C_A \alpha_s(\mu)} + c_1 C_A \alpha_s(\mu) \right] \tag{5.8}$$

with the same values for c_0 , c_1 and b_0 .

N_f	b_0	c_0	c_1
0	16.913	9.052	- 0.133
2	18.383	8.994	- 0.180
3	19.303	8.963	- 0.210

Table 1. Numerical values of parameters for $SU(2)$.

N_f	b_0	c_0	c_1
0	16.913	9.052	- 0.133
2	17.864	9.014	- 0.163
3	18.383	8.994	- 0.180

Table 2. Numerical values of parameters for $SU(3)$.

Although the perturbative correction to the one loop form appears to be converging the actual convergence cannot fully be commented on until a three loop gap equation is available. One indication of the issues related to this is the change in value of c_0 between loop orders. In one sense this is not unexpected since the ansatz we have taken has a relatively simple form

and may not be the best approximation to the full relation for γ as an explicit function of the coupling constant which is not known. To illustrate the subtleties of solving the gap equation at two loops, we had tried to solve (5.6) numerically as a quadratic in the coupling constant. However, this was problematic since for certain values of the parameters, it resulted in solutions where there was an imaginary part. This was in contradiction with the understanding that γ and the coupling constant are real parameters. Moreover, if the solution to the quadratic had turned out to be real, it was not clear whether this would persist at higher loop orders when one would in principle have to solve cubic and quartic equations. The potential proliferation of roots would at some point be problematic and render such an approach meaningless. Therefore, we took the ansatz approach discussed above. As an aside we note that with the new two loop $\overline{\text{MS}}$ gap equation, (5.6), we have verified that the Kugo-Ojima confinement criterion, [34, 35], still holds and that both the Faddeev-Popov and ω_μ^{ab} propagators enhance in the zero momentum limit at two loops, as before.

We turn now to another aspect of the gap equation and that is to do with its form in another renormalization scheme. Whilst the $\overline{\text{MS}}$ scheme is standard in (high order) loop calculations it is not always the most appropriate since it is not a scheme motivated from a physical point of view. One such scheme, however, is the MOM scheme, [70, 71], which has also been used, for example, in lattice calculations of the gluon 2-point function and the evaluation of the renormalization group invariant effective strong coupling constant, [72, 73, 74]. The latter is derived from the gluon ghost vertex, though the triple gluon vertex has also been considered. As the MOM scheme seems to be the one most studied in that context it would seem appropriate to develop the Gribov gap equation in the MOM scheme to see if there is any scheme dependence. Therefore, we repeat the computation of section 3 but for the MOM scheme which is not a trivial exercise.

As a starting point we note that the exact expressions for the one loop 2-point functions are required as a function of γ . These are necessary since the MOM scheme is a mass dependent scheme and therefore the *full* expressions are needed to determine the correct finite parts for the MOM renormalization constants. However, as in the $\gamma = 0$ case the MOM renormalization has to be carried out in such a way that the underlying Slavnov-Taylor identities are not violated. For the Gribov-Zwanziger Lagrangian specifically, this means the renormalization constants for A_μ^a , c^a , ρ_μ^{ab} , ξ_μ^{ab} , ω_μ^{ab} and γ , which are Z_A , Z_c , Z_ρ , Z_ξ , Z_ω and Z_γ , must satisfy, [18, 30, 31],

$$Z_c = Z_\rho = Z_\xi = Z_\omega = \frac{1}{Z_g \sqrt{Z_A}} \quad , \quad Z_\gamma = (Z_A Z_c)^{-1/4} \quad (5.9)$$

where Z_g is the coupling constant renormalization constant. Given this we have proceeded as follows. First, we determined the wave function renormalization constants for A_μ^a , ρ_μ^{ab} and ξ_μ^{ab} by rendering the respective 2-point functions exactly equal to unity when the external momentum satisfies $p^2 = \mu^2$ where μ is the mass scale of the renormalization point. We record the explicit forms for Z_A , Z_ρ and Z_ξ in the MOM scheme are

$$\begin{aligned} Z_A^{\text{MOM}} &= 1 + \left[\frac{13}{6} C_A - \frac{4}{3} T_F N_f \right] \frac{a}{\epsilon} - \frac{20}{9} T_F N_f a \\ &+ \left[\frac{1939}{576} + \frac{7}{64} \ln \left[\frac{[C_A \gamma^4 + \mu^4]}{\mu^4} \right] - \frac{135}{128} \ln \left[\frac{C_A \gamma^4}{\mu^4} \right] - \frac{241\sqrt{2}}{768} \eta_2(\mu^2) \right. \\ &+ \frac{25\mu^2 \sqrt{4C_A \gamma^4 - \mu^4}}{768 C_A \gamma^4} \tan^{-1} \left[-\frac{\sqrt{4C_A \gamma^4 - \mu^4}}{\mu^2} \right] - \frac{131\pi\mu^2}{768 \sqrt{C_A \gamma^2}} \\ &\left. - \frac{37\pi \sqrt{C_A \gamma^2}}{128\mu^2} - \frac{3C_A \gamma^4 \sqrt{4C_A \gamma^4 - \mu^4}}{8\mu^6} \tan^{-1} \left[-\frac{\sqrt{4C_A \gamma^4 - \mu^4}}{\mu^2} \right] \right] \end{aligned}$$

$$\begin{aligned}
& + \left[\frac{35}{64} - \frac{47}{192} \ln \left[1 + \frac{\mu^4}{C_A \gamma^4} \right] \right] \frac{C_A \gamma^4}{\mu^4} - \frac{59\pi C_A^{3/2} \gamma^6}{128\mu^6} \\
& + \frac{11C_A^{3/2} \gamma^6}{64\mu^6} \tan^{-1} \left[\frac{\sqrt{C_A} \gamma^2}{\mu^2} \right] - \frac{7\sqrt{4C_A \gamma^4 - \mu^4}}{192\mu^2} \tan^{-1} \left[-\frac{\sqrt{4C_A \gamma^4 - \mu^4}}{\mu^2} \right] \\
& + \left[\frac{1}{96} \ln \left[\frac{C_A \gamma^4}{\mu^4} \right] - \frac{1}{48} \ln \left[\frac{C_A \gamma^4 + \mu^4}{\mu^4} \right] - \frac{3\sqrt{2}}{1024} \eta_2(\mu^2) \right] \frac{\mu^4}{C_A \gamma^4} \\
& + \left[\frac{19}{192} \tan^{-1} \left[\frac{\sqrt{C_A} \gamma^2}{\mu^2} \right] - \frac{35\sqrt{2}}{384} \eta_1(\mu^2) \right] \frac{\mu^2}{\sqrt{C_A} \gamma^2} \\
& - \left[\frac{25\sqrt{2}}{64} \eta_1(\mu^2) + \frac{23}{48} \tan^{-1} \left[\frac{\sqrt{C_A} \gamma^2}{\mu^2} \right] \right] \frac{\sqrt{C_A} \gamma^2}{\mu^2} C_{Aa} + O(a^2) \quad (5.10)
\end{aligned}$$

and

$$\begin{aligned}
Z_\rho^{\text{MOM}} &= Z_\xi^{\text{MOM}} \\
&= 1 + \frac{3C_A a}{4 \epsilon} + \left[\frac{5}{4} - \frac{3}{8} \ln \left[\frac{C_A \gamma^4 + \mu^4}{\mu^4} \right] - \frac{C_A \gamma^4}{8\mu^4} \ln \left[\frac{C_A \gamma^4}{C_A \gamma^4 + \mu^4} \right] \right. \\
&\quad \left. - \frac{3\pi\sqrt{C_A} \gamma^2}{8\mu^2} + \left[\frac{3\sqrt{C_A} \gamma^2}{4\mu^2} - \frac{\mu^2}{4\sqrt{C_A} \gamma^2} \right] \tan^{-1} \left[\frac{\sqrt{C_A} \gamma^2}{\mu^2} \right] \right] C_{Aa} + O(a^2). \quad (5.11)
\end{aligned}$$

We have checked that the latter is consistent by renormalizing the Faddeev-Popov ghost 2-point function in the same way and verified explicitly that the first of the Slavnov-Taylor identities holds at one loop. Equipped with these renormalization constants then that for γ is now already fixed in the MOM scheme through the second identity of (5.9). In order to verify that this is not inconsistent we have repeated the one loop gap equation computation but using these MOM renormalization constants. This is achieved in the same way as [32], by closing the legs on the mixed propagator which gives the one loop contribution to the gap equation. As this is a vacuum diagram there is no external momentum to set to a mass shell value to extract the MOM scheme expression for Z_γ which is why we have proceeded with the 2-point functions first. Therefore, the renormalization constants which have already been determined will remove the divergences and their finite parts will influence the final form of the gap equation. Ultimately we find the relatively simple expression*

$$\begin{aligned}
1 &= \left[\frac{3}{8} \ln \left[\frac{C_A \gamma^4 + \mu^4}{C_A \gamma^4} \right] - \frac{5}{8} + \frac{C_A \gamma^4}{8\mu^4} \ln \left[\frac{C_A \gamma^4}{C_A \gamma^4 + \mu^4} \right] + \frac{3\pi\sqrt{C_A} \gamma^2}{8\mu^2} \right. \\
&\quad \left. - \left[\frac{3\sqrt{C_A} \gamma^2}{4\mu^2} - \frac{\mu^2}{4\sqrt{C_A} \gamma^2} \right] \tan^{-1} \left[\frac{\sqrt{C_A} \gamma^2}{\mu^2} \right] \right] C_{Aa} + O(a^2) \\
&\equiv \text{gap}(\gamma, \mu, \text{MOM}) C_{Aa} + O(a^2) \quad (5.12)
\end{aligned}$$

where for later purposes we have introduced a shorthand definition of the right hand side of the gap equation. Given that we are following the standard way to proceed in the MOM scheme there could be a doubt as to whether this is ultimately correct. However, in the Gribov-Zwanziger context the main check on this is whether the Kugo-Ojima criterion of Faddeev-Popov ghost enhancement, [34, 35], emerges in the c^a 2-point function in the zero momentum limit when the MOM gap equation of (5.12) is satisfied. We note that not unexpectedly it does so. As a final point we have returned to the renormalization group invariant effective coupling constant defined from the gluon ghost vertex and reconsidered it in the infrared limit similar to section

*This corrects a sign error in the expression given in [75].

3. Using the MOM versions of the respective form factors, $D_A^{\text{MOM}}(p^2)$ and $D_c^{\text{MOM}}(p^2)$ then we define the MOM effective renormalization group invariant coupling constant as

$$\alpha_{\text{eff}}(p^2) \Big|_{\text{MOM}} = \alpha_s(\mu) D_A^{\text{MOM}}(p^2) \left(D_c^{\text{MOM}}(p^2) \right)^2 . \quad (5.13)$$

Equipped with this we find that the coupling constant freezing calculation becomes

$$\alpha_{\text{eff}}(0) \Big|_{\text{MOM}} = \lim_{p^2 \rightarrow 0} \left[\frac{\alpha_s(\mu) \left[1 - C_A \left(\text{gap}(\gamma, \mu, \text{MOM}) + \frac{5}{8} - \frac{11}{16} \right) a \right] (p^2)^2}{C_A \gamma^4 \left[1 - C_A \left(\text{gap}(\gamma, \mu, \text{MOM}) - \frac{\pi p^2}{8\sqrt{C_A} \gamma^2} \right) a \right]^2} \right] \quad (5.14)$$

where we have displayed the rationals in the numerator explicitly in order to compare with the analogous $\overline{\text{MS}}$ computation of [33]. Hence,

$$\alpha_{\text{eff}}(0) \Big|_{\text{MOM}} = \frac{16}{\pi C_A} . \quad (5.15)$$

This is the same value as the $\overline{\text{MS}}$ scheme, [33], as expected and can be regarded as a robust check on the finite parts of the MOM renormalization constants we derived. One final comment on the MOM gap equation in the context of the earlier discussion is that it is evident that inverting (5.12) is not as straightforward as that for the $\overline{\text{MS}}$ scheme and we have not proceeded. This is partly because the two loop expression is not available in order to do a proper comparison but also because if it was, it is clear that nothing substantial would emerge from a complicated explicit expression. Indeed a two loop calculation of the MOM gap equation would require the finite part of the 2-point functions *exactly* which would be a huge computation. To elaborate on the complexity of this problem in order to obtain, for instance, the wave function renormalization constants there are well over 1000 two loop Feynman diagrams correcting all the A_μ^a , ρ_μ^{ab} and ξ_μ^{ab} 2-point functions. Aside from this, it is not clear if all the master scalar two loop self-energy Feynman integrals have been evaluated for all the necessary massive propagator configurations. For instance, the exact expression for the scalar master two loop self-energy corrections with purely 3-point vertices with all masses equal is not known. Even it were available one would still require the expression for different masses in order to determine the expressions for the Gribov mass combinations of $\pm i\sqrt{C_A} \gamma^2$. Indeed to appreciate how complicated this problem would be, one can examine the structure for the simpler two loop sunset self-energy correction for arbitrary masses, discussed in [76]. The arbitrary mass expression in this simplest case involves Lauricella functions where the arguments are a function of the masses and the external momentum. In an MOM renormalization such functions, and the as yet undetermined master integrals for the two loop topologies with four and five propagators, would have to be evaluated exactly at the point where $p^2 = \mu^2$. Therefore, given these considerations it is inconceivable that a two loop MOM gap equation is viable in the immediate future, even if such a quantity were of interest. Finally, we note that the different values for the renormalization group invariant and V -scheme coupling constants at zero momentum are not inconsistent. In this region there is no unique way of defining the strong coupling constant.

6 ξ_μ^{ab} and ρ_μ^{ab} enhancement.

Whilst our potential has been derived from the usual static potential formalism at one loop, it is clear that it lacks a linearly rising part. This is due to the cancellation of similar $1/(p^2)^2$ type terms as $p^2 \rightarrow 0$. However, from experience of the Gribov-Zwanziger Lagrangian any infrared behaviour which is in qualitative agreement with expectations from other work has always

required the explicit use of the gap equation satisfied by γ . For example, the enhancement of the Faddeev-Popov ghost is due to the gap equation, [10], and we recall that the theory can only be regarded as a gauge theory when the gap equation is satisfied. Indeed the ghost enhancement is also a key component of the Kugo-Ojima confinement criterion, [34, 35], in Yang-Mills theory. Its role in the Gribov-Zwanziger path integral has recently been clarified in [77] and is also used as a boundary condition in Dyson Schwinger studies, [29]. Whilst the Faddeev-Popov ghosts and localizing ghosts ω_μ^{ab} satisfy the enhancement, they cannot play a direct role in actually confining a gluon since they are Grassmann fields. Hence they cannot be directly exchanged in gluon-gluon interactions as is evident from the graphs of Figures 1 and 2. Instead one clearly requires a commuting field to enhance to be at least in a situation where a $1/(p^2)^2$ singularity could be exchanged. Unlike the original expectations of Mandelstam and others, [6, 7, 8, 9], this does not appear to be the gluon in the Gribov-Zwanziger set-up. However, as recently pointed out by Zwanziger there appears to be a clue in the enhancement of the propagators of the bosonic ghosts from a Schwinger Dyson analysis, [50]. Therefore, our aim in this section is to first demonstrate that that enhancement can also actually be accessed in perturbation theory and then discuss its implications for the static potential. Aside from the fields c^a and ω_μ^{ab} the explicit forms of the 2-point functions for ξ_μ^{ab} and ρ_μ^{ab} have the potential for enhancement. More concretely the explicit one loop correction to the colour channel of the Lagrangian kinetic term for each of ξ_μ^{ab} and ρ_μ^{ab} , given in appendix B, are exactly equivalent to that of the Faddeev-Popov ghost 2-point function. To illustrate this for completeness here we recall the $p^2 \rightarrow 0$ behaviour of the 2-point functions are,

$$\begin{aligned}
\langle \xi_\mu^{ab}(-p) \xi_\nu^{cd}(p) \rangle^{-1} &= - \left[\delta^{ac} \delta^{bd} \left[1 - C_A \left(\frac{5}{8} - \frac{3}{8} \ln \left(\frac{C_A \gamma^4}{\mu^4} \right) \right) a \right] p^2 + \frac{7}{144} f^{ace} f^{bde} p^2 a \right. \\
&\quad \left. + \frac{11}{288} f^{abe} f^{cde} p^2 a + \frac{7}{24} d_A^{abcd} \frac{p^2}{C_A} a + O(a^2) \right] P_{\mu\nu}(p) \\
&\quad - \left[\delta^{ac} \delta^{bd} \left[1 - C_A \left(\frac{5}{8} - \frac{3}{8} \ln \left(\frac{C_A \gamma^4}{\mu^4} \right) \right) a \right] p^2 + \frac{5}{48} f^{ace} f^{bde} p^2 a \right. \\
&\quad \left. - \frac{5}{96} f^{abe} f^{cde} p^2 a + \frac{5}{8} d_A^{abcd} \frac{p^2}{C_A} a + O(a^2) \right] L_{\mu\nu}(p) \\
&\quad + O((p^2)^2)
\end{aligned} \tag{6.1}$$

and

$$\langle \rho_\mu^{ab}(-p) \rho_\nu^{cd}(p) \rangle^{-1} = - \left[\delta^{ac} \delta^{bd} \left[1 - C_A \left(\frac{5}{8} - \frac{3}{8} \ln \left(\frac{C_A \gamma^4}{\mu^4} \right) \right) a \right] p^2 \right] \eta_{\mu\nu} + O((p^2)^2) \tag{6.2}$$

where to avoid confusion with the propagator we have formally indicated the inverse. The first terms on the right hand side of (6.1) and (6.2) clearly correspond to the one loop gap equation, (5.2), which would imply enhancement similar to the Grassmann ghost fields and the emergence of an infrared dipole form. The inversion of the ρ_μ^{ab} 2-point function to deduce the propagator is similar to that of the Faddeev-Popov ghost and ω_μ^{ab} and so ρ_μ^{ab} will have an enhanced infrared propagator too. However, a ξ_μ^{ab} enhancement is not as straightforward to observe as those fields due to the extra terms in (6.1) and the group structure.

To examine how ξ_μ^{ab} enhancement emerges, we first recall the situation in the Faddeev-Popov case. There one first computes the 2-point function in the zero momentum limit and applies (5.2). This produces a leading term of $O((p^2)^2)$ which one then inverts to discover the dipole infrared behaviour of the Faddeev-Popov ghost. Turning to the ξ_μ^{ab} case the algorithm is the same but not as straightforward due to the mixing in the quadratic part of the $\{A_\mu^a, \xi_\mu^{ab}\}$ sector

of the Lagrangian. So the analogous inversion has to involve the *full* 2×2 mixing matrix. In section 3 this was carried out formally at one loop but without first enforcing the gap equation. Given the potential for ξ_μ^{ab} enhancement of [50] in a Dyson Schwinger analysis, we reconsider the formal matrix inversion in a more general way. Specifically we will focus on the $\{A_\mu^a, \xi_\mu^{ab}\}$ sector and in particular the transverse piece. We do this because at one loop $V = 0$ and so the transverse part of (3.1) becomes block diagonal. It is the upper 2×2 matrix which is of interest. If we now define this 2×2 matrix by $\Lambda_2^{\{ab|cd\}}$, where we can drop the Lorentz indices, then formally

$$\Lambda_2^{\{ab|cd\}} = \begin{pmatrix} \mathcal{X}\delta^{ac} & \mathcal{U}f^{acd} \\ \mathcal{U}f^{cab} & \mathcal{Q}_\xi^{abcd} \end{pmatrix} \quad (6.3)$$

where we use the more general decomposition

$$\mathcal{Q}_\xi^{abcd} = \mathcal{Q}_\xi\delta^{ac}\delta^{bd} + \mathcal{W}_\xi f^{ace}f^{bde} + \mathcal{R}_\xi f^{abe}f^{cde} + \mathcal{S}_\xi d_A^{abcd} + \mathcal{P}_\xi\delta^{ab}\delta^{cd} + \mathcal{T}_\xi\delta^{ad}\delta^{bc} \quad (6.4)$$

and the quantities $\mathcal{X}, \mathcal{U}, \mathcal{Q}_\xi, \mathcal{W}_\xi, \mathcal{R}_\xi$ and \mathcal{S}_ξ are the formal 2-point functions *including* the part from the quadratic part of the Lagrangian. We have used similar notation to sections 2 and 3 but in calligraphic font to indicate that these are not solely the one loop corrections. We have also included two extra terms, \mathcal{P}_ξ and \mathcal{T}_ξ , to complete the basis. Although these are zero up to and including one loop they are required here since we will be multiplying $\Lambda_2^{\{ab|cd\}}$ by its *full* inverse rather than drop the $O(a^2)$ part as was carried out in deriving (3.6). Here there will be extra group structures when, for example, two d_A^{abcd} tensors are partially contracted. Whilst we are aiming at being general our matrix can only really be regarded as one loop in one sense since the colour group structure in the final element may not be the most general. Our choice there is motivated by what actually emerges from the explicit one loop computations. For instance, if quarks are present in higher loop diagrams then the tensor d_F^{abcd} could also be present due to light-by-light subgraphs or some peculiar contraction of this with other tensors. For a comprehensive discussion of potential high rank (adjoint) tensors, see [78]. At present we make no assumptions about the behaviour of (6.3) in the $p^2 \rightarrow 0$ limit but note that like Q_ρ in (6.2), \mathcal{Q}_ξ will be the key function in driving any enhancement. Also the loop order will play a key role in the inversion and we note that

$$\mathcal{X} = \mathcal{U} = \mathcal{Q}_\xi = O(1) \quad , \quad \mathcal{W}_\xi = \mathcal{R}_\xi = \mathcal{S}_\xi = O(a) \quad , \quad \mathcal{P}_\xi = \mathcal{T}_\xi = O(a^2) \quad . \quad (6.5)$$

Given $\Lambda_2^{\{ab|cd\}}$ we define the general inverse $\Pi_2^{\{cd|pq\}}$, which will be the matrix of propagators, in the same formal way by

$$\Pi_2^{\{cd|pq\}} = \begin{pmatrix} \mathcal{A}\delta^{cp} & \mathcal{B}f^{cpq} \\ \mathcal{B}f^{pcd} & \mathcal{D}_\xi^{cdpq} \end{pmatrix} \quad (6.6)$$

where now

$$\mathcal{D}_\xi^{cdpq} = \mathcal{D}_\xi\delta^{cp}\delta^{dq} + \mathcal{J}_\xi f^{cpe}f^{dqe} + \mathcal{K}_\xi f^{cde}f^{pqe} + \mathcal{L}_\xi d_A^{cdpq} + \mathcal{M}_\xi\delta^{cd}\delta^{pq} + \mathcal{N}_\xi\delta^{cq}\delta^{dp} \quad (6.7)$$

similar to (3.4) but allowing for the extra colour tensors to have a basis. For clarity we note that the two matrices must satisfy the standard inversion on the smaller subspace given by

$$\Lambda_2^{\{ab|cd\}}\Pi_2^{\{cd|pq\}} = \begin{pmatrix} \delta^{cp} & 0 \\ 0 & \delta^{cp}\delta^{dq} \end{pmatrix} \quad (6.8)$$

where the right hand side is effectively the unit matrix. Multiplying out the matrices explicitly leads to the formal linear equations satisfied by the 2-point functions and propagators. We have

$$1 = \mathcal{A}\mathcal{X} + C_A\mathcal{U}\mathcal{B} \quad , \quad 0 = \mathcal{X}\mathcal{B} + \left(\mathcal{D}_\xi - \mathcal{N}_\xi + C_A\mathcal{K}_\xi + \frac{1}{2}C_A\mathcal{J}_\xi \right)\mathcal{U}$$

$$\begin{aligned}
0 &= \mathcal{A}U + \left(\mathcal{Q}_\xi + C_A \mathcal{R}_\xi + \frac{1}{2} C_A \mathcal{W}_\xi - \mathcal{T}_\xi \right) \mathcal{B} \\
1 &= \mathcal{Q}_\xi \mathcal{D}_\xi + b_2 \mathcal{L}_\xi \mathcal{W}_\xi + b_2 \mathcal{S}_\xi \mathcal{J}_\xi + a_2 \mathcal{S}_\xi \mathcal{L}_\xi + \mathcal{T}_\xi \mathcal{N}_\xi \\
0 &= \left(\mathcal{Q}_\xi + C_A \mathcal{W}_\xi + \frac{5}{6} C_A^2 \mathcal{S}_\xi + N_A \mathcal{P}_\xi + \mathcal{T}_\xi \right) \mathcal{M}_\xi + \left(C_A \mathcal{J}_\xi + \frac{5}{6} C_A^2 \mathcal{L}_\xi + \mathcal{D}_\xi + \mathcal{N}_\xi \right) \mathcal{P}_\xi \\
&\quad + b_1 \mathcal{W}_\xi \mathcal{L}_\xi + b_1 \mathcal{S}_\xi \mathcal{J}_\xi + a_1 \mathcal{S}_\xi \mathcal{L}_\xi \\
0 &= b_2 \mathcal{L}_\xi \mathcal{W}_\xi + b_2 \mathcal{S}_\xi \mathcal{J}_\xi + a_2 \mathcal{S}_\xi \mathcal{L}_\xi + \mathcal{Q}_\xi \mathcal{N}_\xi + \mathcal{T}_\xi \mathcal{D}_\xi \\
0 &= \mathcal{Q}_\xi \mathcal{L}_\xi + \mathcal{W}_\xi \mathcal{J}_\xi + \mathcal{S}_\xi \mathcal{D}_\xi + b_4 \mathcal{W}_\xi \mathcal{L}_\xi + b_4 \mathcal{S}_\xi \mathcal{J}_\xi + a_4 \mathcal{S}_\xi \mathcal{L}_\xi + \mathcal{S}_\xi \mathcal{N}_\xi + \mathcal{T}_\xi \mathcal{L}_\xi \\
0 &= \mathcal{W}_\xi \mathcal{D}_\xi + \mathcal{Q}_\xi \mathcal{J}_\xi + \frac{1}{6} C_A \mathcal{W}_\xi \mathcal{J}_\xi + 2b_3 \mathcal{S}_\xi \mathcal{J}_\xi + 2a_3 \mathcal{S}_\xi \mathcal{L}_\xi + 2b_3 \mathcal{W}_\xi \mathcal{L}_\xi + \mathcal{W}_\xi \mathcal{N}_\xi + \mathcal{T}_\xi \mathcal{J}_\xi \\
0 &= \mathcal{U} \mathcal{B} + \mathcal{Q}_\xi \mathcal{K}_\xi + \frac{1}{6} C_A \mathcal{W}_\xi \mathcal{J}_\xi + \frac{1}{2} C_A \mathcal{W}_\xi \mathcal{K}_\xi + \frac{1}{2} C_A \mathcal{R}_\xi \mathcal{J}_\xi + C_A \mathcal{R}_\xi \mathcal{K}_\xi - b_3 \mathcal{W}_\xi \mathcal{L}_\xi \\
&\quad - \mathcal{W}_\xi \mathcal{N}_\xi + \mathcal{R}_\xi \mathcal{D}_\xi - \mathcal{R}_\xi \mathcal{N}_\xi - b_3 \mathcal{S}_\xi \mathcal{J}_\xi - a_3 \mathcal{S}_\xi \mathcal{L}_\xi - \mathcal{T}_\xi \mathcal{J}_\xi - \mathcal{T}_\xi \mathcal{K}_\xi \tag{6.9}
\end{aligned}$$

where the coefficients a_i and b_i derive from the group decompositions defined and discussed in appendix A where their explicit forms are given for an arbitrary colour group. It is clear we have nine equations for nine unknowns. So it is a straightforward exercise to determine the general solution. First, we record that

$$\mathcal{A} = \frac{[\mathcal{Q}_\xi + C_A \mathcal{R}_\xi + \frac{1}{2} C_A \mathcal{W}_\xi]}{[(\mathcal{Q}_\xi + C_A \mathcal{R}_\xi + \frac{1}{2} C_A \mathcal{W}_\xi) \mathcal{X} - C_A \mathcal{U}^2]} \quad , \quad \mathcal{B} = - \frac{\mathcal{U}}{[(\mathcal{Q}_\xi + C_A \mathcal{R}_\xi + \frac{1}{2} C_A \mathcal{W}_\xi) \mathcal{X} - C_A \mathcal{U}^2]} \tag{6.10}$$

where we have assumed $\mathcal{P}_\xi = \mathcal{T}_\xi = 0$ initially in accordance to what we found at one loop. The explicit forms of the form factors for ξ_μ^{ab} propagator are cumbersome. So for these cases we record the $SU(3)$ expressions where the values for a_i and b_i of appendix A have been used. We have

$$\begin{aligned}
\mathcal{D}_\xi &= \frac{1}{2\mathcal{Q}_\xi} \left[3(3\mathcal{S}_\xi - 2\mathcal{W}_\xi)(\mathcal{S}_\xi + 2\mathcal{W}_\xi)(\mathcal{S}_\xi + \mathcal{W}_\xi) + 8(7\mathcal{S}_\xi + 3\mathcal{W}_\xi)\mathcal{Q}_\xi^2 \right. \\
&\quad \left. + 16\mathcal{Q}_\xi^3 + 2(27\mathcal{S}_\xi^3 + 20\mathcal{S}_\xi \mathcal{W}_\xi - 8\mathcal{W}_\xi^2)\mathcal{Q}_\xi \right] \\
&\quad \times [2\mathcal{Q}_\xi + 3\mathcal{S}_\xi + 3\mathcal{W}_\xi]^{-1} [2\mathcal{Q}_\xi + 3\mathcal{S}_\xi - 2\mathcal{W}_\xi]^{-1} [2\mathcal{Q}_\xi + \mathcal{S}_\xi + 2\mathcal{W}_\xi]^{-1} \\
\mathcal{J}_\xi &= - \frac{4\mathcal{W}_\xi}{[2\mathcal{Q}_\xi + 3\mathcal{S}_\xi + 3\mathcal{W}_\xi][2\mathcal{Q}_\xi + 3\mathcal{S}_\xi - 2\mathcal{W}_\xi]} \\
\mathcal{K}_\xi &= \frac{1}{\mathcal{Q}_\xi} \left[(4(3\mathcal{S}_\xi - \mathcal{W}_\xi)\mathcal{Q}_\xi + 3(3\mathcal{S}_\xi - 2\mathcal{W}_\xi)(\mathcal{S}_\xi + \mathcal{W}_\xi))(2\mathcal{U}^2 - \mathcal{W}_\xi \mathcal{X} - 2\mathcal{R}_\xi \mathcal{X}) \right. \\
&\quad \left. - 8(\mathcal{R}_\xi \mathcal{X} - \mathcal{U})^2 \mathcal{Q}_\xi^2 \right] \\
&\quad \times [2\mathcal{Q}_\xi \mathcal{X} + 6\mathcal{R}_\xi \mathcal{X} - 6\mathcal{U}^2 + 3\mathcal{W}_\xi \mathcal{X}]^{-1} [2\mathcal{Q}_\xi + 3\mathcal{S}_\xi + 3\mathcal{W}_\xi]^{-1} [2\mathcal{Q}_\xi + 3\mathcal{S}_\xi - 2\mathcal{W}_\xi]^{-1} \\
\mathcal{L}_\xi &= -4 [2\mathcal{Q}_\xi \mathcal{S}_\xi + (3\mathcal{S}_\xi + 2\mathcal{W}_\xi)(\mathcal{S}_\xi - \mathcal{W}_\xi)] \\
&\quad \times [2\mathcal{Q}_\xi + 3\mathcal{S}_\xi + 3\mathcal{W}_\xi]^{-1} [2\mathcal{Q}_\xi + 3\mathcal{S}_\xi - 2\mathcal{W}_\xi]^{-1} [2\mathcal{Q}_\xi + \mathcal{S}_\xi + 2\mathcal{W}_\xi]^{-1} \\
\mathcal{M}_\xi &= 6 [21\mathcal{S}_\xi^3 + \mathcal{S}_\xi^2 \mathcal{W}_\xi - 12\mathcal{S}_\xi \mathcal{W}_\xi^2 - 4\mathcal{W}_\xi^3 + 2(7\mathcal{S}_\xi + 4\mathcal{W}_\xi)\mathcal{Q}_\xi \mathcal{S}_\xi] [2\mathcal{Q}_\xi + 15\mathcal{S}_\xi + 6\mathcal{W}_\xi]^{-1} \\
&\quad \times [2\mathcal{Q}_\xi + 3\mathcal{S}_\xi + 3\mathcal{W}_\xi]^{-1} [2\mathcal{Q}_\xi + 3\mathcal{S}_\xi - 2\mathcal{W}_\xi]^{-1} [2\mathcal{Q}_\xi + \mathcal{S}_\xi + 2\mathcal{W}_\xi]^{-1} \\
\mathcal{N}_\xi &= - \frac{3}{2\mathcal{Q}_\xi} [(3\mathcal{S}_\xi - 2\mathcal{W}_\xi)(\mathcal{S}_\xi + 2\mathcal{W}_\xi)(\mathcal{S}_\xi + \mathcal{W}_\xi) + 2(\mathcal{S}_\xi + 4\mathcal{W}_\xi)\mathcal{Q}_\xi \mathcal{S}_\xi] \\
&\quad \times [2\mathcal{Q}_\xi + 3\mathcal{S}_\xi + 3\mathcal{W}_\xi]^{-1} [2\mathcal{Q}_\xi + 3\mathcal{S}_\xi - 2\mathcal{W}_\xi]^{-1} [2\mathcal{Q}_\xi + \mathcal{S}_\xi + 2\mathcal{W}_\xi]^{-1} . \tag{6.11}
\end{aligned}$$

We have checked that our full arbitrary group solution correctly reproduces the one loop propagator corrections of (3.6). Indeed the gluon propagator remains suppressed in the zero momentum

limit at one loop. Aside from indicating how involved the final expression for the ξ_μ^{ab} propagator is, the main point of (6.11) is to illustrate which of the form factors enhance. From (6.1) the initial terms of the small momentum expansion of \mathcal{Q}_ξ represents the gap equation. Therefore, in this limit when the gap equation is realised \mathcal{Q}_ξ is effectively $O((p^2)^2)$ which corresponds to the same situation with the Faddeev-Popov ghost, ω_μ^{ab} and ρ_μ^{ab} fields giving rise to the enhancement of these fields. From (6.11) the situation is similar since several of the amplitudes have an overall factor of \mathcal{Q}_ξ . Hence these colour channels will enhance whilst the others will not in the zero momentum limit. More specifically the leading order behaviour of the transverse part of both bosonic ghost propagators in the $p^2 \rightarrow 0$ limit for an arbitrary group is

$$\begin{aligned} \langle \xi_\mu^{ab}(p) \xi_\nu^{cd}(-p) \rangle &\sim \left[\frac{4\gamma^2}{\pi\sqrt{C_A}(p^2)^2 a} [\delta^{ad}\delta^{bc} - \delta^{ac}\delta^{bd}] + \frac{8\gamma^2}{\pi C_A^{3/2}(p^2)^2 a} f^{abe} f^{cde} \right] P_{\mu\nu}(p) \\ \langle \rho_\mu^{ab}(p) \rho_\nu^{cd}(-p) \rangle &\sim - \frac{8\gamma^2}{\pi\sqrt{C_A}(p^2)^2 a} \delta^{ac}\delta^{bd} P_{\mu\nu}(p) . \end{aligned} \quad (6.12)$$

So one colour channel in addition to those of the original ξ_μ^{ab} propagator enhances. Although we have used the numerical values deriving from the one loop corrections to \mathcal{Q}_ξ this enhanced behaviour is more general. If instead we examine the leading \mathcal{Q}_ξ behaviour of (6.11) but for a general colour group then we find

$$\mathcal{D}_\xi \sim \frac{1}{2\mathcal{Q}_\xi} , \quad \mathcal{K}_\xi \sim - \frac{1}{C_A \mathcal{Q}_\xi} , \quad \mathcal{N}_\xi \sim - \frac{1}{2\mathcal{Q}_\xi} \quad (6.13)$$

with the other form factors being non-singular in the Laurent expansion in \mathcal{Q}_ξ . This implies that the leading \mathcal{Q}_ξ behaviour of the transverse part of the ξ_μ^{ab} propagator is

$$\langle \xi_\mu^{ab}(p) \xi_\nu^{cd}(-p) \rangle \sim \frac{1}{2\mathcal{Q}_\xi} \left[\delta^{ac}\delta^{bd} - \delta^{ad}\delta^{bc} - \frac{2}{C_A} f^{abe} f^{cde} \right] P_{\mu\nu}(p) . \quad (6.14)$$

So, for instance, when the gap equation is realised in the *three* dimensional Gribov-Zwanziger Lagrangian, then the corresponding ξ_μ^{ab} propagator will also be enhanced together with the Grassmann fields with the *same* colour group structure as four dimensions, (6.12). Interestingly for ξ_μ^{ab} the colour channel which dominates in the infrared is that which is antisymmetric in the colour indices of the field itself. In other words the colour projected field $f^{abc}\xi_\mu^{bc}$ does not enhance at one loop given the relative coefficients of (6.14).

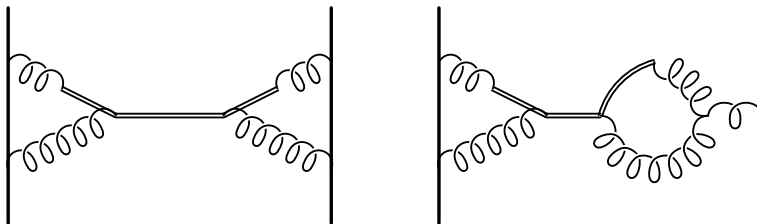


Figure 4: Several two loop topologies with ξ_μ^{ab} exchange.

Having established that ξ_μ^{ab} and ρ_μ^{ab} both enhance we can consider the implications of this for the static potential. These are better candidates for a confinement mechanism since they are bosonic fields and therefore can be exchanged between coloured static sources. However, the same points that were noted in [50] equally apply here in that ξ_μ^{ab} and ρ_μ^{ab} do not couple *directly* to a (static) field such as a quark or gluon. In the context of the static potential, the colour

source only couples to the gluon field, A_μ^a , in (2.3). However, one can have a single ξ_μ^{ab} exchange *indirectly*, for example, through various topologies such as those illustrated in Figure 4. The first graph involves source ξ_μ^{ab} vertex corrections whereas the second graph is a correction to the mixed 2-point function. If we consider the first in an extended computation one can replace the single ξ_μ^{ab} by the enhanced propagator whilst the second graph could be ignored since that is part of our earlier matrix inversion. Given (6.12) this exchange will actually give an $O(a^2)$ contribution to the static potential and not an $O(a^3)$ one. Although this is clearly contrary to a perturbative approach it is a qualitative indication that a reordering of the series will emerge even in a Dyson Schwinger approach as already discussed in [50]. Moreover, a similar reordering to produce the renormalization group invariant effective coupling constant freezing occurred in (3.14). In the context of freezing it is worth noting that as the Lagrangian channel of both ξ_μ^{ab} and ρ_μ^{ab} have enhancement, one could define an effective coupling constant based on either the gluon ξ_μ^{ab} vertex or gluon ρ_μ^{ab} vertex rather than the ghost gluon vertex which has a freezing value the same as (5.15) in either the $\overline{\text{MS}}$ or MOM schemes. Briefly instead of using either the ghost or ω_μ^{ab} 2-point function in the denominator of the definition, one uses instead the first part of (6.1). However, this is offered as an observation since the renormalization group invariance of such a construction is clearly not established and the ξ_μ^{ab} gluon vertex is certainly not on a par with the ghost gluon vertex in the context of non-renormalizability.

If we take the point of view that our reasoning is at a qualitative level, we can then examine some possible implications of ξ_μ^{ab} enhancement on the static potential. We have computed the eight Feynman diagrams contributing to the topology illustrated in the left hand diagram of Figure 4 for the static potential formalism. With the ξ_μ^{ab} propagator of (2.21) we find in the $p^2 \rightarrow 0$ limit that

$$\tilde{V}^{\text{Fig 4a}}(\mathbf{p}) = \left[\frac{5\pi C_A^{3/2}(\mathbf{p}^2)^2}{4608\gamma^6} + O((\mathbf{p}^2)^3) \right] \frac{g^6}{(16\pi^2)^2} \quad (6.15)$$

where, since we are working at two loops, we have put the sources in the adjoint representation. Useful in handling the group theory aspects of this calculation was the `color.h` FORM routine from [57] based on [78]. However, with the enhanced propagator of (6.12) we find in the same limit

$$\tilde{V}^{\text{Fig 4a}}(\mathbf{p}) \Big|_{\text{enhance}}^{SU(3)} = \left[\frac{3\mathbf{p}^2}{14\gamma^4} + O((\mathbf{p}^2)^2) \right] \frac{g^4}{16\pi^2} \quad (6.16)$$

where we record the $SU(3)$ result given that the arbitrary group expression would be too cumbersome. The reason for this is that this leading order term does not derive from the enhanced part of (6.12) but instead the $O(1/p^2)$ correction. In other words the dominant part of the exchange diagram in the zero momentum limit does not depend on the enhancement. This is because the one loop vertex subgraphs corrections are proportional to a structure function. More specifically the colour dependence of the vertex is $f^{abc}T^c$ where the group generator carries the indices of the source legs. Closing to form the Wilson loop leads to a trace over these indices when the other vertex is included. Since the colour channel of the enhanced part of the ξ_μ^{ab} propagator vanishes identically when the indices of this structure function are contracted then that contribution is absent. Indeed we have evaluated the one loop source ξ_μ^{ab} vertex function for the static potential momentum configuration exactly and verified that this colour structure is the source of the cancellation. Moreover, in this set-up the vertex function in principle involves two contributions deriving from the two possible vectors, v_μ and p_μ , which the vertex can be decomposed into since it has one free Lorentz index. It transpires that to this order the form factor of that of the p_μ term is zero leaving only that for v_μ . Hence, we do not need to consider the longitudinal part of the ξ_μ^{ab} propagator since we are in a static situation where $vp = 0$. Whilst there is the possibility of enhancement from the ρ_μ^{ab} propagator through similar topologies to

those illustrated on the left in Figure 4, each of the contributing vertex corrections vanish identically since the $P_{\mu\nu}(k)$ is contracted with k^μ where k is the loop momentum. This occurs because the gluon $\xi_\mu^{ab} \rho_\nu^{cd}$ vertex, which we have not neglected, is essentially proportional to the Landau gauge fixing condition. So in fact (6.16) represents the inclusion of both enhanced propagators of (6.12). Therefore, we appear to be forced to conclude that the single ξ_μ^{ab} exchange process of Figure 4 cannot lead to the dipole behaviour underpinning the linearly rising potential if the one loop enhancement of (6.12) is accepted.

Indeed considering the higher loop corrections to the source ξ_μ^{ab} vertex would not appear to remedy the situation. For instance, one would have to have a colour structure for the vertex which does not involve $f^{abc}T^c$ if the colour structure of (6.12) was preserved beyond one loop. Another candidate would be $d^{abc}T^c$ where d^{abc} is the totally symmetric rank three tensor but it clearly gives zero when contracted with (6.12). Whilst one might contrive something to circumvent this then the coefficient of whatever this colour tensor is would have to be constant in the zero momentum limit. It is not clear at which loop order this could emerge. Alternatively when the higher loop corrections to the propagators are computed then it may be the case that other colour channels aside from \mathcal{Q}_ξ are enhanced. In such a case the colour tensor of (6.12) should be different allowing the enhanced piece to dominate. Clearly such considerations are beyond the scope of the current article but suggest that using resummation methods such as the Schwinger Dyson technique could probe this in more detail. However, it is worth noting the situation with regard to the original observation of bosonic ghost enhancement of Zwanziger, [50]. In [50] an over-enhancement was obtained for various colour channels. In order to obtain a linearly rising potential it was argued, [50], that the quark gluon vertex develops a Lorentz tensor coupling involving $\sigma^{\mu\nu} = [\gamma^\mu, \gamma^\nu]$ together with one momentum vector to reduce the overall exchange to a dipole. Since we have considered in essence static gluons we do not have the same freedom in Lorentz space to accommodate a tensor coupling. However, provided the colour structure did not make the problem trivial then an over-enhancement would clearly reduce the power of momentum in (6.16) at least by another power. Indeed given this it could be the case that the higher loop corrections to (6.1) might also lead to an over-enhanced ξ_μ^{ab} propagator deriving from colour channels other than the propagator one with another colour structure to (6.12). Though we do note that ρ_μ^{ab} enhancement is preserved at *two* loops in $\overline{\text{MS}}$ using (5.6) similar to c^a and ω_μ^{ab} . To verify this enhancement we evaluated the 212 two loop Feynman diagrams of the ρ_μ^{ab} 2-point function in the zero momentum limit using the vacuum bubble expansion. We recall one advantage of the enhancement feature is that it avoids the proliferation of higher order powers in $1/p^2$ which could emerge if one calculated the static potential order by order in perturbation theory as indicated earlier. The use of the gap equation in being central to this appears to be unavoidably essential to any analysis of studying the zero momentum limit. If anything these remarks might only serve to indicate how delicate it is to determine the zero momentum behaviour of the localizing bosonic ghost propagators via the inversion of the matrix of 2-point functions. Having said this it is important to state that we are not ruling out the existence of a linearly rising potential in the Gribov-Zwanziger Lagrangian. There are other avenues one could consider aside from the single exchange of Figure 4. For instance, the enhanced ξ_μ^{ab} propagator can appear inside loop diagrams and hence one would have to use a Schwinger Dyson style of analysis to study the implications for the overall topologies in the infrared. The enhanced propagator would only be significant at low virtual loop momenta. Alternatively the dominant topologies in the infrared could be something such as ladder graphs instead of the simple single ξ_μ^{ab} graphs analysed here. Again that would require techniques beyond those discussed here.

7 Power corrections.

Next, we return to our earlier comments concerning the appearance of power type corrections of the form γ^2/\mathbf{p}^2 at higher loops in the static potential. However, we restrict them to our one loop static potential. First, one widely used tool to probe towards the infrared in QCD is the operator product expansion. In essence it provides a tool to include corrections to perturbative expressions where the corrections involve the vacuum expectation values of gauge invariant operators, such as $G_{\mu\nu}^a G^{a\mu\nu}$. In the conventional perturbative vacuum the expectation value of such operators is zero but in the true non-perturbative vacuum they acquire a non-zero value. Therefore such dimensionful quantities provide the mass scale required to have an expansion in inverse powers of the key momentum in the operator product expansion of the particular Green's function of interest. One situation where this formalism is applied is to the static potential. See, for example, [79, 80]. For instance, in [79] the zero momentum exchange of a single gluon with a one loop self-energy correction in gluon scattering is examined and a $1/(p^2)^3$ correction is produced where the dimensionality is made consistent by the presence of the dimension four quantity $\langle G_{\mu\nu}^a G^{a\mu\nu} \rangle$. However, clearly there is nothing to prevent higher order powers of $1/p^2$ appearing in such analyses and so it is worthwhile considering (4.7) in a similar power series expansion. Therefore, from (4.7) we have

$$\begin{aligned}
\tilde{V}(\mathbf{p}) = & - \frac{4\pi C_F \alpha_s(\mu)}{\mathbf{p}^2} \\
& \times \left[\left[1 - \frac{C_A \gamma^4}{(\mathbf{p}^2)^2} + O\left(\frac{\gamma^8}{(\mathbf{p}^2)^4}\right) \right] \right. \\
& + \left[\left[\frac{31}{9} - \frac{11}{3} \ln \left[\frac{\mathbf{p}^2}{\mu^2} \right] \right] C_A + \left[\frac{4}{3} \ln \left[\frac{\mathbf{p}^2}{\mu^2} \right] - \frac{20}{9} \right] T_F N_f - \frac{2\pi C_A^{3/2} \gamma^2}{\mathbf{p}^2} \right. \\
& + \left[\left[\frac{79}{12} \ln \left[\frac{\mathbf{p}^2}{\mu^2} \right] + \frac{9}{8} \ln \left[\frac{C_A \gamma^4}{(\mathbf{p}^2)^2} \right] - \frac{1315}{72} \right] C_A^2 \right. \\
& + \left. \left. \left[\frac{40}{9} - \frac{8}{3} \ln \left[\frac{\mathbf{p}^2}{\mu^2} \right] \right] T_F N_f \right] \frac{C_A \gamma^4}{(\mathbf{p}^2)^2} + O\left(\frac{\gamma^6}{(\mathbf{p}^2)^3}\right) \right] a \\
& + O(a^2) \left. \right]. \tag{7.1}
\end{aligned}$$

Clearly the leading term in this γ^2/\mathbf{p}^2 expansion is the perturbative result of [36, 37, 38]. Moreover, at leading order in the perturbative expansion the next to leading power correction is $O(\gamma^4/(\mathbf{p}^2)^3)$ which follows trivially since the full term is a function of γ^4 and not γ^2 which the one loop correction clearly is. Therefore, the leading tree part of the potential mimicks the correction observed in [79] although clearly here the quantity used to ensure the dimensions balance is γ^4 and not $\langle G_{\mu\nu}^a G^{a\mu\nu} \rangle$. Though it ought to be stressed here as was emphasised in [79], that this is a short distance approximation to the potential which has not fully been accounted for on the lattice. The reasoning is that the confinement force is in principle accessible at both low and higher energy scales. A recent exposition on this point has been provided in [81]. Though we believe one needs to be careful in this power correction approximation since mathematically a short distance expansion of the full potential can only give an insight into the r dependence for a limited range of r . So before considering the loop correction, the tree part of the potential considered as a power series in γ gives an interesting insight into applying the Fourier transform to coordinate space. As the exact transform is known in (4.15), it can be expanded in powers of γr which is also the combination of variables which appear and not their

square or higher powers. We find

$$V_0(r) = -\frac{C_F g^2}{4\pi r} \left[1 - \frac{C_A^{\frac{1}{4}} \gamma r}{\sqrt{2}} + \frac{C_A^{\frac{3}{4}} \gamma^3 r^3}{6\sqrt{2}} - \frac{C_A \gamma^4 r^4}{24} + O(\gamma^5 r^5) \right]. \quad (7.2)$$

The absence of a term linear in r is consistent with there being no dipole in the momentum space tree potential. However, the one-to-one power series matching clearly breaks down with the appearance of a quadratic correction which would ordinarily be associated with a momentum space term of $1/(\mathbf{p}^2)^{5/2}$ on dimensional grounds.

In the one loop correction of (7.1) one observes that a dipole correction appears at next to leading order in the power expansion rather than the triple pole at leading order. Parenthetically recalling our comments concerning the sign of γ^2 , then this term would then lead to an effective string tension, σ^{eff} , of

$$\sigma^{\text{eff}} = \frac{C_F C_A^{3/2} \gamma^2 g^4}{64\pi^2} \quad (7.3)$$

in the conventional definition of the potential. However, as is evident from our full expression there is actually no net explicit dipole term in (4.7) whose small momentum or large distance potential effectively becomes Coulomb-like. If there was a pure dipole present in addition to the remaining γ dependent part, then performing a power series expansion of the full expression would mean it would be difficult to isolate its contribution *uniquely*. Moreover, it would be difficult to interpret such a correction in an operator power series context since it would involve the square root of the gluon condensate or the vacuum expectation value of a dimension two object. In the Gribov-Zwanziger context such an operator could be $f^{abc} A^a \mu \xi_\mu^{ab}$ which from the equation of motion

$$\xi_\mu^{ab} = i\gamma^2 f^{abc} \frac{1}{\partial^\nu D_\nu} A_\mu^c \quad (7.4)$$

would effectively equate to the presence of the Gribov horizon condition operator. Though one other application of (4.7) could be to use it as a testbed for examining renormalon style corrections, like [80], since the gap equation solution (5.3) is clearly non-perturbative. For instance, in the V -scheme we would have a power correction beyond the perturbative contribution of (4.10) in (4.19) which is

$$\alpha_V(\mathbf{p}) = \alpha_V^{\text{pert}}(\mathbf{p}) - \frac{C_A^{3/2} \gamma^2 \alpha_s^2(\mu)}{2\mathbf{p}^2} + O\left(\frac{\gamma^4}{(\mathbf{p}^2)^2}\right). \quad (7.5)$$

where, [36, 37, 38],

$$\alpha_V^{\text{pert}}(\mathbf{p}) = \alpha_s(\mu) \left[1 + \left[\left[\frac{31}{9} - \frac{11}{3} \ln \left[\frac{\mathbf{p}^2}{\mu^2} \right] \right] C_A + \left[\frac{4}{3} \ln \left[\frac{\mathbf{p}^2}{\mu^2} \right] - \frac{20}{9} \right] T_F N_f \right] a(\mu) + O(a^2) \right]. \quad (7.6)$$

A formally similar power correction was observed in the effective coupling of (5.13) in [33] where the correction had the same sign. In order to compare and for completeness we record that the power correction to this renormalization group invariant coupling in the same notation as (7.6), [33], is

$$\alpha_{\text{eff}}(\mathbf{p}) = \alpha_{\text{eff}}^{\text{pert}}(\mathbf{p}) - \frac{9C_A^{3/2} \gamma^2 \alpha_s^2(\mu)}{16\mathbf{p}^2} + O\left(\frac{\gamma^4}{(\mathbf{p}^2)^2}\right) \quad (7.7)$$

where

$$\alpha_{\text{eff}}^{\text{pert}}(\mathbf{p}) = \alpha_s(\mu) \left[1 + \left[\left[\frac{169}{36} - \frac{11}{3} \ln \left[\frac{\mathbf{p}^2}{\mu^2} \right] \right] C_A + \left[\frac{4}{3} \ln \left[\frac{\mathbf{p}^2}{\mu^2} \right] - \frac{20}{9} \right] T_F N_f \right] a(\mu) + O(a^2) \right]. \quad (7.8)$$

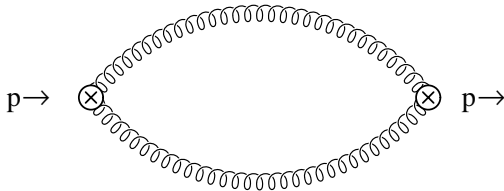


Figure 5: Leading contribution to operator correlation function.

Next, we comment on one aspect concerning potentials and that is whether it is possible to observe *stable* bound states. If there were such states then these could possibly be identified with glueballs. However, since we have demonstrated that the static potential does not have a linear confining part at one loop but a form not dissimilar to that of $V_0(r)$, we expect any states formed in, say, a Schrödinger equation analysis of (4.7) to be unstable. For instance, in [67] a confining piece had to be included in that glueball analysis which assumed a gluon mass. For a similar calculation in the Gribov-Zwanziger context one would have to implement the gap equation for the Gribov mass in some fashion in addition. Aside from this one way of possibly quantifying properties of bound state masses is by considering the correlation of operators with the same quantum numbers as the bound states along the lines of [13]. For glueballs the obvious candidate operators are those involving the field strength given by

$$\mathcal{O}_S = -\frac{1}{4} G_{\mu\nu}^a G^{a\mu\nu} \quad , \quad \mathcal{O}_T^{\mu\nu} = -\frac{1}{4} \left(\frac{\eta^{\mu\nu}}{d} G_{\sigma\rho}^a G^{a\sigma\rho} - G^{a\mu\sigma} G_{\nu\sigma}^a \right) \quad (7.9)$$

since they are gluonic and gauge invariant, where the subscripts S and T denote Lorentz scalar and tensor operators respectively and the second operator is symmetric and traceless. It is based on a similar operator considered in [82]. Indeed Zwanziger has examined the first operator in the context of (2.19) by considering the leading term of the correlator of \mathcal{O}_S , [13]. In [13] it was suggested that there was evidence for a state with mass squared $2\sqrt{C_A}\gamma^2$, in our conventions, by rewriting the correlation function in a spectral representation using tools such as Schwinger and Feynman parameters and searching for physical cuts. However, a full explicit expression for the correlator as a function of the momentum and γ at leading order was not given. Therefore, to partly address this we have computed the leading order term of the correlator of \mathcal{O}_S *exactly*. The Feynman diagram is illustrated in Figure 5 where the crossed circled denotes the location of the operator insertion with momentum p flowing through it. Defining

$$\Pi_S(p^2) = (4\pi)^2 i \int d^4x e^{ipx} \langle 0 | \mathcal{O}_S(x) \mathcal{O}_S(0) | 0 \rangle \quad (7.10)$$

we have

$$\begin{aligned} \Pi_S(p^2) = & \left[\frac{(p^2)^2}{4\epsilon} - \frac{3C_A\gamma^4}{\epsilon} + \frac{C_A\gamma^4 \sqrt{4C_A\gamma^4 - (p^2)^2}}{4p^2} \tan^{-1} \left[\frac{\sqrt{4C_A\gamma^4 - (p^2)^2}}{p^2} \right] \right. \\ & \left. - \frac{\pi C_A^{3/2} \gamma^6}{4p^2} + \frac{p^2}{8} \sqrt{4C_A\gamma^4 - (p^2)^2} \tan^{-1} \left[\frac{\sqrt{4C_A\gamma^4 - (p^2)^2}}{p^2} \right] \right] \end{aligned}$$

$$\begin{aligned}
& + \left[\frac{3}{2} \ln \left[\frac{C_A \gamma^4}{\mu^4} \right] - \frac{3}{2} + \frac{3\sqrt{2}}{16} \eta_2(p^2) \right] C_A \gamma^4 + \left[\frac{3\pi}{8} + \frac{\sqrt{2}}{8} \eta_1(p^2) \right] \sqrt{C_A} \gamma^2 p^2 \\
& + \left[\frac{1}{4} - \frac{1}{8} \ln \left[\frac{C_A \gamma^4}{\mu^2} \right] - \frac{\sqrt{2}}{32} \eta_2(p^2) \right] (p^2)^2 \Big] N_A + O(a) \tag{7.11}
\end{aligned}$$

where the divergent contact terms are included for completeness. These are absorbed by the canonical contact renormalization for operator correlation functions but we note that as there is a Gribov parameter present this contact renormalization actually has a mixing aspect which is not unexpected. Given this one can regard the finite part as the leading piece of the correlation function since the first appearance of an explicit coupling constant is at next order, ignoring the coupling constant implicit in γ , (5.3). We have checked that there are no poles in the expression at obvious places such as $\sqrt{C_A} \gamma^2$, $2\sqrt{C_A} \gamma^2$ or $4\sqrt{C_A} \gamma^2$ and hence regard this correlation function to be regular as a function of p^2 . However, one can see that there is a cut at the same value as observed in [13] which is $p^2 = 2\sqrt{C_A} \gamma^2$ and this is at the same point as the cut in (4.7). Equally it is elementary to verify Zwanziger's other observation in [13] that there are unphysical cuts at $p^2 = \pm 4i\sqrt{C_A} \gamma^2$ in our conventions similar to (4.7). One final point concerning the structure of $\Pi_S(p^2)$ in relation to both glueball states and the physical cut structure and that is that the same conclusion would be obtained if other operators with similar properties to \mathcal{O}_S were considered. For instance, the correlation functions of both the operators $\text{Tr}[(D_\mu G_{\nu\sigma})(D^\mu G^{\nu\sigma})]$ and $\text{Tr}[(D_\mu D_\nu G_{\sigma\rho})(D^\mu D^\nu G^{\sigma\rho})]$ with themselves, where $G_{\mu\nu} = G_{\mu\nu}^a T^a$, will produce the same physical and unphysical cuts as (7.11). These Lorentz scalar operators are both gauge invariant and have the same number of leading gluon legs.

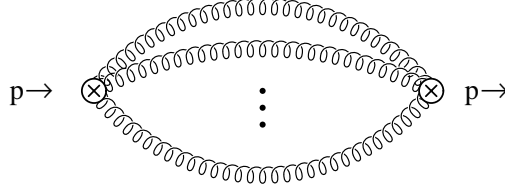


Figure 6: Higher order graphs contributing to operator correlation functions.

For higher loop graphs contributing to the gluonic operator correlation functions it is straightforward to determine the location of the physical cuts. Such graphs are illustrated in Figure 6 where the dots denote more and more gluon propagators. When there are an odd number of gluons then there are unphysical cuts but no physical ones. For an even number of gluons, say $2n$, then there are both types of cuts with the physical ones being at $p^2 = 2n^2\sqrt{C_A} \gamma^2$. The pattern of unphysical cuts cannot be written in as compact a formula. As noted by Zwanziger, [13], for the two gluon case the cuts additional to the physical ones are at $p^2 = \pm 4i\sqrt{C_A} \gamma^2$. It is straightforward to record those for the lowest order cases. For the three gluon situation the only cuts are at $p^2 = \pm i\sqrt{C_A} \gamma^2$, $p^2 = \pm 9i\sqrt{C_A} \gamma^2$ and $p^2 = (\pm 4 \pm 3i)\sqrt{C_A} \gamma^2$ where all possible sign combinations are taken in the final off axis cut. For four gluons, the unphysical cuts are now at $p^2 = \pm 4i\sqrt{C_A} \gamma^2$, $p^2 = \pm 16i\sqrt{C_A} \gamma^2$ and $p^2 = 2(\pm 4 \pm 3i)\sqrt{C_A} \gamma^2$. For other Green's functions, such as the higher loop corrections to (4.7), we expect the physical (and unphysical) cut structure to be the same. Returning to Figure 6 and, for instance, ignoring the presence of internal vertices for the moment, the next physical cut in (7.11) will be at $p^2 = 8\sqrt{C_A} \gamma^2$. If instead of (7.11) one considers the correlation function of a gauge invariant operator involving three gluons in the leading leg term, such as $f^{abc} G_{\mu\nu}^a G^{b\nu}_\sigma G^{c\sigma\mu}$ which was considered in [83], then the first cut would be at $p^2 = 8\sqrt{C_A} \gamma^2$ with the subsequent one at $p^2 = 18\sqrt{C_A} \gamma^2$. In [83] QCD sum rules were used to estimate the masses of various glueball states. For instance, the two gluon

scalar glueball mass was $M_{2g} = (1.50 \pm 0.19)\text{GeV}$ and that for the three gluon bound state was $M_{3g} = 3.1\text{GeV}$ with no errors quoted, [83]. Intriguingly the mass ratio is $M_{3g}/M_{2g} \approx 2$. If we take the ratio of the leading physical cuts for the appropriate gauge invariant gluonic operator correlation functions then we have the *same* ratio deriving from the expression of the ratio in the crude form $\sqrt{8/2}$. By contrast, however, if one was working with gluons which had an ordinary massive propagator instead of the Gribov width, then one would have a canonical cut structure in the corresponding Feynman diagrams. Overlooking the obvious loss of gauge invariance for the moment, then the corresponding ratio for M_{3g}/M_{2g} would be $3/2$. This seems to be too far away to accommodate the mass ratio of [83]. Returning to the Gribov-Zwanziger case, an estimate was also given in [83] for the tensor 2^{++} state which was $M_{2^{++}} = (2.0 \pm 0.1)\text{GeV}$. This gives the ratio $M_{2^{++}}/M_{2g} \approx 4/3$. Such a ratio can be accommodated in terms of ratios of physical cuts, such as $\sqrt{32/18}$ in crude form. Similarly, $M_{3g}/M_{2^{++}}$ can be accommodated by the ratio $\sqrt{18/8}$. However, we acknowledge that the justification of these latter ratios from a simple diagram argument similar to the earlier one seems to be tenuous. This is partly because (4.7) can only really be regarded as being relevant for spinless zero angular momentum bound states such as the lowest lying two and three gluon states. For states such as 2^{++} one requires more detailed structure beyond the simple radial dependence provided in (4.7), such as that considered in depth in [67]. It would be interesting, though, to see if the ratio of $4/3$ could be justified from that point of view in an extended potential incorporating spin and angular momentum. However, even though we are primarily concentrating on Yang-Mills here the issue of degeneracy will arise at some point for the higher states. Whilst not as involved a problem as when quarks are present, which would clearly extend the number of potential bound states, resolving any mixing will require a much more detailed analysis of a potential derived from (2.19). Another test of the ratio hypothesis would be the mass of a four gluon state which ought to be roughly three times that of the lowest state if our reasoning is sound. However, such a state has not been extensively studied, for example on the lattice, as far as we are aware. Finally, in this simple cut analysis we need to temper our remarks with the fact that with the inclusion of higher loops it is not inconceivable that the cut locations will be shifted by corrections. So our method of estimating mass ratios should only be regarded as a rough guide.

Whilst trying to understand the relative sizes of various glueball states is an interesting exercise in itself, ultimately one has to eventually estimate one of the masses which is a non-trivial task. We draw attention to several possibilities in the context of (2.19). In each case one has to somehow fix a mass scale in relation to a measured quantity from other methods such as the lattice in order to obtain a numerical value for $\sqrt{C_A}\gamma^2$ which is the fundamental mass parameter in (2.19). One approach to extract a glueball mass would be to consider the power corrections to (7.11) and apply sum rule technology akin to that used in [82, 83] where the gluon condensate is the quantity used to fix a scale. In [82] a tachyonic gluon mass was introduced to account for apparent discrepancies with experimental data. Performing the detailed analyses for both these approaches is clearly outside the scope of the current article. For example, a proper sum rule analysis would first require a reworking of the original operator product expansion but using the Lagrangian of (2.19) rather than the usual QCD Lagrangian. However, we have computed the leading power correction to (7.11) in the context of the gluonia channels of $\Pi_S(q^2)$ considered in [82]. Therefore, using the same moment definition and notation as [82] we have

$$\Pi_S(M^2) = (\text{parton model}) \left[1 - \frac{6C_A\gamma^4}{M^4} + O\left(\frac{\gamma^8}{M^8}\right) \right] \quad (7.12)$$

where

$$\Pi_S(M^2) \equiv \frac{(p^2)^n}{(n-1)!} \left(\frac{d}{dp^2} \right)^n \Pi_S(p^2) \quad (7.13)$$

and $M^2 = p^2/n$ is finite in the limit of large p^2 and n . As a check on our derivation of this power correction using FORM, [57], we have replaced the gluon propagator of (2.19) by the tachyonic gluon mass propagator of [82] and correctly reproduced the power correction *quadratic* in this mass recorded in [82]. As we are dealing with a gauge invariant operator correlation function in the Gribov-Zwanziger case the first power correction is quartic with the correction numerator being related on dimensional grounds to the gluon condensate. Although in the static potential case the leading order function was a function of γ^4 , the loop correction produced $O(\gamma^2)$ terms in the power series expansion. Such a scenario could emerge for $\Pi_S(p^2)$ when the $O(a)$ correction is computed. Though this is currently beyond the scope of this article as well as using sum rules to estimate scalar or tensor glueball masses akin to [83]. Finally, for the correlation function of the tensor operator $\mathcal{O}_T^{\mu\nu}$, similar power corrections should emerge in each of the scalar amplitudes of its Lorentz decomposition. We record the full expressions for the tensor case for completeness, and for comparison with [82], in appendix C as they are similar to (7.11). However, there is nothing formally different from the scalar case above having, for example, the same physical cut.

Another approach would be to make direct contact with a non-zero vacuum expectation value, whose numerical value is known, by explicit computation using (2.19) itself. This is possible since now the gluon propagator is not massless, (2.21), and so vacuum expectation values of gluonic operators are non-zero. Such an approach has already been used in [84, 85, 86] but where the gluon is assumed to have a canonical mass term. Ignoring the first of these three papers, since it appears to have a result inconsistent with the latter two, an estimate for the gluon mass was deduced by comparing the leading order gluon condensate value with the quark current correlator in the high energy limit at the same order. However, we can also consider the dimension two condensate based on the operator $\frac{1}{2}(A_\mu^a)^2$ which has been measured on the lattice in [72, 73]. At leading order we have

$$\left\langle \frac{1}{2} (A_\mu^a)^2 \right\rangle = \frac{3N_A \sqrt{C_A} \gamma^2}{64\pi} + O(a). \quad (7.14)$$

So, for instance, at leading order we have the formal relation for a glueball mass, if we regard our lowest cut as a glueball mass, of $2\sqrt{C_A}\gamma^2 = (16\pi/3)\langle\frac{1}{2}(A_\mu^a)^2\rangle$. Taking the lattice estimate of $\langle(A_\mu^a)^2\rangle = 3.1\text{GeV}^2$, from [73], for example, then this rough way of estimating would give an unrealistic glueball mass of 5.1GeV. Aside from this one ought not to overlook the gap equation, (5.2), which is assumed to be valid at this order of approximation. If one uses representative numerical values for $\sqrt{C_A}\gamma^2$ derived in this way and a reasonable estimate for $\Lambda_{\overline{\text{MS}}}$ of, say, $\Lambda_{\overline{\text{MS}}} = 300\text{MeV}$ then one would obtain a *negative* value of α_s which is clearly unacceptable. Though this is partly due to the Landau pole problem of the running coupling constant. (We find similar conclusions when the gluon condensate is used similar to [85].) Of course, this simple exercise has been recorded to merely illustrate some of the potential difficulties in estimating a value for the underlying mass parameter of (2.19). Indeed we have only considered leading order and including higher order corrections will in principle change the estimates. However, the full vacuum expectation value should have a non-perturbative piece which would need to be properly incorporated into any deeper analysis as well as dealing with infrared issues which are known to exist in the case of the gluon condensate. The lack of consistency with the Gribov gap equation to the order we considered, clearly indicates that the approximations assumed here could not be validated in a consistent way. By contrast there is no equivalent gap equation constraint on the fundamental gluon mass used in the analyses of [84, 85, 86]. Also, it may be the case that the Gribov gap equation would require a more complete function of a beyond the perturbative approximation. Therefore, whilst carrying out this rough leading order analysis has led to a null conclusion, we feel it is useful to include it as a moderating point of view since it does perhaps illustrate the difficulty in producing a reasonable estimate for the underlying mass parameter of

(2.19). Indeed it may also be indicative that the use of condensates to fix a mass scale may not be compatible when a Gribov mass is present.

8 Discussion.

The main result of this article is the explicit construction of the one loop static potential using the Gribov-Zwanziger Lagrangian. The original motivation was to study a gauge invariant object related to the non-perturbative structure of a formulation of a non-abelian gauge theory which has properties suggesting it describes a confined gluon. Indeed one aim was to see what functions of momentum appeared in the explicit final expression. Whilst a linear potential clearly does not emerge in the final result, there is an intriguing hint with the presence of a pure dipole term but which has a compensating term in the zero momentum limit for positive γ^2 . Ultimately we have to conclude that the usefulness of this approach to the static potential is that it will in principle closely match the full potential if one adds successive loop corrections to (4.7). So it would appear that in the present context a linearly rising potential for a significant range of r arises out of a truly non-perturbative effect. Indeed it is hard to see how the compensating term could be split from the pure dipole in higher loop corrections to leave a net dipole as well as no net higher order momentum poles. Therefore, some non-perturbative feature must be taken into account.

In the context of this field theoretic approach in the Gribov set-up the most promising candidate for this is the (non-perturbative) Gribov gap equation. To this end we revisited the behaviour of the bosonic ρ_μ^{ab} and ξ_μ^{ab} localizing ghosts which dominate in the infrared and are responsible in essence for implementing the horizon condition in (2.19). We have been able to derive enhancement for both bosonic localizing ghosts, together with the colour structure but it differs from that derived in Zwanziger's Schwinger Dyson analysis, [50]. Moreover, we do not find the over-enhancement discovered in [50]. We have discussed various possibilities that might lead to similar behaviour but this would at least require a higher loop computation. One lesson appears to be that the inversion of the matrix of 2-point functions to obtain the propagators is intricately tied to the colour group structure of the corrections. For instance, to extend the perturbative analysis to the two loop level is in principle possible in the zero momentum limit but requires the computation of over 1000 Feynman diagrams since one has to consider the full matrix of 2-point functions in the $\{A_\mu^a, \xi_\mu^{ab}\}$ sector. This would at least give some indication of the zero momentum behaviour of the colour channels not present in the original Lagrangian and whether the gap equation emerges in the corrections similar to (6.1). It could be the case that additional enhancement arises in other channels or an over-enhancement akin to that of [50]. The aim of such an analysis would be to see if a dipole dominated the exchange between the static colour sources of the formalism but in such a way that higher order poles were excluded.

Further, one underlying feature of the static potential formalism is the absence of a direct coupling of the source to either ρ_μ^{ab} or ξ_μ^{ab} which prevents the direct single ρ_μ^{ab} or ξ_μ^{ab} field exchange with an enhanced propagator being the simple explanation for a linear potential, provided such a vertex did not depend on the exchange momentum. Though one would naively believe ξ_μ^{ab} has to play some role in this way since from its equation of motion it is a non-local projection of the gluon. Perhaps the original Wilson loop static potential formalism would need to be reconsidered in the Gribov-Zwanziger case due to the restriction of the path integral to the Gribov region of configuration space. From another point of view, although the Gribov-Zwanziger Lagrangian is consistent with the Kugo-Ojima confinement criterion, [34, 35], that is a necessary but not sufficient condition for confinement which would imply that an additional feature might be necessary in (2.19) to obtain a confining potential. For instance, the Gribov construction is

founded on the *infinitesimal* behaviour of the gauge fixing condition, [10], and the less local aspects of that construction might need to be included now.

Throughout the article we have concentrated on what is referred to now as the conformal or scaling solution. In recent years there has been interest in an alternative point of view which is called the decoupling solution, [22, 23, 24, 25, 26, 27, 28, 29]. Essentially this scenario differs from the gluon suppression and ghost enhancement properties of the conformal solution, in having no Faddeev-Popov ghost enhancement and the gluon propagator freezes to a finite non-zero value excluding suppression. The evidence for this behaviour derives from both lattice gauge theory and Schwinger Dyson analyses, [22, 23, 24, 25, 26, 27, 28, 29]. As yet there is no definitive consensus as to which of the conformal or decoupling solutions is the correct picture of infrared Landau gauge Yang-Mills theory.

One proposal to explain the lack of suppression and enhancement in the Gribov-Zwanziger Lagrangian is the condensation of the BRST invariant operator $\bar{\phi}_\mu^{ab}\phi^{ab\mu} - \bar{\omega}_\mu^{ab}\omega^{ab\mu}$, [52, 53], using the notation of the original localizing fields. With a non-zero value for the vacuum expectation value of this operator the observed behaviour of the gluon and Faddeev-Popov ghost propagators could be accommodated. However, to include such an operator one applies the local composite operator formalism developed in [87, 88, 89]. Briefly the method introduces a new source coupled to the dimension two operator and then constructs the effective potential of the operator. Studying the minima of this effective potential one observes that the perturbative vacuum solution is unstable in favour of a vacuum solution where the operator condenses. Hence a new dynamically generated mass is introduced which modifies the propagators of the appropriate fields. In the application to the Gribov-Zwanziger Lagrangian, [52, 53], both sets of localizing ghosts acquire a mass and induce extra mass dependence in the gluon and Faddeev-Popov ghost propagators. Moreover, the corresponding gap equation is insufficient to produce a Faddeev-Popov enhancement.

This raises several points for our static potential calculation. First, we have taken the point of view that the ρ_μ^{ab} , ξ_μ^{ab} and ω_μ^{ab} localizing fields are purely *internal* fields with no coupling to external sources in the way the gluon does. Therefore, it seems unclear how to incorporate all the dynamically modified propagators at the outset since including them would require coupling an *operator* of internal fields to an external source. Moreover, to have a homogeneous renormalization group interpretation in the local composite operator formalism one has to allow for the generation of the square of this external source. However, even if one relaxed such assumptions or used the modified propagators directly in the analogous computation of (4.7) then it seems difficult to see how a linearly rising term could emerge in the corresponding static potential due to the absence of enhancement.

This leads on to the other point of view we examined and that was the enhancement of ρ_μ^{ab} and ξ_μ^{ab} . It now appears evident, at least in the conformal solution, that the enhancement of the Faddeev-Popov ghost, ρ_μ^{ab} , ξ_μ^{ab} and ω_μ^{ab} are on the same footing and inextricably linked. Therefore, if there is a loss of enhancement in the decoupling solution for the Faddeev-Popov ghost it would seem inevitable that this would be the case for the localizing fields too. Whilst we analysed the simple two loop contribution of Figure 4 to the static potential with enhanced ξ_μ^{ab} and ρ_μ^{ab} propagators, it was insufficient with the enhancement to produce a dipole behaviour at one loop primarily due to group theory considerations. If there was a non-enhanced ξ_μ^{ab} propagator in the decoupling case then there would appear to be no emergence of anything like a dipole behaviour in the zero momentum limit. However, the behaviour of the ρ_μ^{ab} and ξ_μ^{ab} propagators in the infrared for the decoupling solution has not been established yet. If the decoupling solution is established as the correct description of the infrared properties of Landau gauge Yang-Mills it would be interesting to see how the linearly rising potential emerges in

the field theory context. For instance, in [19] the Wilson loop was considered in the context of (2.19) and it was shown that the string tension of a linearly rising potential depended on the zero momentum value of a particular combination of the gluon and Faddeev-Popov ghost propagator form factors. Briefly, if the gluon propagator froze to a zero or non-zero value but the Faddeev-Popov ghost was *enhanced* then a linear potential emerged. If the argument of [19] remains valid in the decoupling scenario then the lack of Faddeev-Popov enhancement would seem to exclude a linear potential in that case.

Acknowledgement. The author thanks Dr F.R. Ford, Prof. S.J. Hands, Dr P.E.L. Rakow, Prof. S.P. Sorella and Prof. D. Zwanziger for useful discussions. Support from IHES, Paris, France, where part of this work was carried out, is also gratefully acknowledged.

A Group theory.

In this appendix we discuss the decomposition of products of group generators into the basis of Casimirs. For a comprehensive review of such Casimirs we refer the reader to [78]. In section 6 we introduced the two sets of coefficients $\{a_i\}$ and $\{b_i\}$ where

$$d_A^{abpq} d_A^{cdpq} = a_1 \delta^{ab} \delta^{cd} + a_2 (\delta^{ac} \delta^{bd} + \delta^{ad} \delta^{bc}) + a_3 (f^{ace} f^{bde} + f^{ade} f^{bce}) + a_4 d_A^{abcd} \quad (\text{A.1})$$

and

$$f^{ape} f^{bqe} d_A^{cdpq} = b_1 \delta^{ab} \delta^{cd} + b_2 (\delta^{ac} \delta^{bd} + \delta^{ad} \delta^{bc}) + b_3 (f^{ace} f^{bde} + f^{ade} f^{bce}) + b_4 d_A^{abcd}. \quad (\text{A.2})$$

These coefficients can be computed by the projection method. By this we mean that each tensor on the right hand side is used in sequence to multiply each equation. Using the properties of the Lie algebra this leads to a set of linear equations for the a_i and b_i which can be solved by simple matrix inversion. It transpires that the matrix which needs to be inverted is the same for both (A.1) and (A.2) and is

$$M = \begin{pmatrix} N_A^2 & 2N_A & 2C_A N_A & \frac{5}{6} C_A^2 N_A \\ 2N_A & 2N_A(N_A + 1) & -2C_A N_A & \frac{5}{3} C_A^2 N_A \\ 2C_A N_A & -2C_A N_A & 3C_A^2 N_A & 0 \\ \frac{5}{6} C_A^2 N_A & \frac{5}{3} C_A^2 N_A & 0 & d_A^{abcd} d_A^{abcd} \end{pmatrix}. \quad (\text{A.3})$$

To determine a_i and b_i the inverse of M multiplies the respective vectors

$$\begin{pmatrix} \frac{25}{36} C_A^4 N_A \\ 2d_A^{abcd} d_A^{abcd} \\ \frac{2}{3} C_A d_A^{abcd} d_A^{abcd} \\ d_A^{abcd} d_A^{cdpq} d_A^{abpq} \end{pmatrix} \quad \text{and} \quad \begin{pmatrix} \frac{5}{6} C_A^3 N_A \\ 0 \\ 2d_A^{abcd} d_A^{abcd} \\ \frac{1}{3} C_A d_A^{abcd} d_A^{abcd} \end{pmatrix}. \quad (\text{A.4})$$

Hence, we find

$$\begin{aligned} a_1 &= - \left[540 C_A^2 N_A (N_A - 3) d_A^{abcd} d_A^{cdpq} d_A^{abpq} + 144 (2N_A + 19) (d_A^{abcd} d_A^{abcd})^2 \right. \\ &\quad \left. - 150 C_A^4 N_A (3N_A + 11) d_A^{abcd} d_A^{abcd} + 625 C_A^8 N_A^2 \right] \\ &\quad \times \frac{1}{54 N_A (N_A - 3) [12 (N_A + 2) d_A^{efgh} d_A^{efgh} - 25 C_A^4 N_A]} \end{aligned}$$

$$\begin{aligned}
a_2 &= \left[144(11N_A - 8) \left(d_A^{abcd} d_A^{abcd} \right)^2 - 1080C_A^2 N_A (N_A - 3) d_A^{abcd} d_A^{cdpq} d_A^{abpq} \right. \\
&\quad \left. + 625C_A^8 N_A^2 - 3000C_A^4 N_A d_A^{abcd} d_A^{abcd} \right] \\
&\quad \times \frac{1}{108N_A(N_A - 3)[12(N_A + 2)d_A^{efgh} d_A^{efgh} - 25C_A^4 N_A]} \\
a_3 &= \frac{[12(N_A + 2)d_A^{abcd} d_A^{abcd} - 25C_A^4 N_A]}{54C_A N_A (N_A - 3)} \\
a_4 &= \frac{[216(N_A + 2)d_A^{abcd} d_A^{cdpq} d_A^{abpq} - 125C_A^6 N_A - 360C_A^2 d_A^{abcd} d_A^{abcd}]}{18[12(N_A + 2)d_A^{efgh} d_A^{efgh} - 25C_A^4 N_A]} \tag{A.5}
\end{aligned}$$

and

$$b_1 = -2b_2 = \frac{[5C_A^4 N_A - 12d_A^{abcd} d_A^{abcd}]}{9C_A N_A (N_A - 3)}, \quad b_3 = \frac{[6(N_A - 1)d_A^{abcd} d_A^{abcd} - 5C_A^4 N_A]}{9C_A^2 N_A (N_A - 3)}, \quad b_4 = \frac{C_A}{3}. \tag{A.6}$$

These expressions have been derived by making use of the `color.h` package of [57, 78]. Both sets of coefficients can be evaluated explicitly for $SU(N_c)$ and for completeness we note the values of the various Casimirs in this instance are

$$N_A = N_c^2 - 1, \quad C_A = N_c, \quad \frac{d_A^{abcd} d_A^{abcd}}{N_A} = \frac{N_c^2 [N_c^2 + 36]}{24} \tag{A.7}$$

where the last expression is given in [90]. The set $\{a_i\}$ also require $d_A^{abcd} d_A^{cdpq} d_A^{abpq}$ which we have evaluated directly using the $SU(N_c)$ identity of [91]

$$f^{abe} f^{cde} = \frac{2}{N_c} [\delta^{ac} \delta^{bd} - \delta^{ad} \delta^{bc}] + d^{ace} d^{bde} - d^{ade} d^{bce} \tag{A.8}$$

and relations for products of the structure functions and the totally symmetric rank 3 tensor d^{abc} , [91]. As an intermediate step we have

$$d_A^{abcd} = \frac{2}{3} [\delta^{ab} \delta^{cd} + \delta^{ac} \delta^{bd} + \delta^{ad} \delta^{bc}] + \frac{N_c}{12} [d^{abe} d^{cde} + d^{ace} d^{bde} + d^{ade} d^{bce}] \tag{A.9}$$

for $SU(N_c)$ which we have checked correctly reproduces the final expression of (A.7). Hence, we found

$$\frac{d_A^{abcd} d_A^{cdpq} d_A^{abpq}}{N_A} = \frac{N_c^2 [N_c^4 + 135N_c^2 + 324]}{216}. \tag{A.10}$$

We have checked the consistency of this expression by explicitly evaluating the left hand side for both colour groups $SU(2)$ and $SU(3)$. To do this we used the explicit respective 3×3 and 8×8 matrix representations of the adjoint group generators using FORM. Although it is not required here, as a corollary we have also determined the $SU(N_c)$ value for $d_A^{abcdef} d_A^{abcdef}$ which is introduced in [78]. We find

$$\frac{d_A^{abcdef} d_A^{abcdef}}{N_A} = \frac{N_c^2 [N_c^4 + 666N_c^2 + 1800]}{1920}. \tag{A.11}$$

Equipped with the $SU(N_c)$ values of these Casimirs we have

$$a_1 = \frac{7N_c^2}{12}, \quad a_2 = -\frac{N_c^2}{24}, \quad a_3 = \frac{N_c(N_c^2 - 9)}{108}, \quad a_4 = \frac{(N_c^2 + 9)}{9} \tag{A.12}$$

and

$$b_1 = -2b_2 = \frac{N_c}{2}, \quad b_3 = \frac{(N_c^2 + 18)}{36}, \quad b_4 = \frac{N_c}{3}. \tag{A.13}$$

It is worth noting that some of the numerator factors as well as the denominator factors of a_i , which are N_A , $(N_A^2 - 3)$ and $[12(N_A + 2)d_A^{abcd}d_A^{abcd} - 25C_A^4N_A]$, have zeroes at $N_c = 1, 2$ and 3 . Therefore, one cannot directly evaluate a_i for the latter two values of N_c but must derive the N_c dependent expressions first before determining numerical values.

B Transverse parts.

In this appendix we collect the explicit one loop $\overline{\text{MS}}$ expressions for the transverse parts of the 2-point functions of (3.1). We have

$$\begin{aligned}
X = & \left[-\frac{37\pi}{128}\sqrt{C_A^3}\gamma^2 - \left[\frac{23}{48}\tan^{-1}\left[\frac{\sqrt{C_A}\gamma^2}{p^2}\right] + \frac{25\sqrt{2}}{64}\eta_1(p^2) \right] \sqrt{C_A^3}\gamma^2 \right. \\
& - \frac{7C_A\sqrt{4C_A\gamma^4 - (p^2)^2}}{192}\tan^{-1}\left[-\frac{\sqrt{4C_A\gamma^4 - (p^2)^2}}{p^2} \right] \\
& - \frac{3C_A^2\gamma^4}{8(p^2)^2}\sqrt{4C_A\gamma^4 - (p^2)^2}\tan^{-1}\left[-\frac{\sqrt{4C_A\gamma^4 - (p^2)^2}}{p^2} \right] \\
& - \frac{59\pi}{128}\frac{\sqrt{C_A^5}\gamma^6}{(p^2)^2} + \frac{11}{64}\frac{\sqrt{C_A^5}\gamma^6}{(p^2)^2}\tan^{-1}\left[\frac{\sqrt{C_A}\gamma^2}{p^2}\right] \\
& + \left[\frac{35}{64} - \frac{47}{192}\ln\left[1 + \frac{(p^2)^2}{C_A\gamma^4}\right] \right] \frac{C_A^2\gamma^4}{p^2} + \left[\frac{4}{3}\ln\left[\frac{p^2}{\mu^2}\right] - \frac{20}{9} \right] T_F N_f p^2 \\
& + \left[\frac{1939}{576} - \frac{135}{128}\ln\left[\frac{C_A\gamma^4}{\mu^4}\right] + \frac{7}{64}\ln\left[\frac{[(p^2)^2 + C_A\gamma^4]}{\mu^4}\right] \right. \\
& \quad \left. - \frac{53}{192}\ln\left[\frac{p^2}{\mu^2}\right] - \frac{241\sqrt{2}}{768}\eta_2(p^2) \right] C_A p^2 \\
& + \frac{25(p^2)^2}{768\gamma^4}\sqrt{4C_A\gamma^4 - (p^2)^2}\tan^{-1}\left[-\frac{\sqrt{4C_A\gamma^4 - (p^2)^2}}{p^2} \right] - \frac{131\pi}{768}\frac{\sqrt{C_A}(p^2)^2}{\gamma^2} \\
& + \left[\frac{19}{192}\tan^{-1}\left[\frac{\sqrt{C_A}\gamma^2}{p^2}\right] - \frac{35\sqrt{2}}{384}\eta_1(p^2) \right] \frac{\sqrt{C_A}(p^2)^2}{\gamma^2} \\
& + \left[\frac{1}{96}\ln\left[\frac{C_A\gamma^4}{\mu^4}\right] - \frac{1}{48}\ln\left[\frac{[(p^2)^2 + C_A\gamma^4]}{\mu^4}\right] \right. \\
& \quad \left. + \frac{1}{48}\ln\left[\frac{p^2}{\mu^2}\right] - \frac{3\sqrt{2}}{1024}\eta_2(p^2) \right] \frac{(p^2)^3}{C_A\gamma^4} \Big] a + O(a^2) \tag{B.1}
\end{aligned}$$

$$\begin{aligned}
U = & i \left[C_A \left[\frac{1}{64}\ln\left[1 + \frac{(p^2)^2}{C_A\gamma^4}\right] - \frac{31}{64} \right] - \frac{C_A^2\gamma^4}{96(p^2)^2}\ln\left[1 + \frac{(p^2)}{C_A\gamma^4}\right] + \frac{179\pi\sqrt{C_A^3}\gamma^2}{384p^2} \right. \\
& - \frac{11\sqrt{C_A^3}\gamma^2}{192p^2}\tan^{-1}\left[\frac{\sqrt{C_A}\gamma^2}{p^2}\right] \\
& + \left[\frac{7C_A}{16p^2} - \frac{7p^2}{64\gamma^4} \right] \sqrt{4C_A\gamma^4 - (p^2)^2}\tan^{-1}\left[-\frac{\sqrt{4C_A\gamma^4 - (p^2)^2}}{p^2} \right] - \frac{39\pi\sqrt{C_A}p^2}{128\gamma^2} \\
& - \left[\frac{1}{24}\tan^{-1}\left[\frac{\sqrt{C_A}\gamma^2}{p^2}\right] + \frac{7\sqrt{2}}{64}\eta_1(p^2) \right] \frac{\sqrt{C_A}p^2}{\gamma^2}
\end{aligned}$$

$$\begin{aligned}
& + \left[\frac{5}{192} \ln \left[\frac{[(p^2)^2 + C_A \gamma^4]}{\mu^4} \right] - \frac{3}{128} \ln \left[\frac{C_A \gamma^4}{\mu^4} \right] - \frac{1}{192} \ln \left[\frac{p^2}{\mu^2} \right] + \frac{5\sqrt{2}}{256} \eta_2(p^2) \right] \frac{(p^2)^2}{\gamma^4} \\
& - \frac{\pi(p^2)^3}{256\sqrt{C_A}\gamma^6} + \left[\frac{1}{64} \tan^{-1} \left[\frac{\sqrt{C_A}\gamma^2}{p^2} \right] - \frac{\sqrt{2}}{512} \eta_1(p^2) \right] \frac{(p^2)^3}{\sqrt{C_A}\gamma^6} \gamma^2 a + O(a^2) \quad (\text{B.2})
\end{aligned}$$

$$V = W_\rho = R_\rho = S_\rho = O(a^2) \quad (\text{B.3})$$

$$\begin{aligned}
Q_\xi = Q_\rho = & \left[\frac{3\sqrt{C_A^3}\gamma^2}{4} \tan^{-1} \left[\frac{\sqrt{C_A}\gamma^2}{p^2} \right] - \frac{3\pi\sqrt{C_A^3}\gamma^2}{8} + \frac{C_A^2\gamma^4}{8p^2} \ln \left[1 + \frac{(p^2)^2}{C_A\gamma^4} \right] \right. \\
& + \frac{5C_A p^2}{4} - \frac{3C_A p^2}{8} \ln \left[\frac{C_A\gamma^4}{\mu^4} \right] - \left. \frac{\sqrt{C_A}(p^2)^2}{4\gamma^2} \tan^{-1} \left[\frac{\sqrt{C_A}\gamma^2}{p^2} \right] \right] a \\
& + O(a^2) \quad (\text{B.4})
\end{aligned}$$

$$\begin{aligned}
W_\xi = & \left[\frac{\pi}{24} \sqrt{C_A}\gamma^2 - \frac{\sqrt{C_A}\gamma^2}{9} \tan^{-1} \left[\frac{\sqrt{C_A}\gamma^2}{p^2} \right] \right. \\
& - \left. \frac{\sqrt{4C_A\gamma^4 - (p^2)^2}}{72} \tan^{-1} \left[-\frac{\sqrt{4C_A\gamma^4 - (p^2)^2}}{p^2} \right] \right. \\
& - \frac{\pi}{192} \frac{\sqrt{C_A^3}\gamma^6}{(p^2)^2} + \frac{1}{96} \frac{\sqrt{C_A^3}\gamma^6}{(p^2)^2} \tan^{-1} \left[\frac{\sqrt{C_A}\gamma^2}{p^2} \right] + \left[\frac{1}{96} - \frac{1}{36} \ln \left[1 + \frac{(p^2)^2}{C_A\gamma^4} \right] \right] \frac{C_A\gamma^4}{p^2} \\
& + \left[-\frac{1}{96} - \frac{5}{96} \ln \left[\frac{C_A\gamma^4}{\mu^4} \right] + \frac{5}{96} \ln \left[\frac{[(p^2)^2 + C_A\gamma^4]}{\mu^4} \right] - \frac{\sqrt{2}}{72} \eta_2(p^2) \right] p^2 \\
& + \frac{(p^2)^2}{288C_A\gamma^4} \sqrt{4C_A\gamma^4 - (p^2)^2} \tan^{-1} \left[-\frac{\sqrt{4C_A\gamma^4 - (p^2)^2}}{p^2} \right] - \frac{\pi}{144} \frac{(p^2)^2}{\sqrt{C_A}\gamma^2} \\
& + \left[\frac{13}{288} \tan^{-1} \left[\frac{\sqrt{C_A}\gamma^2}{p^2} \right] - \frac{\sqrt{2}}{288} \eta_1(p^2) \right] \frac{(p^2)^2}{\sqrt{C_A}\gamma^2} \\
& + \left[\frac{1}{576} \ln \left[\frac{C_A\gamma^4}{\mu^4} \right] - \frac{1}{288} \ln \left[\frac{[(p^2)^2 + C_A\gamma^4]}{\mu^4} \right] + \frac{1}{288} \ln \left[\frac{p^2}{\mu^2} \right] \right] \frac{(p^2)^3}{C_A\gamma^4} a \\
& + O(a^2) \quad (\text{B.5})
\end{aligned}$$

$$\begin{aligned}
R_\xi = & \left[\frac{5\pi}{96} \sqrt{C_A}\gamma^2 - \frac{11\sqrt{C_A}\gamma^2}{72} \tan^{-1} \left[\frac{\sqrt{C_A}\gamma^2}{p^2} \right] \right. \\
& - \left. \frac{\sqrt{4C_A\gamma^4 - (p^2)^2}}{72} \tan^{-1} \left[-\frac{\sqrt{4C_A\gamma^4 - (p^2)^2}}{p^2} \right] \right. \\
& + \frac{C_A\gamma^4 \sqrt{4C_A\gamma^4 - (p^2)^2}}{12(p^2)^2} \tan^{-1} \left[-\frac{\sqrt{4C_A\gamma^4 - (p^2)^2}}{p^2} \right] + \frac{13\pi}{192} \frac{\sqrt{C_A^3}\gamma^6}{(p^2)^2} \\
& + \frac{1}{32} \frac{\sqrt{C_A^3}\gamma^6}{(p^2)^2} \tan^{-1} \left[\frac{\sqrt{C_A}\gamma^2}{p^2} \right] - \left[\frac{5}{96} + \frac{17}{288} \ln \left[1 + \frac{(p^2)^2}{C_A\gamma^4} \right] \right] \frac{C_A\gamma^4}{p^2} \\
& + \left[-\frac{1}{96} - \frac{1}{32} \ln \left[\frac{C_A\gamma^4}{\mu^4} \right] + \frac{1}{32} \ln \left[\frac{[(p^2)^2 + C_A\gamma^4]}{\mu^4} \right] - \frac{\sqrt{2}}{72} \eta_2(p^2) \right] p^2 \\
& - \frac{(p^2)^2}{576C_A\gamma^4} \sqrt{4C_A\gamma^4 - (p^2)^2} \tan^{-1} \left[-\frac{\sqrt{4C_A\gamma^4 - (p^2)^2}}{p^2} \right] + \frac{5\pi}{576} \frac{(p^2)^2}{\sqrt{C_A}\gamma^2} \\
& + \left[-\frac{5}{288} \tan^{-1} \left[\frac{\sqrt{C_A}\gamma^2}{p^2} \right] + \frac{\sqrt{2}}{576} \eta_1(p^2) \right] \frac{(p^2)^2}{\sqrt{C_A}\gamma^2}
\end{aligned}$$

$$\begin{aligned}
& + \left[-\frac{1}{288} \ln \left[\frac{C_A \gamma^4}{\mu^4} \right] + \frac{1}{144} \ln \left[\frac{[(p^2)^2 + C_A \gamma^4]}{\mu^4} \right] \right. \\
& \quad \left. - \frac{1}{144} \ln \left[\frac{p^2}{\mu^2} \right] - \frac{\sqrt{2}}{768} \eta_2(p^2) \right] \frac{(p^2)^3}{C_A \gamma^4} a + O(a^2) \tag{B.6}
\end{aligned}$$

and

$$\begin{aligned}
S_\xi &= \left[\frac{\pi \gamma^2}{4\sqrt{C_A}} - \frac{2\gamma^2}{3\sqrt{C_A}} \tan^{-1} \left[\frac{\sqrt{C_A} \gamma^2}{p^2} \right] - \frac{\sqrt{4C_A \gamma^4 - (p^2)^2}}{12C_A} \tan^{-1} \left[-\frac{\sqrt{4C_A \gamma^4 - (p^2)^2}}{p^2} \right] \right. \\
& \quad - \frac{\pi \sqrt{C_A} \gamma^6}{32 (p^2)^2} + \frac{1}{16} \frac{\sqrt{C_A} \gamma^6}{(p^2)^2} \tan^{-1} \left[\frac{\sqrt{C_A} \gamma^2}{p^2} \right] + \left[\frac{1}{16} - \frac{1}{6} \ln \left[1 + \frac{(p^2)^2}{C_A \gamma^4} \right] \right] \frac{\gamma^4}{p^2} \\
& \quad + \left[-\frac{1}{16} - \frac{5}{16} \ln \left[\frac{C_A \gamma^4}{\mu^4} \right] + \frac{5}{16} \ln \left[\frac{[(p^2)^2 + C_A \gamma^4]}{\mu^4} \right] - \frac{\sqrt{2}}{12} \eta_2(p^2) \right] \frac{p^2}{C_A} \\
& \quad + \frac{(p^2)^2}{48 C_A^2 \gamma^4} \sqrt{4C_A \gamma^4 - (p^2)^2} \tan^{-1} \left[-\frac{\sqrt{4C_A \gamma^4 - (p^2)^2}}{p^2} \right] - \frac{\pi}{24} \frac{(p^2)^2}{\sqrt{C_A^3} \gamma^2} \\
& \quad + \left[\frac{13}{48} \tan^{-1} \left[\frac{\sqrt{C_A} \gamma^2}{p^2} \right] - \frac{\sqrt{2}}{48} \eta_1(p^2) \right] \frac{(p^2)^2}{\sqrt{C_A^3} \gamma^2} \\
& \quad + \left[\frac{1}{96} \ln \left[\frac{C_A \gamma^4}{\mu^4} \right] - \frac{1}{48} \ln \left[\frac{[(p^2)^2 + C_A \gamma^4]}{\mu^4} \right] + \frac{1}{48} \ln \left[\frac{p^2}{\mu^2} \right] \right] \frac{(p^2)^3}{C_A^2 \gamma^4} a + O(a^2). \tag{B.7}
\end{aligned}$$

Taking the zero momentum limit of each expression we find

$$\begin{aligned}
X &= \left[\left[\frac{101}{72} - \frac{121}{128} \ln \left[\frac{C_A \gamma^4}{\mu^4} \right] - \frac{53}{192} \ln \left[\frac{p^2}{\mu^2} \right] \right] C_A p^2 - \frac{69\pi}{128} \sqrt{C_A^3} \gamma^2 \right. \\
& \quad \left. + \left[\frac{4}{3} \ln \left[\frac{p^2}{\mu^2} \right] - \frac{20}{9} \right] T_F N_f p^2 + O((p^2)^2) \right] a + O(a^2) \\
U &= i \left[-\frac{31\pi}{192} \sqrt{C_A} p^2 + O((p^2)^2) \right] \gamma^2 a + O(a^2) \\
V &= W_\rho = R_\rho = S_\rho = O(a^2) \\
Q_\xi &= Q_\rho = \left[\left[\frac{5}{8} - \frac{3}{8} \ln \left[\frac{C_A \gamma^4}{\mu^4} \right] \right] C_A p^2 + O((p^2)^2) \right] a + O(a^2) \\
W_\xi &= \left[-\frac{7p^2}{144} + O((p^2)^2) \right] a + O(a^2) \quad , \quad R_\xi = \left[-\frac{11p^2}{288} + O((p^2)^2) \right] a + O(a^2) \\
S_\xi &= \left[-\frac{7p^2}{24C_A} + O((p^2)^2) \right] a + O(a^2). \tag{B.8}
\end{aligned}$$

C Longitudinal parts.

In this appendix we provide the one loop $\overline{\text{MS}}$ expressions for the longitudinal parts of the 2-point functions of (3.1). We find

$$\begin{aligned}
X^L &= \left[-\frac{69}{64} \sqrt{C_A^3} \gamma^2 \tan^{-1} \left[\frac{\sqrt{C_A} \gamma^2}{p^2} \right] + \frac{9C_A \sqrt{4C_A \gamma^4 - (p^2)^2}}{64} \tan^{-1} \left[-\frac{\sqrt{4C_A \gamma^4 - (p^2)^2}}{p^2} \right] \right. \\
& \quad \left. + \frac{9C_A^2 \gamma^4}{8(p^2)^2} \sqrt{4C_A \gamma^4 - (p^2)^2} \tan^{-1} \left[-\frac{\sqrt{4C_A \gamma^4 - (p^2)^2}}{p^2} \right] + \frac{177\pi}{128} \frac{\sqrt{C_A^5} \gamma^6}{(p^2)^2} \right]
\end{aligned}$$

$$\begin{aligned}
& - \frac{33}{64} \frac{\sqrt{C_A^5} \gamma^6}{(p^2)^2} \tan^{-1} \left[\frac{\sqrt{C_A} \gamma^2}{p^2} \right] + \left[-\frac{105}{64} + \frac{9}{64} \ln \left[1 + \frac{(p^2)^2}{C_A \gamma^4} \right] \right] \frac{C_A^2 \gamma^4}{p^2} \\
& + \left[\frac{9}{128} \ln \left[\frac{C_A \gamma^4}{\mu^4} \right] + \frac{27}{64} \ln \left[\frac{[(p^2)^2 + C_A \gamma^4]}{\mu^4} \right] - \frac{63}{64} \ln \left[\frac{p^2}{\mu^2} \right] \right] C_A p^2 \Big] a + O(a^2) \quad (C.1)
\end{aligned}$$

$$\begin{aligned}
U^L = & i \left[C_A \left[\frac{3}{32} - \frac{15}{64} \ln \left[1 + \frac{(p^2)^2}{C_A \gamma^4} \right] \right] - \frac{C_A^2 \gamma^4}{32(p^2)^2} \ln \left[1 + \frac{(p^2)^2}{C_A \gamma^4} \right] + \frac{\pi \sqrt{C_A^3} \gamma^2}{32p^2} \right. \\
& + \frac{5\sqrt{C_A^3} \gamma^2}{16p^2} \tan^{-1} \left[\frac{\sqrt{C_A} \gamma^2}{p^2} \right] + \frac{3C_A \sqrt{4C_A \gamma^4 - (p^2)^2}}{16p^2} \tan^{-1} \left[-\frac{\sqrt{4C_A \gamma^4 - (p^2)^2}}{p^2} \right] \\
& - \frac{3p^2 \sqrt{4C_A \gamma^4 - (p^2)^2}}{64\gamma^4} \tan^{-1} \left[-\frac{\sqrt{4C_A \gamma^4 - (p^2)^2}}{p^2} \right] - \frac{\sqrt{C_A} p^2}{4\gamma^2} \tan^{-1} \left[\frac{\sqrt{C_A} \gamma^2}{p^2} \right] \\
& + \left. \left[\frac{1}{64} \ln \left[\frac{[(p^2)^2 + C_A \gamma^4]}{\mu^4} \right] - \frac{3}{128} \ln \left[\frac{C_A \gamma^4}{\mu^4} \right] + \frac{1}{64} \ln \left[\frac{p^2}{\mu^2} \right] \right] \frac{(p^2)^2}{\gamma^4} \right] \gamma^2 a \\
& + O(a^2) \quad (C.2)
\end{aligned}$$

$$\begin{aligned}
V^L = & i \left[C_A \left[\frac{3}{32} \ln \left[1 + \frac{(p^2)^2}{C_A \gamma^4} \right] - \frac{1}{16} \right] + \frac{\pi \sqrt{C_A^3} \gamma^2}{32p^2} \right. \\
& - \frac{\sqrt{C_A^3} \gamma^2}{16p^2} \tan^{-1} \left[\frac{\sqrt{C_A} \gamma^2}{p^2} \right] + \frac{3\sqrt{C_A} p^2}{16\gamma^2} \tan^{-1} \left[\frac{\sqrt{C_A} \gamma^2}{p^2} \right] \\
& + \left. \left[-\frac{1}{32} \ln \left[\frac{[(p^2)^2 + C_A \gamma^4]}{\mu^4} \right] + \frac{1}{16} \ln \left[\frac{p^2}{\mu^2} \right] \right] \frac{(p^2)^2}{\gamma^4} \right] \gamma^2 a + O(a^2) \quad (C.3)
\end{aligned}$$

$$W_\rho^L = R_\rho^L = S_\rho^L = O(a^2) \quad (C.4)$$

$$\begin{aligned}
Q_\xi^L = Q_\rho^L = & \left[\frac{3\sqrt{C_A^3} \gamma^2}{4} \tan^{-1} \left[\frac{\sqrt{C_A} \gamma^2}{p^2} \right] - \frac{3\pi \sqrt{C_A^3} \gamma^2}{8} + \frac{C_A^2 \gamma^4}{8p^2} \ln \left[1 + \frac{(p^2)^2}{C_A \gamma^4} \right] \right. \\
& + \frac{5C_A p^2}{4} - \frac{3C_A p^2}{8} \ln \left[\frac{C_A \gamma^4}{\mu^4} \right] - \frac{\sqrt{C_A} (p^2)^2}{4\gamma^2} \tan^{-1} \left[\frac{\sqrt{C_A} \gamma^2}{p^2} \right] \Big] a \\
& + O(a^2) \quad (C.5)
\end{aligned}$$

$$\begin{aligned}
W_\xi^L = & \left[\frac{5\pi}{48} \sqrt{C_A} \gamma^2 - \frac{5\sqrt{C_A} \gamma^2}{24} \tan^{-1} \left[\frac{\sqrt{C_A} \gamma^2}{p^2} \right] + \frac{\pi}{64} \frac{\sqrt{C_A^3} \gamma^6}{(p^2)^2} \right. \\
& - \frac{1}{32} \frac{\sqrt{C_A^3} \gamma^6}{(p^2)^2} \tan^{-1} \left[\frac{\sqrt{C_A} \gamma^2}{p^2} \right] - \frac{1}{32} \frac{C_A \gamma^4}{p^2} \\
& + \left[\frac{1}{32} - \frac{5}{32} \ln \left[\frac{C_A \gamma^4}{\mu^4} \right] + \frac{5}{32} \ln \left[\frac{[(p^2)^2 + C_A \gamma^4]}{\mu^4} \right] - \frac{\sqrt{2}}{24} \eta_2(p^2) \right] p^2 \\
& - \frac{5\pi}{96} \frac{(p^2)^2}{\sqrt{C_A} \gamma^2} + \left[\frac{5}{32} \tan^{-1} \left[\frac{\sqrt{C_A} \gamma^2}{p^2} \right] - \frac{\sqrt{2}}{48} \eta_1(p^2) \right] \frac{(p^2)^2}{\sqrt{C_A} \gamma^2} \\
& + \left[\frac{1}{192} \ln \left[\frac{C_A \gamma^4}{\mu^4} \right] - \frac{1}{96} \ln \left[\frac{[(p^2)^2 + C_A \gamma^4]}{\mu^4} \right] + \frac{1}{96} \ln \left[\frac{p^2}{\mu^2} \right] + \frac{\sqrt{2}}{384} \eta_2(p^2) \right] \frac{(p^2)^3}{C_A \gamma^4} \Big] a \\
& + O(a^2) \quad (C.6)
\end{aligned}$$

$$\begin{aligned}
R_\xi^L = & \left[-\frac{5\pi}{96}\sqrt{C_A}\gamma^2 + \frac{5\sqrt{C_A}\gamma^2}{12}\tan^{-1}\left[\frac{\sqrt{C_A}\gamma^2}{p^2}\right] \right. \\
& + \left[\frac{1}{8} - \frac{C_A\gamma^4}{4(p^2)^2} \right] \sqrt{4C_A\gamma^4 - (p^2)^2} \tan^{-1}\left[-\frac{\sqrt{4C_A\gamma^4 - (p^2)^2}}{p^2}\right] - \frac{13\pi}{64}\frac{\sqrt{C_A^3}\gamma^6}{(p^2)^2} \\
& - \frac{3}{32}\frac{\sqrt{C_A^3}\gamma^6}{(p^2)^2}\tan^{-1}\left[\frac{\sqrt{C_A}\gamma^2}{p^2}\right] + \left[\frac{5}{32} + \frac{5}{32}\ln\left[1 + \frac{(p^2)^2}{C_A\gamma^4}\right] \right] \frac{C_A\gamma^4}{p^2} \\
& + \left[\frac{1}{32} + \frac{5}{32}\ln\left[\frac{C_A\gamma^4}{\mu^4}\right] - \frac{5}{32}\ln\left[\frac{[(p^2)^2 + C_A\gamma^4]}{\mu^4}\right] + \frac{\sqrt{2}}{48}\eta_2(p^2) \right] p^2 \\
& - \frac{(p^2)^2}{64C_A\gamma^4}\sqrt{4C_A\gamma^4 - (p^2)^2}\tan^{-1}\left[-\frac{\sqrt{4C_A\gamma^4 - (p^2)^2}}{p^2}\right] + \frac{5\pi}{192}\frac{(p^2)^2}{\sqrt{C_A}\gamma^2} \\
& + \left[-\frac{5}{32}\tan^{-1}\left[\frac{\sqrt{C_A}\gamma^2}{p^2}\right] + \frac{\sqrt{2}}{96}\eta_1(p^2) \right] \frac{(p^2)^2}{\sqrt{C_A}\gamma^2} \\
& + \left[-\frac{1}{96}\ln\left[\frac{C_A\gamma^4}{\mu^4}\right] + \frac{1}{48}\ln\left[\frac{[(p^2)^2 + C_A\gamma^4]}{\mu^4}\right] \right. \\
& \quad \left. - \frac{1}{48}\ln\left[\frac{p^2}{\mu^2}\right] - \frac{\sqrt{2}}{768}\eta_2(p^2) \right] \frac{(p^2)^3}{C_A\gamma^4} a + O(a^2)
\end{aligned} \tag{C.7}$$

and

$$\begin{aligned}
S_\xi^L = & \left[\frac{5\pi\gamma^2}{8\sqrt{C_A}} - \frac{5\gamma^2}{4\sqrt{C_A}}\tan^{-1}\left[\frac{\sqrt{C_A}\gamma^2}{p^2}\right] \right. \\
& + \frac{3\pi}{32}\frac{\sqrt{C_A}\gamma^6}{(p^2)^2} - \frac{3}{16}\frac{\sqrt{C_A}\gamma^6}{(p^2)^2}\tan^{-1}\left[\frac{\sqrt{C_A}\gamma^2}{p^2}\right] - \frac{3}{16}\frac{\gamma^4}{p^2} \\
& + \left[\frac{3}{16} - \frac{15}{16}\ln\left[\frac{C_A\gamma^4}{\mu^4}\right] + \frac{15}{16}\ln\left[\frac{[(p^2)^2 + C_A\gamma^4]}{\mu^4}\right] - \frac{\sqrt{2}}{4}\eta_2(p^2) \right] \frac{p^2}{C_A} \\
& - \frac{5\pi}{16}\frac{(p^2)^2}{\sqrt{C_A^3}\gamma^2} + \left[\frac{15}{16}\tan^{-1}\left[\frac{\sqrt{C_A}\gamma^2}{p^2}\right] - \frac{\sqrt{2}}{8}\eta_1(p^2) \right] \frac{(p^2)^2}{\sqrt{C_A^3}\gamma^2} \\
& + \left[\frac{1}{32}\ln\left[\frac{C_A\gamma^4}{\mu^4}\right] - \frac{1}{16}\ln\left[\frac{[(p^2)^2 + C_A\gamma^4]}{\mu^4}\right] + \frac{1}{16}\ln\left[\frac{p^2}{\mu^2}\right] + \frac{\sqrt{2}}{64}\eta_2(p^2) \right] \frac{(p^2)^3}{C_A^2\gamma^4} a \\
& + O(a^2) .
\end{aligned} \tag{C.8}$$

As in the previous appendix, taking the zero momentum limit of each expression we find

$$\begin{aligned}
X^L &= \left[\left[\frac{35}{32} + \frac{63}{128}\ln\left[\frac{C_A\gamma^4}{\mu^4}\right] - \frac{63}{64}\ln\left[\frac{p^2}{\mu^2}\right] \right] C_A p^2 - \frac{69\pi}{128}\sqrt{C_A^3}\gamma^2 + O\left((p^2)^2\right) \right] a + O(a^2) \\
U^L &= i \left[-\frac{7\pi}{128}\sqrt{C_A}p^2 + O\left((p^2)^2\right) \right] \gamma^2 a + O(a^2) \\
V^L &= i \left[\frac{3\pi}{32}\sqrt{C_A}p^2 + O\left((p^2)^2\right) \right] \gamma^2 a + O(a^2) \\
W_\rho^L &= R_\rho^L = S_\rho^L = O(a^2) \\
Q_\xi^L &= Q_\rho^L = \left[\left[\frac{5}{8} - \frac{3}{8}\ln\left[\frac{C_A\gamma^4}{\mu^4}\right] \right] C_A p^2 + O\left((p^2)^2\right) \right] a + O(a^2) \\
W_\xi^L &= \left[-\frac{5p^2}{48} + O\left((p^2)^2\right) \right] a + O(a^2) \quad , \quad R_\xi^L = \left[\frac{5p^2}{96} + O\left((p^2)^2\right) \right] a + O(a^2)
\end{aligned}$$

$$S_\xi^L = \left[-\frac{5p^2}{8C_A} + O((p^2)^2) \right] a + O(a^2). \quad (\text{C.9})$$

Interestingly the $O(\gamma^2)$ part of X^L is equivalent to the $O(\gamma^2)$ term of X in the same limit.

D Tensor operator correlation function.

In this appendix we record the explicit form of the correlation function of the Lorentz tensor operator $\mathcal{O}_T^{\mu\nu}$ which is defined by

$$\Pi_T^{\{\mu\nu|\sigma\rho\}}(p^2) = (4\pi)^2 i \int d^4x e^{ipx} \langle 0 | \mathcal{O}_T^{\mu\nu}(x) \mathcal{O}_T^{\sigma\rho}(0) | 0 \rangle. \quad (\text{D.1})$$

We decompose this into a similar basis of Lorentz tensors to that used in [82] with the only difference being that we work completely in d -dimensions and not four dimensions, as we use dimensional regularization. We have

$$\begin{aligned} \Pi_T^{\{\mu\nu|\sigma\rho\}}(p^2) &= \left[\eta_{\mu\sigma}\eta_{\nu\rho} + \eta_{\mu\rho}\eta_{\nu\sigma} - \frac{2}{d}\eta_{\mu\nu}\eta_{\sigma\rho} \right] \Pi_1^T(p^2) \\ &+ \left[\frac{4}{d^2}\eta_{\mu\nu}\eta_{\sigma\rho} + \left(\eta_{\mu\sigma}\frac{p_\nu p_\rho}{p^2} + \eta_{\nu\rho}\frac{p_\mu p_\sigma}{p^2} + \eta_{\mu\rho}\frac{p_\nu p_\sigma}{p^2} + \eta_{\nu\sigma}\frac{p_\mu p_\rho}{p^2} \right) \right. \\ &\quad \left. - \frac{4}{d} \left(\eta_{\mu\nu}\frac{p_\sigma p_\rho}{p^2} + \eta_{\sigma\rho}\frac{p_\mu p_\nu}{p^2} \right) \right] \Pi_2^T(p^2) \\ &+ \left[\frac{1}{d^2}\eta_{\mu\nu}\eta_{\sigma\rho} - \frac{1}{d} \left(\eta_{\mu\nu}\frac{p_\sigma p_\rho}{p^2} + \eta_{\sigma\rho}\frac{p_\mu p_\nu}{p^2} \right) + \frac{p_\mu p_\nu p_\sigma p_\rho}{(p^2)^2} \right] \Pi_3^T(p^2). \quad (\text{D.2}) \end{aligned}$$

To determine the scalar amplitudes $\Pi_i^T(p^2)$ we use a projection method. This involves multiplying the original correlator by a Lorentz tensor which is a linear combination of the three basis Lorentz tensors defining the decomposition, (D.2). The construction of each of the three projection tensors is similar to that used in appendix A for the decomposition of colour group tensors. We first construct a matrix where the entries are determined by multiplying (D.2) by each basis tensor in turn. This produces the d -dependent matrix

$$P_T = \begin{pmatrix} 2(d-1)(d+2) & \frac{4}{d}(d-1)(d+2) & \frac{2}{d}(d-1) \\ \frac{4}{d}(d-1)(d+2) & \frac{4}{d^2}(d-1)(d^2+4d-4) & \frac{4}{d^2}(d-1)^2 \\ \frac{2}{d}(d-1) & \frac{4}{d^2}(d-1)^2 & \frac{(d-1)^2}{d^2} \end{pmatrix}. \quad (\text{D.3})$$

The coefficients of the basis tensors in each of the three projectors are then determined from the inverse which is

$$P_T^{-1} = \frac{1}{(d^2-1)(d-2)} \begin{pmatrix} \frac{1}{2}(d-1) & -\frac{1}{2}(d-1) & (d-2) \\ -\frac{1}{2}(d-1) & \frac{1}{4}(d^2+d-4) & -(d^2-4) \\ (d-2) & -(d^2-4) & (d^2-4)(d+4) \end{pmatrix}. \quad (\text{D.4})$$

Equipped with this we find the three scalar amplitudes are

$$\begin{aligned} \Pi_1^T(p^2) &= \left[\frac{(p^2)^2}{160\epsilon} - \frac{C_A\gamma^4}{12\epsilon} + \frac{C_A^2\gamma^8\sqrt{4C_A\gamma^4-(p^2)^2}}{120(p^2)^3} \tan^{-1} \left[\frac{\sqrt{4C_A\gamma^4-(p^2)^2}}{p^2} \right] \right. \\ &\quad \left. - \frac{\pi C_A^{5/2}\gamma^{10}}{120(p^2)^3} + \frac{C_A^2\gamma^8}{120(p^2)^2} + \frac{C_A\gamma^4\sqrt{4C_A\gamma^4-(p^2)^2}}{60p^2} \tan^{-1} \left[\frac{\sqrt{4C_A\gamma^4-(p^2)^2}}{p^2} \right] \right] \end{aligned}$$

$$\begin{aligned}
& - \frac{\pi C_A^{3/2} \gamma^6}{64 p^2} + \frac{p^2}{320} \sqrt{4 C_A \gamma^4 - (p^2)^2} \tan^{-1} \left[\frac{\sqrt{4 C_A \gamma^4 - (p^2)^2}}{p^2} \right] \\
& + \left[\frac{1}{24} \ln \left[\frac{C_A \gamma^4}{\mu^4} \right] - \frac{71}{1440} + \frac{3\sqrt{2}}{640} \eta_2(p^2) \right] C_A \gamma^4 \\
& + \left[\frac{\pi}{128} + \frac{3\sqrt{2}}{1280} \eta_1(p^2) \right] \sqrt{C_A} \gamma^2 p^2 \\
& + \left[\frac{9}{1600} - \frac{1}{320} \ln \left[\frac{C_A \gamma^4}{\mu^2} \right] - \frac{\sqrt{2}}{1280} \eta_2(p^2) \right] (p^2)^2 N_A + O(a) \tag{D.5}
\end{aligned}$$

$$\begin{aligned}
\Pi_2^T(p^2) = & \left[- \frac{(p^2)^2}{160\epsilon} - \frac{C_A^2 \gamma^8 \sqrt{4 C_A \gamma^4 - (p^2)^2}}{20(p^2)^3} \tan^{-1} \left[\frac{\sqrt{4 C_A \gamma^4 - (p^2)^2}}{p^2} \right] \right. \\
& + \frac{\pi C_A^{5/2} \gamma^{10}}{20(p^2)^3} - \frac{C_A^2 \gamma^8}{20(p^2)^2} - \frac{C_A \gamma^4 \sqrt{4 C_A \gamma^4 - (p^2)^2}}{160 p^2} \tan^{-1} \left[\frac{\sqrt{4 C_A \gamma^4 - (p^2)^2}}{p^2} \right] \\
& - \frac{p^2}{320} \sqrt{4 C_A \gamma^4 - (p^2)^2} \tan^{-1} \left[\frac{\sqrt{4 C_A \gamma^4 - (p^2)^2}}{p^2} \right] \\
& + \left[- \frac{1}{160} + \frac{\sqrt{2}}{1920} \eta_2(p^2) \right] C_A \gamma^4 - \left[\frac{\pi}{192} + \frac{\sqrt{2}}{960} \eta_1(p^2) \right] \sqrt{C_A} \gamma^2 p^2 \\
& \left. + \left[- \frac{9}{1600} + \frac{1}{320} \ln \left[\frac{C_A \gamma^4}{\mu^2} \right] + \frac{\sqrt{2}}{1280} \eta_2(p^2) \right] (p^2)^2 N_A + O(a) \tag{D.6}
\right.
\end{aligned}$$

and

$$\begin{aligned}
\Pi_3^T(p^2) = & \left[\frac{(p^2)^2}{120\epsilon} + \frac{2 C_A^2 \gamma^8 \sqrt{4 C_A \gamma^4 - (p^2)^2}}{5(p^2)^3} \tan^{-1} \left[\frac{\sqrt{4 C_A \gamma^4 - (p^2)^2}}{p^2} \right] \right. \\
& - \frac{2\pi C_A^{5/2} \gamma^{10}}{5(p^2)^3} + \frac{2 C_A^2 \gamma^8}{5(p^2)^2} + \frac{C_A \gamma^4 \sqrt{4 C_A \gamma^4 - (p^2)^2}}{120 p^2} \tan^{-1} \left[\frac{\sqrt{4 C_A \gamma^4 - (p^2)^2}}{p^2} \right] \\
& + \frac{\pi C_A^{3/2} \gamma^6}{24 p^2} + \frac{p^2}{240} \sqrt{4 C_A \gamma^4 - (p^2)^2} \tan^{-1} \left[\frac{\sqrt{4 C_A \gamma^4 - (p^2)^2}}{p^2} \right] \\
& + \left[- \frac{3}{40} + \frac{\sqrt{2}}{160} \eta_2(p^2) \right] C_A \gamma^4 - \frac{\sqrt{2}}{480} \sqrt{C_A} \gamma^2 p^2 \eta_1(p^2) \\
& \left. + \left[\frac{17}{3600} - \frac{1}{240} \ln \left[\frac{C_A \gamma^4}{\mu^2} \right] - \frac{\sqrt{2}}{960} \eta_2(p^2) \right] (p^2)^2 N_A + O(a) \right. \tag{D.7}
\end{aligned}$$

Again we have included the divergent parts of the correlation functions which are absorbed by a contact renormalization. We note, though, that there is only mixing for the first amplitude. Aside from several terms involving the factors $1/(p^2)^2$ and $1/(p^2)^3$ the actual functions appearing in each of the amplitudes are the same as for $\Pi_S(p^2)$. So, for example, the cut structure is the same with a physical cut at $p^2 = 2\sqrt{C_A} \gamma^2$. Repeating the same moment calculation for the scalar operator of section 7, we find that

$$\Pi_1^T(M^2) = (\text{parton model}) \left[1 - \frac{10 C_A \gamma^4}{3 M^4} + O\left(\frac{\gamma^8}{M^8}\right) \right] \tag{D.8}$$

and there are no $O\left(\frac{C_A \gamma^4}{M^4}\right)$ corrections for the other two scalar amplitudes. Further, if one considered the correlation function of the energy momentum tensor, as in [82], then the same power correction as $\Pi_1^T(M^2)$ would emerge.

References.

- [1] D.J. Gross & F.J. Wilczek, Phys. Rev. Lett. **30** (1973), 1343.
- [2] H.D. Politzer, Phys. Rev. Lett. **30** (1973), 1346.
- [3] S. Perantonis & C. Michael, Nucl. Phys. **B347** (1990), 854.
- [4] C. Michael, Phys. Lett. **B283** (1992), 103.
- [5] G.S. Bali, K. Schilling & A. Wachter, Phys. Rev. **D56** (1997), 2566.
- [6] S. Mandelstam, Phys. Rept. **67** (1980), 109.
- [7] R. Anishetty, M. Baker, J.S. Ball, S.K. Kim & F. Zachariasen, Phys. Lett. **B86** (1979), 52.
- [8] S. Mandelstam, Phys. Rev. **D20** (1979), 3223.
- [9] G.B. West, Phys. Lett. **B115** (1982), 468.
- [10] V.N. Gribov, Nucl. Phys. **B139** (1978), 1.
- [11] D. Zwanziger, Nucl. Phys. **B209** (1982), 336.
- [12] D. Zwanziger, Nucl. Phys. **B321** (1989), 591.
- [13] D. Zwanziger, Nucl. Phys. **B323** (1989), 513.
- [14] G. Dell'Antonio & D. Zwanziger, Nucl. Phys. **B326** (1989), 333.
- [15] G. Dell'Antonio & D. Zwanziger, Commun. Math. Phys. **138** (1991), 291.
- [16] D. Zwanziger, Nucl. Phys. **B364** (1991), 127.
- [17] D. Zwanziger, Nucl. Phys. **B378** (1992), 525.
- [18] D. Zwanziger, Nucl. Phys. **B399** (1993), 477.
- [19] D. Zwanziger, Nucl. Phys. **B412** (1994), 657.
- [20] D. Zwanziger, Phys. Rev. **D65** (2002), 094039.
- [21] D. Zwanziger, Phys. Rev. **D69** (2004), 016002.
- [22] A. Cucchieri & T. Mendes, PoS LAT2007 (2007), 297.
- [23] I.L. Bogolubsky, E.M. Ilgenfritz, M. Müller-Preussker & A. Sternbeck, PoS LAT2007 (2007), 290.
- [24] A. Cucchieri & T. Mendes, Phys. Rev. Lett. **100** (2008), 241601.
- [25] A. Cucchieri & T. Mendes, Phys. Rev. **D 78** (2008), 094503.
- [26] O. Oliveira & P.J. Silva, Phys. Rev. **D79** (2009), 031501.
- [27] Ph. Boucaud, J.P. Leroy, A.L. Yaounac, J. Micheli, O. Pène & J. Rodríguez-Quintero, JHEP **06** (2008), 099.
- [28] A.C. Aguilar, D. Binosi & J. Papavassiliou, Phys. Rev. **D78** (2008), 025010.

- [29] C.S. Fischer, A. Maas & J.M. Pawłowski, *Annals Phys.* **324** (2009), 2408.
- [30] N. Maggiore & M. Schaden, *Phys. Rev.* **D50** (1994), 6616.
- [31] D. Dudal, R.F. Sobreiro, S.P. Sorella & H. Verschelde, *Phys. Rev.* **D72** (2005), 014016.
- [32] J.A. Gracey, *Phys. Lett.* **B632** (2006), 282.
- [33] J.A. Gracey, *JHEP* **05** (2006), 052.
- [34] T. Kugo & I. Ojima, *Prog. Theor. Phys. Suppl.* **66** (1979), 1; *Prog. Theor. Phys. Suppl.* **77** (1984), 1121.
- [35] T. Kugo, hep-th/9511033.
- [36] L. Susskind, “Coarse Grained Quantum Chromodynamics” in ‘Les Houches 1976, Proceedings Weak and Electromagnetic Interactions at High Energy’, (North-Holland Publishing Company, Amsterdam, 1977), 207.
- [37] W. Fischler, *Nucl. Phys.* **B129** (1977), 157.
- [38] T. Appelquist, M. Dine & I.J. Muzinich, *Phys. Rev.* **D17** (1978), 2074.
- [39] M. Peter, *Phys. Rev. Lett.* **78** (1997), 602.
- [40] M. Peter, *Nucl. Phys.* **B501** (1997), 471.
- [41] Y. Schröder, “The Static Potential in QCD” DESY-THESIS-1999-021.
- [42] Y. Schröder, *Phys. Lett.* **B447** (1999), 321.
- [43] B.A. Kniehl, A.A. Penin, Y. Schröder, V.A. Smirnov & M. Steinhauser, *Phys. Lett.* **B607** (2005), 96.
- [44] A.V. Smirnov, V.A. Smirnov & M. Steinhauser, *Phys. Lett.* **B668** (2008), 293.
- [45] A.V. Smirnov, V.A. Smirnov & M. Steinhauser, *PoS RADCOR2007* (2007), 024.
- [46] A.V. Smirnov, V.A. Smirnov & M. Steinhauser, *Nucl. Phys. Proc. Suppl.* **183** (2008), 308.
- [47] C. Anzai, Y. Kiyo & Y. Sumino, arXiv:0911.4335 [hep-ph].
- [48] A.V. Smirnov, V.A. Smirnov & M. Steinhauser, arXiv:0911.4742 [hep-ph].
- [49] Y.M. Makeenko, *Surveys High Energ. Phys.* **10** (1997), 1.
- [50] D. Zwanziger, arXiv:0904.2380 [hep-th].
- [51] J.C. Taylor, *Nucl. Phys.* **B33** (1971), 436.
- [52] D. Dudal, S.P. Sorella, N. Vandersickel & H. Verschelde, *Phys. Rev.* **D77** (2008), 071501.
- [53] D. Dudal, J.A. Gracey, S.P. Sorella, N. Vandersickel & H. Verschelde, *Phys. Rev.* **D78** (2008), 065047.
- [54] J.G.M. Gatheral, *Phys. Lett.* **B133** (1983), 90.
- [55] J. Frenkel & J.C. Taylor, *Nucl. Phys.* **B246** (1984), 231.
- [56] S. Titard & F.J. Yndurain, *Phys. Rev.* **D49** (1994), 6007.

- [57] J.A.M. Vermaseren, math-ph/0010025.
- [58] R.F. Sobreiro & S.P. Sorella, JHEP **06** (2005), 054.
- [59] P. Nogueira, J. Comput. Phys. **105** (1993), 279.
- [60] S.A. Larin & J.A.M. Vermaseren, Phys. Lett. **B303** (1993), 334.
- [61] A.D. Dolgov, A. Lepidi & G. Piccinelli, JCAP **02** (2009), 027.
- [62] G. Gabadadze & R.A. Rosen, JCAP **02** (2009), 016.
- [63] P. Gaete & E. Spallucci, Phys. Lett. **B675** (2009), 145.
- [64] G. Gabadadze & D. Pirtskhalava, JCAP **05** (2009), 017.
- [65] A.D. Dolgov, A. Lepidi & G. Piccinelli, Phys. Rev. **D80** (2009), 125009.
- [66] M. Lüscher, Nucl. Phys. **B180** (1981), 317.
- [67] J.M. Cornwall & A. Soni, Phys. Lett. **B120** (1983), 431.
- [68] W. Buchmüller, G. Grunberg & S.-H. H. Tye, Phys. Rev. Lett. **45** (1980), 103; Phys. Rev. Lett. **45** (1980), 587.
- [69] S.J. Brodsky, G.P. Lepage & P.B. Mackenzie, Phys. Rev. **D28** (1983), 228.
- [70] W. Celmaster & R.J. Gonsalves, Phys. Rev. **D20** (1979), 1420.
- [71] E. Braaten & J.P. Leveille, Phys. Rev. **D24** (1981), 1369.
- [72] P. Boucaud, G. Burgio, F. di Renzo, J.P. Leroy, J. Micheli, C. Parrinello, O. Pène, C. Pittori, J. Rodríguez-Quintero, C. Roiesnel & K. Sharkey, JHEP **04** (2000), 006.
- [73] P. Boucaud, F. de Soto, J.P. Leroy, A. Le Yaouanc, J. Micheli, H. Moutarde, O. Pène & J. Rodríguez-Quintero, Phys. Rev. **D74** (2006), 034505.
- [74] P. Boucaud, J.P. Leroy, A. Le Yaouanc, A.Y. Lokhov, J. Micheli, O. Pène, J. Rodríguez-Quintero & C. Roiesnel, JHEP **01** (2006), 037.
- [75] J.A. Gracey, “Recent results for Yang-Mills theory restricted to the Gribov region” in ‘Path Integrals - New Trends and Perspectives’, (World Scientific, Singapore, 2008), 167.
- [76] F.A. Berends, M. Böhm, M. Buza & R. Scharf, Z. Phys. **C63** (1994), 227.
- [77] D. Dudal, S.P. Sorella, N. Vandersickel & H. Verschelde, Phys. Rev. **D79** (2009), 121701.
- [78] T. van Ritbergen, A.N. Schellekens & J.A.M. Vermaseren, Int. J. Mod. Phys. **A14** (1999), 41.
- [79] A. Soni & M.D. Tran, Phys. Lett. **B109** (1982), 393.
- [80] R. Akhoury & V.I. Zakharov, Phys. Lett. **B438** (1998), 165.
- [81] S. Narison & V.I. Zakharov, Phys. Lett. **B679** (2009), 355.
- [82] K.G. Chetyrkin, S. Narison & V.I. Zakharov, Nucl. Phys. **B550** (1999), 353.
- [83] S. Narison, Nucl. Phys. **B509** (1998), 312.

- [84] F.R. Graziani, Z. Phys. **C33** (1987), 397.
- [85] V.P. Spiridonov & K.G. Chetyrkin, Sov. J. Nucl. Phys. **47** (1988), 522.
- [86] J. Liu & W. Wetzel, hep-ph/9611250.
- [87] H. Vershelde, Phys. Lett. **B351** (1995), 242.
- [88] H. Vershelde, S. Schelstraete & M. Vanderkelen, Z. Phys. **C76** (1997), 161.
- [89] H. Vershelde, K. Knecht, K. van Acoleyen & M. Vanderkelen, Phys. Lett. **B516** (2001), 307.
- [90] T. van Ritbergen, J.A.M. Vermaseren & S.A. Larin, Phys. Lett. **B400** (1997), 379.
- [91] A.J. Macfarlane, A. Sudbery & P.H. Weisz, Commun. Math. Phys. **11** (1968), 77.